

South Dakota State University

Open PRAIRIE: Open Public Research Access Institutional Repository and Information Exchange

Electronic Theses and Dissertations

2021

Analysis of Volatile Organic Compounds: Petroleum Emissions and Microbial Degradation

A K M Ahsan Ahmed
South Dakota State University

Follow this and additional works at: <https://openprairie.sdstate.edu/etd>

 Part of the [Chemistry Commons](#)

Recommended Citation

Ahmed, A K M Ahsan, "Analysis of Volatile Organic Compounds: Petroleum Emissions and Microbial Degradation" (2021). *Electronic Theses and Dissertations*. 5251.
<https://openprairie.sdstate.edu/etd/5251>

This Dissertation - Open Access is brought to you for free and open access by Open PRAIRIE: Open Public Research Access Institutional Repository and Information Exchange. It has been accepted for inclusion in Electronic Theses and Dissertations by an authorized administrator of Open PRAIRIE: Open Public Research Access Institutional Repository and Information Exchange. For more information, please contact michael.biondo@sdstate.edu.

ANALYSIS OF VOLATILE ORGANIC COMPOUNDS: PETROLEUM EMISSIONS AND
MICROBIAL DEGRADATION

BY

A K M AHSAN AHMED

A dissertation submitted in partial fulfillment of the requirements for the

Doctor of Philosophy

Major in Chemistry

South Dakota State University

2021

DISSERTATION ACCEPTANCE PAGE

A K M Ahsan Ahmed

This dissertation is approved as a creditable and independent investigation by a candidate for the Doctor of Philosophy degree and is acceptable for meeting the dissertation requirements for this degree. Acceptance of this does not imply that the conclusions reached by the candidate are necessarily the conclusions of the major department.

Douglas Raynie
Advisor

Date

Douglas Raynie
Department Head

Date

Nicole Lounsbery, PhD
Director, Graduate School

Date

This dissertation is dedicated to my parents, Salah Uddin Ahmed and Syeda Rahela Khatun. I am grateful for their love, support, and sacrifices. Without them, I might not be the person I am today.

ACKNOWLEDGEMENTS

I would like to express my sincere gratitude and appreciation to my advisor, Dr. Douglas Raynie, for his continuous support and valuable suggestions throughout this journey. His vast knowledge and expertise in analytical chemistry have significantly helped in developing the methodology and answering research questions of this work. His insightful feedbacks were instrumental in the fulfillment of this dissertation work.

I would also like to thank our collaborators, Pavan Kulkarni, and Dr. Bleakley from the Biology & Microbiology Department, for their valuable contribution to accomplish chapter two of this dissertation. I would also like to offer my appreciation to all my committee members for their assistance and guidance. I extend my thanks to my colleagues from Green Chemistry Lab, Department of Chemistry and Biochemistry, and all the staff and faculty members for their help and encouragement.

I would like to thank my late father, Salah Uddin Ahmed, my mother, Syeda Rahela Khatun, and my elder brother, Sawket Ahmed, for their love, sacrifice, and belief in me. Many thanks to my in-laws, family, and friends for their never-ending support and encouragement. I would like to thank the most special person in my life, my wife Sharmin Sultana, without whom this journey would not have been possible. Thank you for providing me your constant support, love, and encouragement to make this journey easier, especially during the challenging time, by helping me stay focused on my work.

TABLE OF CONTENTS

Abbreviations	xi
List of Tables	xiv
List of Figures	xv
Abstract	xix
1 Chapter 1. Introduction and background	1
1.1 Overall significance	1
1.2 Project objectives	2
1.3 Volatile organic compounds (VOCs)	3
1.4 Sources of VOCs	4
1.5 Petroleum hydrocarbons	5
1.6 Gasoline	6
1.6.1 Composition of gasoline	7
1.7 Kerosene	9
1.7.1 Composition of kerosene	9
1.8 Analytical techniques used for petroleum hydrocarbons and other VOCs analysis	
9	
2 CHAPTER 2. Evaporative emission from ethanol-blended gasoline	10
2.1 Introduction	10
2.2 Background	12
2.2.1 Gasoline emission	12

2.2.2 Environmental effect of gasoline emissions	13
2.2.3 Oxygenates in gasoline	14
2.2.4 History of oxygenates and its uses in gasoline	15
2.2.5 Use of ethanol as oxygenates	16
2.2.6 Emission characteristics of ethanol-blended gasoline-literature review	16
2.3 Experimental	18
2.3.1 Gasoline sample fuels	18
2.3.2 Standard sample	18
2.3.3 Evaporative emission testing method	21
2.3.4 Sample preparation	21
2.3.5 Headspace SPME-GC-MS analysis of ethanol blended gasoline	21
2.3.6 Determination of headspace composition of gasoline and ethanol- blended gasoline	22
2.4 Results and Discussion	23
2.4.1 Optimization of SPME fiber and extraction time	23
2.4.2 Headspace SPME-GC-MS analysis of ethanol-blended gasoline	24
2.4.3 Effect of headspace composition of gasoline with ethanol addition	26
2.4.3.1 Effect at room temperature	26
2.4.3.2 Effect at 38 °C	28

2.4.3.3 Effect at 49 °C	29
2.4.4 Effect of headspace composition of gasoline with the change of temperature	32
2.4.5 Change of percentage composition with regards to both temperature and ethanol	37
2.5 Conclusion	39
2.6 Acknowledgement	40
3 CHAPTER 3. Microbial degradation of petroleum hydrocarbons in kerosene and biosurfactants production	41
3.1 Acknowledgment	41
3.2 Introduction	41
3.3 Background	44
3.3.1 Petroleum hydrocarbons pollutions and its effect	44
3.3.2 Bioremediation	44
3.3.3 Biodegradation of petroleum hydrocarbons	44
3.3.4 Biosurfactants	45
3.3.5 Role of biosurfactants in bioremediation	46
3.3.6 Biosurfactant producing bacteria	46
3.3.7 Lipopeptide biosurfactants	47
3.3.7.1 Iturin	47
3.3.7.2 Surfactin	47

3.3.8 <i>Bacillus amyloliquifaciens</i>	48
3.3.9 <i>B. amyloliquefaciens</i> and lipopeptide biosurfactants	48
3.4 Experimental	49
3.4.1 Bacterial isolates.....	49
3.4.2 Culture media	49
3.4.2.1 Composition and preparation of culture media	49
3.4.3 Inoculation of bacterial isolates into culture media.....	50
3.4.4 Biodegradation studies of kerosene in culture media.....	50
3.4.5 GC-MS conditions.....	51
3.4.6 Growth studies to investigate bacterial growth	51
3.4.7 Production of lipopeptide biosurfactants from 1BA and 1D3 isolates	51
3.4.8 Extraction of lipopeptides from the culture media	52
3.4.9 RP-UHPLC-UV analysis of lipopeptides.....	52
3.5 Results and discussion.....	54
3.5.1 Analysis of hydrocarbon degradation by GC-MS	54
3.5.2 Determination of bacterial growth by growth studies	57
3.5.2.1 Growth studies of <i>B. amyloliquefaciens</i> 1BA and 1D3 in TSB media	57

3.5.2.2 Growth studies of <i>B. amyloliquefaciens</i> 1BA and 1D3 in minimal media	57
3.5.3 UHPLC analysis of lipopeptide biosurfactants	58
3.5.4 Determination of concentrations of extracted surfactin	64
3.6 Conclusion	66
4 Chapter 4. Dry herb vaporizer as a headspace sampler for solid-phase microextraction	
68	
4.1 Introduction	68
4.2 Background	69
4.2.1 Headspace analysis	69
4.2.2 Principal of headspace analysis	70
4.2.3 Types of headspace analysis	72
4.2.4 Headspace solid-phase microextraction analysis	73
4.2.5 Field analytical chemistry	74
4.2.6 Importance of field analytical chemistry	75
4.2.7 Portable field laboratory instruments	75
4.2.8 Vaporizer device	75
4.3 Experimental	76
4.3.1 Samples	76
4.3.2 Dry herb vaporizer	76

4.3.3 Analytical procedure	77
4.3.3.1 Procedure A (using vape)	77
4.3.3.2 Procedure B (using conventional headspace set up)	79
4.3.4 Headspace solid-phase microextraction (HS-SPME) analysis.....	79
4.3.5 GC-MS analysis	80
4.3.6 Data analysis.....	81
4.4 Results and discussion.....	81
4.4.1 HS-SPME-GC-MS analysis of horseradish components	81
4.4.2 HS-SPME-GC-MS analysis of cinnamon components.....	86
4.4.3 HS-SPME-GC-MS analysis of gasoline spiked soil	91
4.5 Conclusion.....	97
5 Conclusion.....	98
6 REFERENCES.....	100

ABBREVIATIONS

AITC: Allyl isothiocyanate

ATC: Allyl thiocyanate

BPN: Benzenepropanenitrile

BTEX: Benzene, toluene, ethyl benzene and xylenes

CAA: Clean Air Act Amendments

CAR: Carboxen

CDS: Chromatography Data System

CFU: Colony forming units

DAD: Diode array detection

DVB: Divinylbenzene

E0: 0 v/v % ethanol content fuel

E10: 10 v/v % ethanol content fuel

E20: 20 v/v % ethanol content fuel

FAME: Fatty acid methyl ester

FID: Flame ionization detection

GC: Gas Chromatography

HC: Hydrocarbon

HS: Headspace

HSA: Headspace analysis

IR: Infrared

MA: Immunoassay

MON: Motor octane number

MS: Mass Spectrometry

MSD: Mass spectrometric detection

MTBE: Methyl tertiary butyl ether

NIST: National Institute Standard and Technology

NO_x: Oxides of nitrogen

OD: Optimal density

PDMS: polydimethylsiloxane

PH: Petroleum hydrocarbons

PITC: 2-phenylethyl isothiocyanate

PM: Particulate matter

POM: Particulate organic matter

RFG: Reformulated Gasoline

RON: Research octane number

RT: Room temperature

RVP: Reid vapor pressure

SPME: Solid-phase microextraction

SVOCs: Semi-volatile organic compounds

TEL: Tetraethyl lead

TFA: trifluoro acetic acid

THC: Total hydrocarbon

TIC: Total ion chromatogram

TSB: Tryptic soy broth

UHPLC: Ultra-High Performance Liquid Chromatography

UV: Ultraviolet

Vape: Vaporizer

VOCs: Volatile organic compounds

VVOC: Very volatile organic compounds

WHO: World Health Organization

XRF: X-ray fluorescence

LIST OF TABLES

Table 1. General Summary of Product Type and Distillation Range. ¹¹	6
Table 2. Increase in the number of isomers with carbon numbers. ¹¹	7
Table 3. Average composition of gasoline. ⁵	8
Table 4. Chemicals used in this work with their purity and the name of manufacturer. .	19
Table 5. Mass and Volume % of prepared standard solution	20
Table 6. R ² values and curve equation for calibration curve used for surfactin quantification	65
Table 7. Concentration of extracted surfactin in TSB by <i>B. amyloliquefaciens</i> 1D3 in absence of kerosene.	65
Table 8. Concentration (in ppm) of extracted surfactin in TSB by <i>B. amyloliquefaciens</i> 1D3 in presence of kerosene.	66
Table 9. Time (s) required to reach incubation and extraction temperature	78
Table 10. Relative Percent Peak Area of Horseradish Components.....	84
Table 11. Relative percent peak area of cinnamon components.....	89
Table 12. Relative percent peak area of gasoline spiked soil components.....	95

LIST OF FIGURES

Figure 1. Optimization of SPME fiber and extraction time: a) effect of fiber stationary phase and b) effect of extraction time using PDMS-CAR.....	24
Figure 2. Total ion chromatogram of components of gasoline in (a) standard (E0), (b) high-density gasoline (E0) fuels, and (c) high-density gasoline (E0) fuels with expanded y-axis at room temperature ($\times 10^6$) is plotted against retention times in min.	25
Figure 3. Effect of ethanol on headspace composition of (A) Standard, (B) High-density gasoline and (C) Medium-density gasoline samples at room temperature	27
Figure 4. Effect of ethanol on headspace composition of (A) Standard, (B) High-density gasoline and (C) Medium-density gasoline samples at 38 °C	28
Figure 5. Effect of ethanol on headspace composition of (A) Standard, (B) High-density gasoline and (C) Medium-density gasoline samples at 49 °C	30
Figure 6. Effect of ethanol on overall evaporative emission of all studied compounds (a) at room temperature, (b) at 38 °C, and (c) at 49 °C. The total GC-MS peak area ($\times 10^8$) is plotted against E0, E10 and E20 fuels.....	32
Figure 7. Effect of temperature on the headspace composition of (a) Standard, (b) High-density gasoline and (c) Medium-density gasoline E0 samples	33
Figure 8. Effect of temperature on the headspace composition of (a) Standard, (b) High-density gasoline and (c) Medium-density gasoline with E10 samples	35
Figure 9. Effect of temperature on the headspace composition of (a) Standard, (b) High-density gasoline and (c) Medium-density gasoline with E20 samples	36
Figure 10. Change of monoaromatics percentage composition with ethanol and temperature (a) medium-density gasoline and (b) high-density gasoline.....	37

Figure 11. Change of paraffins percentage composition (a) medium-density gasoline and (b) high-density gasoline, and i-paraffins composition (c) medium-density gasoline and (d) high-density gasoline with respect to ethanol and temperature	38
Figure 12. Change of mononaphthene percentage composition with ethanol and temperature (a) medium-density gasoline and (b) high-density gasoline	39
Figure 13. Cyclic structure of Iturin. ¹⁰⁰	47
Figure 14. Cyclic structure of Surfactin. ¹⁰⁰	48
Figure 15. Sample chromatogram showing components of extracted kerosene in control (TSB with kerosene but no bacteria) and in TSB with bacteria but no kerosene	55
Figure 16. Degradation of kerosene by <i>B. amyloliquifaciens</i> 1BA and 1D3 in TSB media	56
Figure 17. Degradation of kerosene by <i>B. amyloliquifaciens</i> 1BA and 1D3 in minimal media.....	56
Figure 18. Growth curve of <i>B. amyloliquifaciens</i> 1D3 and 1BA using CFU counts	57
Figure 19. Growth curve of <i>B. amyloliquifaciens</i> 1D3 and 1BA using OD600 measurements.....	58
Figure 20. Sample chromatogram of standard conc. of iturin A and surfactin (100 ppm), extracted lipopeptide from TSB culture broth containing <i>B. amyloliquifaciens</i> 1D3, and extracted TSB media with no bacteria in absence of kerosene after day 10.....	59
Figure 21. Chromatogram showing iturin A fractions (zoomed in version of Figure 20).	60
Figure 22. Chromatogram showing surfactin fractions (zoomed in version of Figure 20).	60

Figure 23. Chromatogram showing extracted minimal media with no bacteria, lipopeptides from the culture broth (minimal media) of <i>B. amyloliquefaciens</i> 1D3 and 1BA in absence of kerosene after day 10 and standard mixture of iturin A and surfactin (100ppm).....	61
Figure 24. Chromatogram showing extracted minimal media with no bacteria and extracted lipopeptides from the culture broth (minimal media) of <i>B. amyloliquefaciens</i> 1D3 and 1BA in presence of kerosene after day 10, and standard mixture of iturin A and surfactin (100 ppm).....	62
Figure 25. Chromatogram showing extracted lipopeptides from the culture broth (TSB media) of <i>B. amyloliquefaciens</i> 1D3 and 1BA in absence of kerosene after day 10 and standard conc. of surfactin at 1600 ppm	63
Figure 26. Chromatogram showing extracted TSB media with no bacteria and extracted lipopeptides from the culture broth (TSB media) of <i>B. amyloliquefaciens</i> 1D3 and 1BA in presence of kerosene after day 10, and standard conc. of surfactin at 600ppm.....	64
Figure 27. Jedi dry herb vaporizer (a) with mouthpiece (b), top hat cap, and (d) aluminum foil container	77
Figure 28. Experimental set up for vape extraction a) sample loading b) incubation c) extraction.....	78
Figure 29. Experimental set up for conventional headspace extraction a) vial and cap b) sample incubation c) sample extraction	79
Figure 30. Structure of horseradish components chosen for analysis.....	82
Figure 31. Chromatograms of extracted horseradish components at different temperature using both vape and headspace method. The abundance ($\times 10^5$) is plotted against	

retention times in min. 1. Allyl thiocyanate, 2. Allyl isothiocyanate, 3.	
Benzenepropanenitrile and 4. Phenethyl isothiocyanate	83
Figure 32. Chromatograms of extracted horseradish components at different temperature with expanded y-axis (a) vapo method and (b) headspace method	84
Figure 33. Horseradish samples (a) pre-extraction, (b) post-extraction at 150 °C, (c) post-extraction at 200 °C, and (d) post-extraction at 240 °C.....	86
Figure 34. Structure of cinnamon components chosen for analysis	87
Figure 35. Chromatograms of extracted cinnamon components at different temperature using both vapo and headspace method. The abundance ($\times 10^6$) is plotted against retention times in min. 1. E-cinnamaldehyde, 2. α -copaene, 3. α -muurolene and 4. δ -cadinene	88
Figure 37. Cinnamon samples (a) pre-extraction, (b) post-extraction at 150 °C, (c) post-extraction at 200 °C, and (d) post-extraction at 240 °C.....	91
Figure 38. Structure of gasoline spiked soil components chosen for analysis.....	92
Figure 39. Chromatograms of components of gasoline spiked soil at different temperature using both vapo and headspace method. The abundance ($\times 10^7$ (for vapo) and $\times 10^6$ (for headspace)) is plotted against retention times in min. 1. 2,2,3,3-tetramethylbutane, 2. Toluene, 3. p-Xylene, 4. Nonane, 5. Propylbenzene, 6. m-Ethylmethylbenzene, 7. p-Ethylmethylbenzene, 8. 1,2,3-trimethylbenzene, 9. o-Ethylmethylbenzene, 10. 1,2,4-trimethylbenzene, and 11. Undecane	93
Figure 40. Chromatograms of components of gasoline spiked soil at different temperature with expanded y-axis (a) vapo method and (b) headspace method.	93

ABSTRACT

ANALYSIS OF VOLATILE ORGANIC COMPOUNDS: PETROLEUM EMISSIONS AND
MICRBIAL DEGRADATION

A K M AHSAN AHMED

2021

Volatile organic compounds (VOCs) are abundant in nature and can occur in various forms in a wide variety of sources. Petroleum is one of the major sources of VOCs. Petroleum being the most widely used energy resources of the world, often released to the environment due to emission and leakage or accidental spillage during exploration, transportation and manufacturing. Once released to the environment, petroleum poses a serious threat to the environment due to some of its toxic organic components. Therefore, the analysis of petroleum is critical to understand its effect on the environment and remediation. This dissertation is focused on the analysis of VOCs from petroleum to understand their emission characteristics and microbial degradation.

In Chapter 2, the effect of ethanol on the evaporative emission characteristics of ethanol-blended medium and high-density gasoline was studied by measuring the vapor phase composition at different temperatures (room temperature, 38, and 49 °C) using headspace solid-phase microextraction (HS-SPME) coupled with gas chromatography-mass spectrometry (GC-MS). A standard mixture of gasoline was prepared based on the detailed hydrocarbon analysis of high-density gasoline by mixing 16 selected compounds and tested. Ethanol was added in different percentages to prepare E0, E10, and E20 (0, 10

and 20 v/v % ethanol) fuel samples. The results obtained from GC-MS were calculated in terms of percentage compositions of compounds separated into four groups (paraffins, *i*-paraffins, monoaromatics, and mononaphthene). The results showed the decrease of vapor phase composition of monoaromatics with the increasing ethanol percentages for most of the tested fuels at all tested temperatures. Similar results were also obtained in paraffin and *i*-paraffins except for *i*-paraffins in standard and high-density gasoline and paraffins in medium-density gasoline at room temperature. The percentage decrease is much higher from 0 % to 20 v/v % ethanol containing fuel.

In Chapter 3, we investigated the biodegradation ability of petroleum hydrocarbons from kerosene in tryptic soy broth (TSB) and minimal culture media by *Bacillus amyloliquefaciens*. Two isolates (1BA and 1D3) of *B. amyloliquefaciens* were grown in TSB and minimal media supplemented with 1% kerosene to understand if the isolates could co-metabolize (or metabolize in case of minimal media) the petroleum hydrocarbons from kerosene by utilizing them. The degradation was measured using GC-MS. The result showed the decrease of residual kerosene to below 50% after 4 and 6 days by 1BA and 1D3 respectively. However, beyond this period, the results for control showed more degradation compared to media containing isolates. Although the residual percentage kerosene was comparatively less, meaning more degradation by 1BA and 1D3 compared to control in minimal media, the difference was comparatively low to determine whether the degradation was due to bacterial isolates or not. Further studies were done in terms of iturin A and surfactin biosurfactant production using UHPLC with diode array detection to find out the degradation of petroleum hydrocarbons if a correlation between biosurfactant production and hydrocarbon utilization could be

established or not. The UHPLC results confirmed the production of surfactin by only 1D3, but no iturin A by any isolates. Based on the results, 1D3 produced surfactin both in the presence and absence of kerosene in TSB media. However, the concentration in absence of kerosene was much higher (more than double) than in presence of kerosene. Although no surfactin isoform peaks were produced by 1D3 in the presence of kerosene in minimal culture media, it gave some peaks, but very low in intensity in the absence of kerosene, hence concentration was seemed to be very low when compared to 100 ppm standard solution. Since UHPLC results did not find any correlation between surfactin production and kerosene utilization, based on the result, it is less likely that the studied bacteria isolates were utilizing the kerosene to grow and producing lipopeptide surfactants.

In Chapter 4, we developed an analytical technique using a commercial dry herb vaporizer (vape) to be used for sample heating and direct extraction of analyte compounds from the headspace of the vape using headspace solid-phase microextraction (HS-SPME) coupled with GC-MS. VOCs from three samples (horseradish, cinnamon, and gasoline spiked soil) were analyzed, and the results were compared with the traditional headspace method. Although comparable results were obtained in term of relative area percentage for both methods, the vape method was found to be more concentrated, since the abundance in the total ion chromatogram obtained for identified peaks were much higher than traditional headspace method.

1 CHAPTER 1. INTRODUCTION AND BACKGROUND

1.1 Overall significance

Volatile organic compounds (VOCs) are abundant in nature. They can occur in various forms and emit from various sources, from natural sources such as trees and plants to human sources such as power plants. The use and evaporation of petroleum and other industrial chemicals and burning of domestic wastes are some of the example sources of VOCs. Many hydrocarbon rich fluids such as gasoline and other industrial solvents like paint, varnish, various cleaning, and degreasing products are the significant contributors of VOCs in the atmosphere.^{1, 2} Petroleum hydrocarbons or other volatile organic compound contamination is a severe threat to the environment because of potentially toxic organic components. Contamination of petroleum hydrocarbons or other VOCs can occur in several ways. Petroleum hydrocarbons are the most widely used energy resource in the world, may get polluted due to leakage or accidental spillage from underground storage tanks or during exploration, transportation, and manufacturing. Gasoline, another source of VOCs, often releases to the environment through exhaust gases from gasoline powered vehicles due to the incomplete combustion of unburned hydrocarbons. The VOCs can also emit to air due to the evaporation of gasoline from fuel tanks or pipelines. Once released into the environment, they accumulate in the air, water, and soils, hence adversely affecting the environment and human health. Some VOCs such as BTEX compounds (benzene, toluene, ethylbenzene, and xylenes) are irritants. These compounds can contaminate the air, drinking, and agricultural water supply or persist in soil for a long time, causing adverse effect on both human health and the environment. The VOCs in air play an important part in forming ground-level ozone by reacting with

oxides of nitrogen (NO_x) from the atmosphere. Ground-level ozone is the main components of smog, which can irritate the eye, nose, and throat and can also reduce lung functions, aggravate asthma, and lead to a wide range of respiratory systems.^{3, 4}

Therefore, the analysis of VOCs from petroleum or other hydrocarbon sources is very important to understand their emission characteristics and degradation. Emission characteristics research is mainly focused on gasoline-based petroleum hydrocarbon sources. Gasoline is the widely used fuel in vehicles. Most gasoline fuel in the US is blended with ethanol to improve the octane rating. Since gasoline contains high-octane aromatics that can produce disproportionate amounts of carbon monoxide (CO), by replacing it with ethanol, CO and hydrocarbons' emissions can be reduced.⁵ So development of an analytical method is necessary to understand the emission level of VOCs from ethanol-blended gasoline, which will help develop measures needed to curb or control the emissions. Research on the degradation of petroleum hydrocarbons is also fundamental since petroleum hydrocarbon is contaminated through accidental spills (whether marine, ground, or underground oil spills) pose a serious threat to the environment and living organisms. There is a need to develop environmentally friendly methods to clean up the oil spills to remove the toxic VOCs from the contaminated site.

1.2 Project objectives

The objective of this work consists of:

- 1) To study the emission characteristics of ethanol-blended gasoline at different temperatures
- 2) To investigate the microbial degradation of hydrocarbons in kerosene in culture media by *Bacillus amyloliquefaciens*

3) To analyze the production of lipopeptide biosurfactants in order to find the correlation between lipopeptide production and kerosene utilizations by *Bacillus amyloliquefaciens*

4) Development of an analytical technique using a commercial dry herb vaporizer (vape) as a headspace sampling device to analyze the volatile organic compounds extracted from the headspace of the vaporizer.

Chapter 2 describes the study of emission characteristics of ethanol blended gasoline by analyzing their headspace vapor composition at different temperatures using headspace solid-phase microextraction gas chromatography- mass spectrometry (HS-SPME-GC-MS). Chapter 3 explains the investigation of microbial degradation of hydrocarbons present in kerosene in bacterial culture media by *B. amyloliquefaciens* using a GC-MS method. This chapter also addresses the correlation between lipopeptide biosurfactant production and kerosene utilization by *B. amyloliquefaciens* by analyzing the lipopeptide biosurfactants production in bacterial culture media using UHPLC with diode array detection. Chapter 4 describes the development of analytical technique using vape as a headspace sampling vial plus heating medium to substitute traditional in-house heating arrangements to analyze various food and environmental compounds directly from the headspace of the vape using HS-SPME-GC-MS.

1.3 Volatile organic compounds (VOCs)

Volatile organic compounds are carbon-containing compounds excluding elemental carbon, carbon monoxide, and carbon dioxide, that have a very higher vapor pressure at room temperature.⁶ The higher vapor pressure is due to their low boiling points, which causes the evaporation of a large number of molecules to the surrounding

air. The VOCs are a wide range of compounds, and WHO classified these compounds into four categories: very volatile organic compounds (VVOC) (boiling point range from $< 0\text{ }^{\circ}\text{C}$ to $50\text{-}100\text{ }^{\circ}\text{C}$), volatile organic compounds (VOCs) (boiling point range from $50\text{-}100\text{ }^{\circ}\text{C}$ to $240\text{-}260\text{ }^{\circ}\text{C}$), semi-volatile organic compounds (SVOCs) (boiling point range from $240\text{-}260\text{ }^{\circ}\text{C}$ to $380\text{-}400\text{ }^{\circ}\text{C}$), and organic compounds associated with particulate matter (POM) (boiling point range $> 380\text{ }^{\circ}\text{C}$).⁷ Although there are several types, this study mainly deals with the VOCs.

1.4 Sources of VOCs

VOCs are ubiquitous in our daily life. They evaporate at ambient temperatures, and therefore produce gases from solids and liquids. The sources of VOCs are mainly natural and anthropogenic. The origin of natural VOCs are comprised of terrestrial and ocean biogenic reactions, while anthropogenic VOCs are originated from man-made sources, primarily from the evaporation of organic solvents and burning of fossil fuel.⁸ Some of the sources of VOCs include commercial, household, and industrial products such as gasoline, kerosene, diesel, paint, varnishes, caulks, adhesives, carpet, vinyl flooring, rubber, plastics etc. VOCs are also available in home and personal care products (air fresheners, perfumes, cleaning products, cosmetics, pharmaceuticals). It is also used in dry cleaning, refrigeration, burning woods, cooking, etc. Fruits and vegetables are also a source of VOCs. Plants of some vegetables and fruits usually have some type of base level scent, designated as “standard level of volatile” and compounds like monoterpenes, sesquiterpenes and other aromatic compounds can present in specific gland or storage site of plants, which are later released, and can be found in fruits and vegetables as aroma and flavoring ingredients.⁹ Although there are many VOCs sources, the current study deals

with and analyzes the VOCs found in petroleum sources such as gasoline, kerosene and some food sources such as cinnamon and horseradish.

1.5 Petroleum hydrocarbons

Petroleum fuel contains a wide variety of VOCs and it is one of the primary sources of VOCs in the environment. The group of compounds comprised of petroleum oil and products refined from oil such as gasoline and diesel are known as petroleum hydrocarbons (PH). It is a complex mixture of several hundreds of chemicals, consist mainly of hydrogen and carbon, and some other impurities such as oxygen, sulfur, and nitrogen. Some common petroleum hydrocarbons chemicals include benzene, toluene, xylene, ethylbenzene, naphthalene, fluorine, as well as constituents of gasoline, jet fuels, diesel, kerosene, mineral oil, and other petroleum products.

Petroleum hydrocarbons can be of different types and combinations, from petroleum products (such as gasoline) used in cars or other type of internal combustion engines to natural gas used for cooking and heating. The various types of petroleum hydrocarbons can be classified into three major groups: alkanes, alkenes, and aromatics. Alkanes, which are also known as saturated hydrocarbons, are the major constituents of petroleum products. Alkanes include linear or branch alkanes (paraffins) and cycloalkanes (cycloparaffins). The second major group of hydrocarbons is the alkenes, also known as unsaturated hydrocarbons, which are usually not found in crude oil, rather these compounds are the by-products of several refining process.¹⁰ The third basic type of hydrocarbons in petroleum products includes aromatics. Aromatics can be of different types: some containing one benzene ring such as benzene, toluene, xylene, and

ethylbenzene, and some containing more than one benzene ring such as naphthalene and benzo (a) pyrene.

1.6 Gasoline

Gasoline is a mixture of volatile and flammable liquid. It is derived from petroleum or crude oil and used as fuel in motor vehicles or other internal combustion engines. The boiling point of gasoline falls between -1°C (30°F) and 216°C (421°F) (Table 1).¹¹ It is a mixture of hydrocarbons containing several hundred isomers in it (Table 2).¹¹ The hydrocarbon constituents in the above boiling ranges can have 4-12 carbons atoms in their molecular structure and can be categorized into paraffins (including the cycloparaffins and branched materials), olefins, and aromatics.¹¹

Table 1. General Summary of Product Type and Distillation Range.¹¹

Product	Lower Carbon Limit	Upper Carbon Limit	Lower Boiling Point $^{\circ}\text{C}$	Upper Boiling Point $^{\circ}\text{C}$	Lower Boiling Point $^{\circ}\text{F}$	Upper Boiling Point $^{\circ}\text{F}$
Refinery Gas	C1	C4	-161	-1	-259	31
Liquefied petroleum gas	C3	C4	-42	-1	-44	31
Naphtha	C5	C17	36	302	97	575
Gasoline	C4	C12	-1	216	31	421
Kerosene/diesel fuel	C8	C18	126	258	302	575
Aviation turbine fuel	C8	C16	126	287	302	548
Fuel oil	C12	>C20	216	421	>343	>649
Lubricating oil	>C20		>343		>649	
Was	C17	>C20	302	>343	575	>649
Asphalt	>C20		>343		>649	
Coke	>C50 *		>1000*		>1832*	

*Carbon number and boiling point difficult to assess; inserted for illustrative purposes only

Table 2. Increase in the number of isomers with carbon numbers.¹¹

Carbon Atoms	Number of Isomers
1	1
2	1
3	1
4	2
5	3
6	5
7	9
8	18
9	35
10	75
15	4347
20	366319
25	36,797,588
30	4,111,846,763
40	62,491,178,805,831

1.6.1 Composition of gasoline

Gasoline is a petroleum product that consist of a mixture of hydrocarbons, additives, and blending agents. Gasoline composition may vary based on the type of crude oil used, the process used to refine it, product specifications, and demand. Gasoline is the refined product of crude oil. Gasoline is the refined product of crude oil. Crude oil after pumped out of the ground, sent to the refinery, where the conversion of crude oil to gasoline and other value-added products (jet fuel, kerosene, diesel, lubricating oil, paraffin wax etc.) occurs after undergoing several processes such distillation, conversion (catalytic cracking, hydrocracking, isomerization, reforming, and alkylation) and blending. The composition of gasoline varies widely, depending on the crude oil used, refinery processes, product demand, and product specifications. However, gasoline typically includes saturated hydrocarbons or alkanes, unsaturated hydrocarbons or olefins, naphthene or cyclic hydrocarbons, aromatics, oxygenates, and other hetero-atom compounds.⁵ So gasoline may contain several hundreds of hydrocarbons, of which the

most major hydrocarbons of a typical gasoline mixture can be classified into six major groups (Table 3).

Table 3. Average composition of gasoline.⁵

Groups	% composition	Hydrocarbons
n-paraffins	15	n-pentane
		n-hexane
		n-heptane
		n-octane
		n-decane
		n-dodecane
		n-tetradecan
iso-paraffins	30	2-methylpropane
		2-methylbutane
		2-methylpentane
		3-methylpentane
		2-methylhexane
		3-methylhexane
		2,2-dimethylpentane
		2,2,3-trimethylbutane
		2,2,4-trimethylpentane
cycloparaffins	12	Cyclopentane
		Methylcyclopentane
		Cyclohexane
		Methylcyclohexane
aromatics	35	Benzene
		Toluene
		ethyl benzene
		meta-xylene
		para-xylene
		ortho-xylene
		1,3,5-trimethylbenzene
		1,2,4-trimethylbenzene
olefins	8	2-pentene
		2-methylbutene-2
		2-methylpentene-2
		cyclopentene
		1-methylcyclopentene
		1,3 cyclopentadiene
		dicyclopentadiene
oxygenates		methanol
		ethanol
		iso-propyl alcohol

1.7 Kerosene

Kerosene, a flammable liquid mixture of chemicals, is produced from the distillation of crude oil. It is produced in a distillation tower in a similar process as gasoline or diesel.¹² It is a middle distillate, so comparatively less volatile than gasoline. Kerosene is the major component of aviation oil and is also used as heating oil and as a cleaning agent.¹²

1.7.1 Composition of kerosene

Kerosene is a complex mixture of hydrocarbons containing 10- 16 carbon atoms per molecule with an average of 12 carbon atoms per molecule. Typically kerosene is a mixture of three major classes of hydrocarbons: alkanes or paraffins (35%), cyclic alkanes or naphthenes (60%), and aromatics (15%).¹³

1.8 Analytical techniques used for petroleum hydrocarbons and other VOCs analysis

Several techniques have been developed to analyze petroleum hydrocarbons and other volatile organic compounds (VOCs) from various fields of interest. These include separation techniques such as gas chromatography with flame ionization detection (GC-FID), mass spectrometric detection (GC-MS) or electron capture detection, spectroscopic techniques such as atomic emission spectroscopy, ultraviolet (UV), infrared (IR), fluorescence, Raman spectroscopy, and other techniques such as gravimetry and immunoassay (IMA).¹⁴⁻²⁰ Among these, gas chromatography coupled with different detectors is the most commonly used technique for analyzing petroleum hydrocarbons and other VOCs.²¹ However, GC-MS has become the most preferred method due to its high potential ability to confirm compounds.²² MSD, when combined with GC, has the ability to detect compounds in very low concentrations and provide compound specific

information, which is very helpful in determining aromatic hydrocarbon compounds such as alkylbenzenes.^{14, 23}

2 CHAPTER 2. EVAPORATIVE EMISSION FROM ETHANOL-BLENDED GASOLINE

2.1 Introduction

Increasing air pollution is one of the most important problems of developed countries today, and there is no denying that vehicles play a major part in contributing air pollution. Vehicles are powered by gasoline, which is a mixture of a wide range of hydrocarbons. When vehicles burn gasoline, emit noxious chemicals like carbon dioxide, nitrogen oxides, carbon monoxide, or various unburnt hydrocarbons through their tailpipe. Besides the tailpipe emissions, vehicles produce another type of emissions that can also contribute to air pollution. These are known as evaporative emissions, which are involved the release of volatile organic compounds (VOCs) in the air resulting from the evaporation of gasoline from fuel tanks or pipelines. Evaporative emissions constitute a significant source of ambient VOCs in the air,²⁴⁻²⁶ which are important ozone and PM_{2.5} precursors.²⁷⁻²⁹ Tailpipe emissions are now well controlled with the development of new technologies and advanced after treatments. However, the evaporative emissions, which also contribute a fair share of hydrocarbons emission in the air need more attention.

Ethanol has been added to gasoline as an oxygenate for decades. Ethanol has higher octane number (both research octane number (RON) and motor octane number (MON)) than the US regular-grade gasoline.^{30, 31} So the addition of ethanol will be expected to increase the overall octane number of gasoline.^{30, 31} A higher octane number means higher resistance to knocking during combustion, resulting in improved engine

efficiency. In addition to improving octane rating, ethanol also increases the fuel's oxygen content, hence improving the combustion process and lowering the emission of CO. The addition of ethanol in gasoline also changes the vapor pressure of gasoline. Although the Reid Vapor Pressure or RVP (vapor pressure measured at 100 °F or 37.8 °C in a chamber at a vapor to liquid ratio of 4:1) of gasoline is much higher than the RVP of pure ethanol,^{32, 33} but when mixed together, the overall RVP of the mixture increases.^{32, 34} As a result, components of ethanol blended gasoline vaporize more easily than the components of base gasoline.

Since ethanol is the most widely used oxygenate in the US, and nearly all gasoline in the US consists of some percentage of ethanol, it has instigated a surge of research to investigate the emission characteristics of ethanol-blended gasoline. Several studies have been conducted to understand the emission characteristics of ethanol-blended gasoline,³⁵⁻⁴⁵ of which most of the researches were focused on the tailpipe emission. However, there is not enough research done on evaporative emission of VOCs from the gasoline fuel. So, there is a need to investigate the evaporative emission of ethanol-blended gasoline, to understand how much VOCs escape to the environment due to evaporation from the gasoline-powered vehicles.

To understand how much gasoline vaporizes upon the addition of ethanol, a method is needed to quantify the component concentration of gasoline in the vapor phase. GC-MS has been an established technique for the analysis of volatile and semivolatile compounds in crude oil.⁴⁶ Headspace (HS) and solid-phase microextraction (SPME) is also considered convenient methods for the analysis of VOCs.^{47, 48} HS-SPME provides high sensitivity and selectivity because of its extremely low blank in VOCs analysis.⁴⁸

When combined, HS-SPME-GC-MS can become a powerful technique in analysis of VOCs.

The objective of this work was to study the evaporative emission of ethanol-blended gasoline. This was accomplished by analyzing the component concentrations of gasoline in the vapor phase with different ethanol percentages at different temperatures using HS-SPME-GC-MS.

2.2 Background

2.2.1 Gasoline emission

The internal combustion engine drives a motor vehicle by transforming gasoline's chemical energy into mechanical energy by combustion of hydrocarbons. This process produces exhaust gases, which emits through the tailpipe. These are known as exhaust or tailpipe emissions. These exhaust emissions comprise of combustion product water and carbon dioxides, as well as combustion byproducts such as oxides of nitrogen (NO_x), carbon monoxide (CO), volatile organic compounds (VOCs), and particulate matter (PM). NO_x is formed at high temperatures in the combustion chambers from the reaction of ambient nitrogen and oxygen, while CO, VOCs, and particulate matter are the product of incomplete combustion of unburned hydrocarbons. In addition to tailpipe emissions, there is another type of emission, known as evaporative emission. Gasoline in fuel tank or pipeline slowly evaporates overtime, and releases VOCs into the air. Unlike exhaust emissions, evaporative emissions can happen all the time. Car makers are developing new technologies and advanced after treatments to control tailpipe emission. However, much attention needs to be paid to control evaporative emissions, which contributes substantial amounts of hydrocarbons emission to the environment.

2.2.2 Environmental effect of gasoline emissions

The main effects associated with exposure to fine PM (referred to as PM_{2.5}) are premature mortality, aggravation of cardiovascular disease, aggravated asthma, acute respiratory symptoms, and chronic bronchitis.⁴² Nearly 200,000 premature deaths per year in the U.S. are attributed to PM_{2.5} emissions,⁴³ and the World Health Organization (WHO) estimates 3 million worldwide annual deaths caused by particulate pollution.⁴⁴ In 2012, the EPA lowered the primary annual fine particulate standard from 15 $\mu\text{g}/\text{m}^3$ to 12 $\mu\text{g}/\text{m}^3$ in an effort to combat these health effects.

Surface ozone is produced by the reaction of VOCs and nitrogen oxides (NO_x) under the influence of sunlight.⁴⁹ Ozone is the main component of smog, which can reduce lung function, aggravate asthma, and lead to a wide range of respiratory symptoms.^{3, 4}

Gasoline is a toxic and highly flammable liquid. It is comprised of hundreds of hydrocarbons, many of which are highly volatile. Some of these hydrocarbons are also very hazardous and toxic, such as BTEX compounds (benzene, toluene, ethylbenzene, and xylene). Benzene is a known carcinogen and is linked to the development of leukemia and lymphoma.⁵⁰ Air pollution is one of the major problems of modern world, and the contribution of volatile organic compounds (VOCs) present in gasoline in the chemistry of air pollution is very significant at the local, regional, and global level. There are many ways in which these VOCs are released to the environment and cause air pollution. However, the main anthropogenic sources of VOCs in the urban area are originated from automobiles.⁵¹ The most common and discussed pathway for air pollution caused by automobiles is through tailpipe, where it produces many harmful

substances such as carbon dioxide, carbon monoxide, nitrogen oxides, particulate matter, and unburned hydrocarbons when gasoline is burned. There is another type of emission, known as evaporative emission, which is not discussed as prominently as tailpipe emission, and sometimes underestimated, contributes substantial amount of hydrocarbons emission to the environment. Like tailpipe emissions, evaporative emission also constitutes a major source of ambient VOCs in the air,²⁴⁻²⁶ which are important ozone and PM_{2.5} precursors.²⁷⁻²⁹ Exposure to ozone has been associated with decrease in lung function,^{52, 53} aggravation of asthma or chronic airways,⁵⁴ and acute respiratory symptoms.⁵⁵

2.2.3 Oxygenates in gasoline

Oxygenates are oxygen-containing compounds and are one of the most important used additives in gasoline. Some commonly used oxygenates are methanol, ethanol, tertiary butyl alcohol, MTBE (methyl tertiary butyl ether), etc. Oxygenates are antiknock agents, which can prevent or reduce knocking during auto-ignition by increasing the octane value (measure of fuels resistance to engine knocking) of fuel. Higher octane value means the fuel has more resistance to pre-ignition at high temperature and pressure. So, oxygenates or antiknock agents help the cars to ignite at the correct time, thus reducing pre-detonation and saving the car engine. Oxygenates can also replace the high-octane aromatics in gasoline. As the burning of aromatics during combustion can produce disproportionate amounts of CO and hydrocarbons emissions, the use of oxygenates in fuel can reduce CO and hydrocarbons emissions.⁵

2.2.4 History of oxygenates and its uses in gasoline

The use of oxygenates dates back to 1979 when methyl tert-butyl ether (MTBE) was added to gasoline.⁵⁶ Before the use of MTBE, tetraethyl lead (TEL) was used widely in gasoline to increase the octane rating. Due to poisonous characteristics possessed by TEL, the use of leaded gasoline was banned in the United States for all on-road vehicles as of January 1, 1996.⁵⁷

As part of The Clean Air Act Amendments (CAA) of 1990, Oxygenated Fuels Program and the Reformulated Gasoline (RFG) Program was established to reduce carbon monoxide (CO) and ground-level ozone in most polluted city of the United States, which requires the presence of oxygen to be at least 2.7 % by weight for oxygenated fuel and 2.0 percent by weight for reformulated gasoline.⁵⁸ The oxygenate requirement made ethanol and MTBE the most widely used oxygenates in gasoline, and the requirement can be met by adding either 11 % MTBE or 5.7 % ethanol by volume.⁵⁶ Due to its cheap production cost and good blending properties, MTBE was the most preferred oxygenates.⁵⁹ However, MTBE is highly soluble in water and can spread rapidly in groundwater and thus contaminate drinking water. The use of MTBE in the United States has declined due to its environmental and health concern, and in order to help refineries in phasing out MTBE uses, the Energy Policy Act in 2005 removed the oxygenates requirement in RFG. Currently, many states in USA have passed legislation to ban or restrict the use of MTBE in gasoline.⁶⁰ As MTBE use has been phasing out, ethanol has become a strong candidate for replacing MTBE.

2.2.5 Use of ethanol as oxygenates

Ethanol has been added as oxygenates in gasoline for decades. Ethanol is a biomass fuel, biodegradable, and has low toxicity.^{61, 62} Ethanol also has good anti-knock characteristics.⁶³ Ethanol, when substituted with MTBE, can reduce water contamination and possess no significant adverse impacts on public health and environment.⁵⁶

2.2.6 Emission characteristics of ethanol-blended gasoline-literature review

Ethanol is one of the most widely used oxygenates in gasoline. The presence of ethanol in gasoline not only increases the octane value of fuel, but also affects its emission characteristics. Research shows the consequence of ethanol blended gasoline on emission of greenhouse gases, particulates, and other toxic pollutants.

Fred et al. studied the tailpipe emissions and evaporative emissions of pre-1985 passenger motor vehicles and found that ethanol-blended gasoline (8.8% ethanol by volume) produces lower tailpipe emissions of total hydrocarbons (THC) and carbon monoxide (CO) compared to regular base fuel (0% ethanol by volume), but they got mixed results for evaporative emissions, diurnal evaporative emissions were less from the oxygenated fuel, while hot-soak evaporative emissions were greater from the oxygenated fuel (for all vehicles except MU098).³⁵

Kenneth et al. studied the effect of ethanol fuel on the emissions of vehicles over a wide range of temperatures (75, 0, and -20 °F), and found a reduction in THC and CO emission for most vehicles with the use of E10 fuel (gasoline containing 10 % ethanol by volume), while the NOx emission increases at -20 °F, however, at other temperatures the NOx emissions decreases with E10 fuel.³⁶

Ching-Huei et al. studied the exhaust emissions of two-stroke motorcycles, and found that ethanol-blended gasoline produces lower THC, CO, and NO_x emissions than emissions from ethanol-free gasoline.³⁷

Shing et al. studied the applicability of gasoline containing ethanol as Thailand's alternative fuel to curb toxic VOC pollutants from automobile emission and found that the emission rates of BTEX compounds (benzene, toluene, m-xylene) of ethanol-blended gasoline reduced with E10 and E15 fuel.³⁸

Poulopoulos and Philippopoulos investigated the effect of adding oxygenated compounds to gasoline on automotive exhaust emissions and found that the addition of ethanol decreased benzene emission (4-50%).³⁹

He et al. studied the emission characteristics of an EFI engine with ethanol-blended gasoline fuels, and found the decrease of the engine-out total hydrocarbon emissions (THC) at operating conditions and engine-out THC, CO, and NO_x emissions at idle speed with E30.⁴⁰

Suarez-Bertoa et al. studied the impact of ethanol containing gasoline blends on emissions from a flex-fuel vehicle tested over the Worldwide Harmonized Light Duty Test Cycle (WLTC), and concluded that carbon monoxide, methane, carbonyls and ethanol emission increase for E85 and E75 blends, compared to E5, E10 and E15 blends.⁴¹

Li et al. investigated the exhaust and evaporative emissions from motorcycles fueled with ethanol gasoline blends. They found that for 10% ethanol blend (E10), the emission factor THC and CO decreased while the emission factor of NO_x increased. Their results also showed that the exhaust emissions of VOCs (benzene, toluene, styrene,

and xylene) decreased for E10. Their evaporative emission results showed not so much difference in evaporative THC, while the evaporative emissions of BTEX (benzene, toluene, ethylbenzene, and xylene) showed a slight growth for E10.⁴²

Yüksel and Yüksel studied the use of ethanol–gasoline blend as a fuel in an SI engine and concluded 80% and 50% reduction of CO and HC emissions respectively, while 20% increase of CO₂ emission.⁴³

Najafi et al. investigate the performance and exhaust emissions of a gasoline engine with ethanol blended gasoline fuels using artificial neural network and found that ethanol blended gasoline decreased CO and HC emissions while increased CO₂ and NO_x emissions.⁴⁴

Koç et al. investigated the effects of ethanol-unleaded gasoline blends (E50 and E85) on engine performance and exhaust emissions in a spark-ignition engine. Their results showed that the addition of ethanol to unleaded gasoline reduced carbon monoxide (CO), nitrogen oxides (NO_x), and hydrocarbon (HC) emissions.⁴⁵

2.3 Experimental

2.3.1 Gasoline sample fuels

Two gasoline sample fuels were used: medium-density and high-density gasoline fuel. These fuels were supplied by ICM, Inc. These fuels were base fuels for neat or E0 (gasoline containing 0 % ethanol by volume), E10 (gasoline containing 10 % ethanol by volume), and E20 (gasoline containing 20 % ethanol by volume)

2.3.2 Standard sample

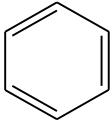
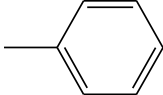
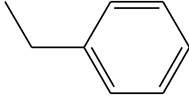
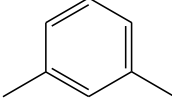
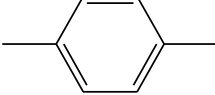
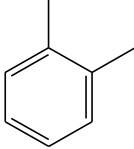
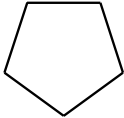
A standard mixture of gasoline fuel was prepared according to the volume percentage (v/v %) given in Table 5. The volume percentage of the mixture in the table

were based on detailed hydrocarbon analysis of high-density fuel results provided by ICM, Inc and the standards in the following table covers over 50% of the fuel. This standard mixture will also be a standard test fuel for neat or E0, E10, and E20. The compounds analyzed in this study were also classified into four groups based on their chemical structures: paraffins, *i*-paraffins, monoaromatics and mononaphthenes (also known as cycloparaffins). The structure of the compounds is also shown in Table 5.

Table 4. Chemicals used in this work with their purity and the name of manufacturer.

Substance	Purity	Manufacturer
n-butane	99%	SPEX CertiPrep
2-methyl butane	99.5%	Sigma Aldrich
Cyclopentane	95%	SPEX CertiPrep
2-methyl pentane	99%	SPEX CertiPrep
3-methyl pentane	99%	SPEX CertiPrep
n-hexane	95% Optima	Fisher Chemical
Benzene	99.9%	Alfa Aesar
2-methyl hexane	99%	Acros Organics
3-methyl hexane	95%	SPEX CertiPrep
2,2,4-trimethyl pentane	99%	Acros Organics
2,3,4-trimethyl pentane	98%	Alfa Aesar
Toluene	Certified ACS	Fisher Scientific
Ethyl benzene	99.8%	SPEX CertiPrep
<i>m</i> -xylene	99%	SPEX CertiPrep
<i>p</i> -xylene	99%	SPEX CertiPrep
<i>o</i> -xylene	98%	SPEX CertiPrep
Ethanol	Absolute (200 Proof)	Fisher Scientific

Table 5. Mass and Volume % of prepared standard solution

Groups	Compound name	Structures	Vol %
Paraffins	n-butane	$\text{CH}_3\text{CH}_2\text{CH}_2\text{CH}_3$	8.41
	n-hexane	$\text{CH}_3(\text{CH}_2)_4\text{CH}_3$	8.46
<i>i</i> - paraffins	2-methylpentane	$\text{CH}_3\text{CH}(\text{CH}_3)(\text{CH}_2)_2\text{CH}_3$	3.60
	3-methylpentane	$\text{CH}_3\text{CH}_2\text{CH}(\text{CH}_3)\text{CH}_2\text{CH}_3$	4.03
	2-methylhexane	$\text{CH}_3\text{CH}(\text{CH}_3)(\text{CH}_2)_3\text{CH}_3$	4.28
	3-methylhexane	$\text{CH}_3\text{CH}_2\text{CH}(\text{CH}_3)(\text{CH}_2)_2\text{CH}_3$	2.24
	2,2,4-trimethylpentane	$(\text{CH}_3)_2\text{CHCH}_2\text{C}(\text{CH}_3)_3$	11.74
	2,3,4-trimethylpentane	$(\text{CH}_3)_2\text{CHCH}(\text{CH}_3)\text{CH}(\text{CH}_3)_2$	1.96
	2-methylbutane	$(\text{CH}_3)_2\text{CHCH}_2\text{CH}_3$	10.22
Monoaromatics	Benzene		0.68
	Toluene		16.47
	Ethylbenzene		1.99
	m- xylene		4.99
	p-xylene		2.52
	o-Xylene		1.94
Mononaphthene	Cyclopentane		16.47

2.3.3 Evaporative emission testing method

The purpose of the study was to analyze the headspace composition of evaporative emission of ethanol-blended gasoline, and how that composition changes with the addition of ethanol into gasoline at different temperatures. This was done by quantifying the component concentration in the headspace at increasing temperature. Three temperatures were chosen: room temperature (RT), 38°C, and 49°C and the headspace component concentration was determined using headspace SPME-GC-MS

2.3.4 Sample preparation

E0, E10 and E20 were prepared from the medium and high-density gasoline base fuels by adding 0%, 10% and 20% (v/v) ethanol in it. Then 1 mL of these samples were added to 20 mL screw top headspace vials. The vials were then placed into an auto-sampler for headspace SPME-GC-MS analysis

2.3.5 Headspace SPME-GC-MS analysis of ethanol blended gasoline

Headspace composition of ethanol-blended gasoline was analyzed using an Agilent 7890B gas chromatograph (Agilent Technologies, Little Falls, DE) coupled to an Agilent Technologies 5977B mass spectrometer and fitted with a 30-m x 0.25-mm, 0.25- μm DB-5MS column (Agilent Technologies, Little Falls, DE). The SPME extractor and the fiber used in this experiment was purchased from Supelco (Bellefonte, PA, USA). Three SPME fibers were tested: carboxen/polydimethylsiloxane (CAR/PDMS) (StableflexTM/SS, thickness: 85 μm), divinylbenzene/carboxen/polydimethylsiloxane (DVB/CAR/PDMS) (StableflexTM/SS, thickness: 50/30 μm), and polydimethylsiloxane/divinylbenzene (PDMS/DVB) (StableflexTM/SS, thickness: 65 μm), and four extraction time were tested: 10, 20, 30, and 40 min for optimization of fibers and

extraction time. The silica fibers were coated with an 65 μ m film of polydimethylsiloxane/divinylbenzene (PDMS/DVB). Before the extraction, the sample was incubated at three different temperatures: room temperature, 38 $^{\circ}$ C and 49 $^{\circ}$ C for 5 minutes. Each fiber was conditioned for 30 minutes before the extraction, and followed by a 20 minutes post extraction conditioned, at the manufactured recommended maximum operation temperatures. The liquid sample phase was under constant agitation at 250 rpm during the incubation and extraction. The extracted sample was desorbed in the injection port of the GC with a temperature of 250 $^{\circ}$ C for 5 min. The GC method begins with an initial oven temperature of 35 $^{\circ}$ C for 1 min, then ramped at 10 $^{\circ}$ C/minute to 220 $^{\circ}$ C and held for 1 min, followed by a final ramp at 50 $^{\circ}$ C/minute to 250 $^{\circ}$ C and held for 5 min for a total run time of 26.10 min. The hydrogen carrier flow was kept constant at 1.2 ml/min. Split injection (50:1) was performed with a PAL RSI 120 automatic sampler with an injection port at 250 $^{\circ}$ C. The mass spectrometer was operated in electron ionization mode (with 70 eV ionizing voltage). The transfer line temperature was kept at 250 $^{\circ}$ C. The MS temperatures were ion source 250 $^{\circ}$ C and quadrupole 150 $^{\circ}$ C. The scan range was 30-400 U (3.9 scans/s)

2.3.6 Determination of headspace composition of gasoline and ethanol-blended gasoline

Headspace composition of ethanol and ethanol-blended gasoline was determined by calculating the percentage composition of each compounds listed in Table 4. The % composition of the gasoline and ethanol-blended gasoline was approximated by comparing the relative peak areas obtained from HS-SPME-GC-MS analysis. To obtain the percentage composition, all the peak area of identified compounds were added, and

then to calculate the percentage of any compounds (listed in table 4), the individual area of a particular compounds was divided by total area, and multiplied the result by 100. All the samples were run in triplicate, with the percentage composition results presented according to the group classified in Table 5. In terms of environmental perspective, the monoaromatics and mononaphthenes are the group of compounds that are regulated by EPA. In addition to these compounds, the effect of ethanol on the headspace composition of total paraffins and *i*-paraffins were also studied.

2.4 Results and Discussion

2.4.1 Optimization of SPME fiber and extraction time

The selection of the appropriate SPME fiber for any analysis is very important as the amount of analyte extracted depends on the physiochemical properties of respective fiber coating (stationary phases of the fiber).⁶⁴ Extraction time is also an important parameter, which tells the minimum time required to reach equilibrium and maximum extraction of analyte. Three different fibers: CAR/PDMS, DVB/CAR/PDMS, and PDMS/DVB were tested to extract the components of standard gasoline mixture. According to the results shown in figure 1a, the most effective fiber was PDMS-CAR and the least effective fiber was PDMS, as extracted peak area in the case of PDMS-CAR was almost three times higher than the peak area extracted using PDMS fiber. The PDMS-CAR-DVB fiber was also very effective compared to PDMS, but its performance fell short compared to PDMS-CAR in terms of peak area response. Since PDMS-CAR gave the maximum peak area response compared to the other two fibers, it was chosen as the most suitable fiber for the extraction of studied compounds

After the fiber was optimized, the extraction time was also optimized, and based on the results shown in figure 1b, the optimum extraction time for extraction of studied compounds was 30 min, since at 30 min maximum peak area response were achieved, and also 30 min was sufficient to obtain a good response.

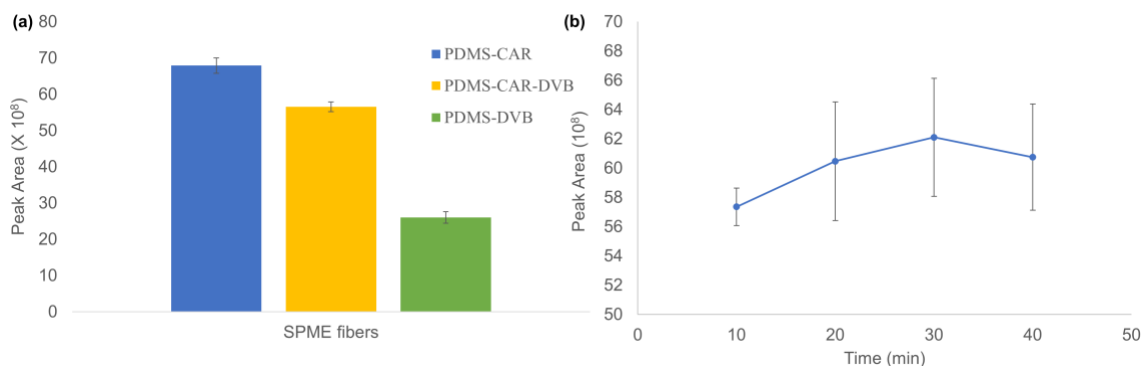


Figure 1. Optimization of SPME fiber and extraction time: a) effect of fiber stationary phase and b) effect of extraction time using PDMS-CAR

2.4.2 Headspace SPME-GC-MS analysis of ethanol-blended gasoline

The evaporative emissions of standard and gasoline (high and medium dense) samples (neat (EO) and blended (E10 and E20)) were analyzed by determining their headspace percent composition at room temperature (RT), 38°C, and 49°C using the HS-SPME-GC-MS method described above.

The sample chromatogram of one standard E0 fuel and one high-density gasoline E0 gasoline are showed in Figure 2. The retention times for standard solution were recorded at 1.179 (2-methyl butane), 1.424 (cyclopentane), 1.568 (n-hexane), 1.976 (benzene), 2.015 (2-methyl hexane), 2.220 (2,2,4-trimethyl pentane), 2.896 (2,3,4-trimethyl pentane) and 3.139 min (toluene) and for high density gasoline were recorded at 1.091 (n-butane), 1.178 (2-methyl butane), 1.423 (cyclopentane), 1.489 (3-methyl pentane), 1.566 (n-hexane), 1.975 (benzene), 2.011(2-methyl hexane), 2.090 (3-methyl

hexane), 2.214 (2,2,4-trimethyl pentane), 2.894 (2,3,4-trimethyl pentane), 3.136 (toluene), 4.499 (ethyl benzene), 4.656 (m-xylene), 4.677 (p-xylene) and 5.009 min (o-xylene).

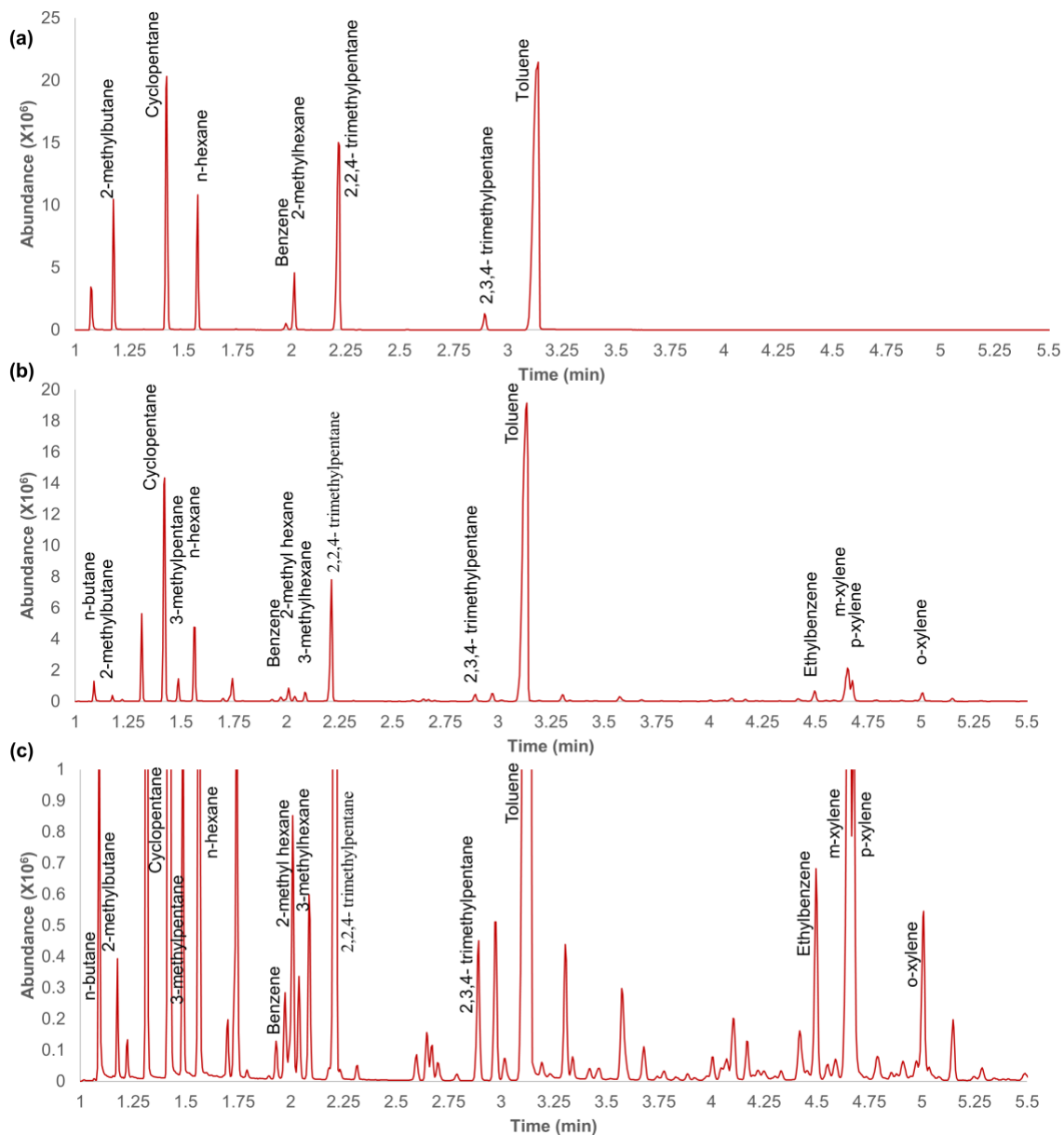


Figure 2. Total ion chromatogram of components of gasoline in (a) standard (E0), (b) high-density gasoline (E0) fuels, and (c) high-density gasoline (E0) fuels with expanded y-axis at room temperature (X 10⁶) is plotted against retention times in min.

Similar chromatogram was obtained in case of medium-density gasoline samples. So, out of 16 studied compounds, 8 were detected and identified for standard solution (butane, 2-methyl pentane, 3-methyl pentane, 3-methyl hexane, ethylbenzene, and xylenes could not be detected), while 15 were detected and identified for medium and high-density gasoline samples (2-methyl pentane could not be detected). The identification of the compounds was done by comparing with the retention times of standard solution and using the database of National Institute Standard and Technology (NIST).

2.4.3 Effect of headspace composition of gasoline with ethanol addition

In order to understand the effect of ethanol addition on the headspace composition, three different samples (standard, high and medium density gasoline) were tested at room temperature, 38 °C, and 49 °C. The outcome is explained below.

2.4.3.1 Effect at room temperature

The influence of ethanol addition on the headspace composition of paraffins, *i*-paraffins, monoaromatics, and mononaphthene for standard, high and medium-density gasoline samples at room temperatures are shown in Figure 3. As it can be seen from the figure, the total monoaromatics percentage composition decreases with increasing ethanol percentages for all fuel samples. However, the decrease is more significant in EO to E20 than E0 to E10 samples. The results for other groups did not follow any pattern, and gave mixed results, as percentage composition increased for *i*-paraffins percentage in E10 standard and high-density gasoline fuels, and for mononaphthene in E10 high-density gasoline fuel. However, the percent changes with ethanol addition were very much similar for paraffins in all samples.

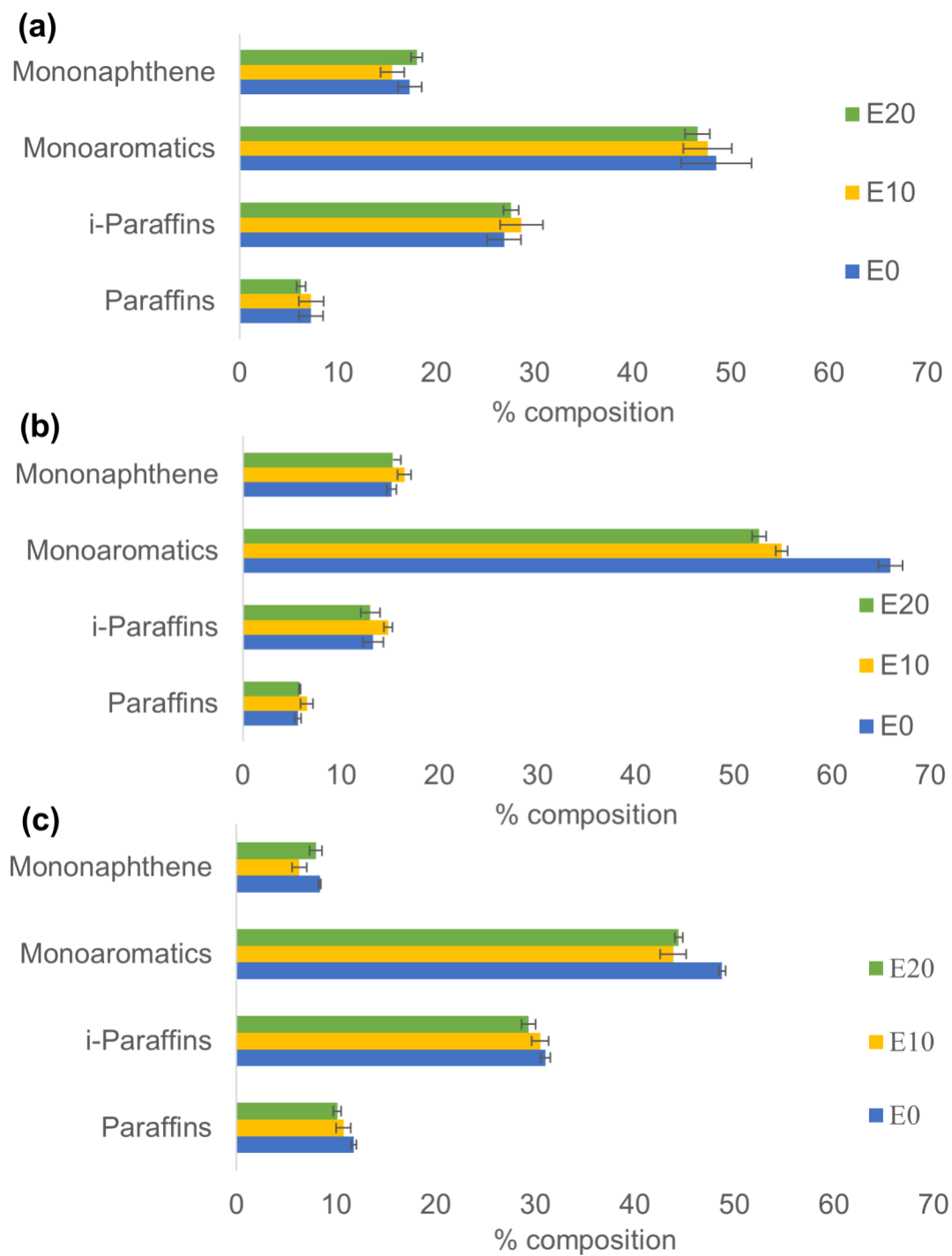


Figure 3. Effect of ethanol on headspace composition of (A) Standard, (B) High-density gasoline and (C) Medium-density gasoline samples at room temperature

2.4.3.2 Effect at 38 °C

Figure 4 illustrates that the influence of ethanol addition at 38 °C. Based on the

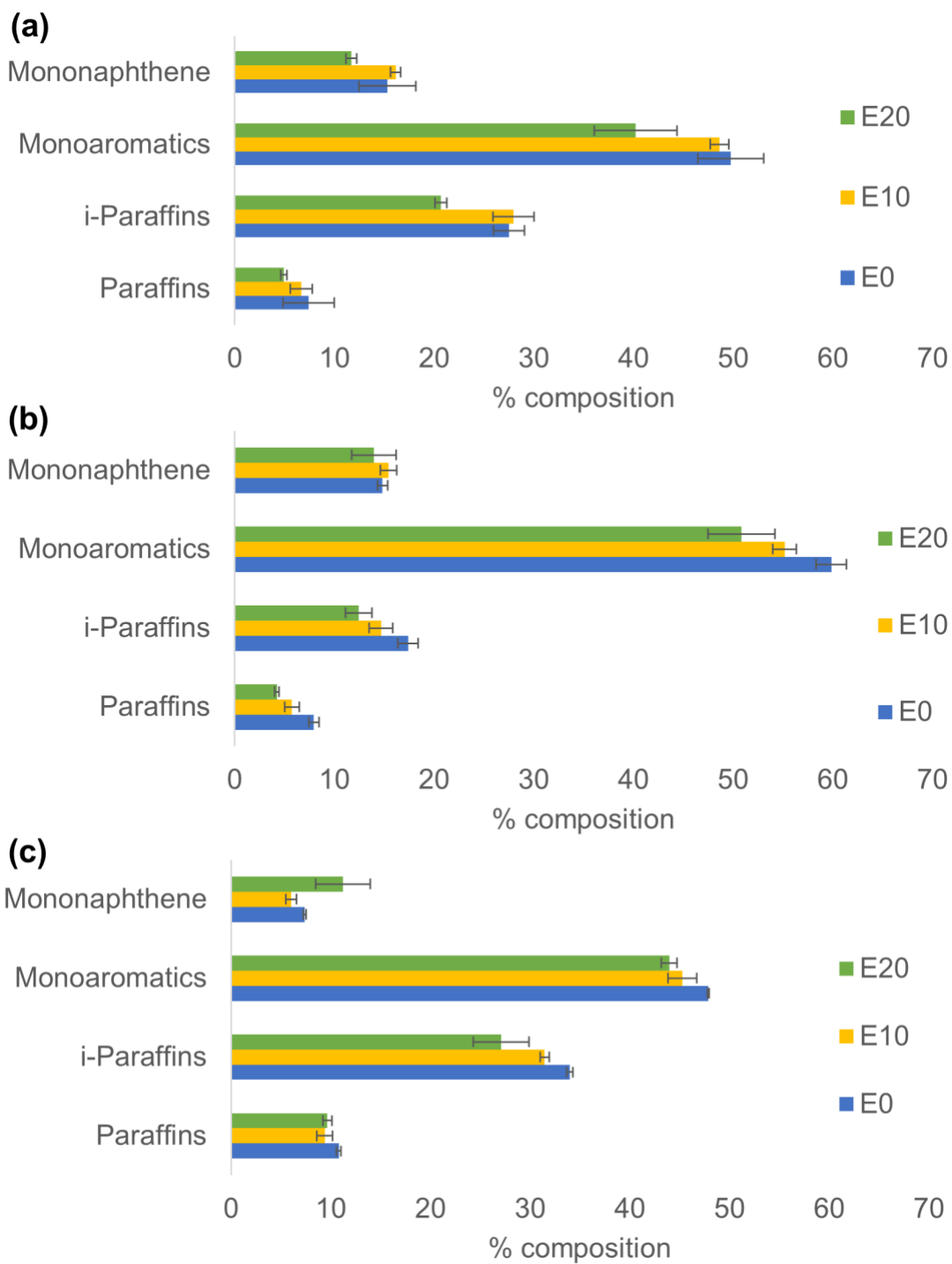


Figure 4. Effect of ethanol on headspace composition of (A) Standard, (B) High-density gasoline and (C) Medium-density gasoline samples at 38 °C

result, the monoaromatics percentage decreased with increasing ethanol percentages. Paraffins and *i*-paraffins followed a similar trend as monoaromatics as ethanol addition decreased the vapor phase composition for all sample except for E10 standard. However, mixed results were obtained for mononaphthene, as in some fuels (E10 standard, high-density gasoline, and E20 medium-density gasoline fuel), the percentage composition increased from E0 fuel.

2.4.3.3 Effect at 49 °C

Figure 5 shows the influence of ethanol on the headspace percent composition at 49 °C. Results similar to 38 °C and room temperature were obtained at 49 °C for monoaromatics, as the percentage composition decreased with E10 and E20 (10 and 20% v/v ethanol) samples. For paraffins and *i*-paraffins, although with ethanol addition, all the samples showed a decrease in percentage composition, however, with overlapping error bars, the percentage compositions were very similar between E0 and E10 standard (in case of paraffins and *i*-paraffins percentage composition) and E10 and E20 high and medium density gasoline fuel (for paraffins percentage composition). Similar to room temperature results, mononaphthene gave mixed results, as the percentage composition increased in E10 standard, high-density gasoline, and E20 medium-density gasoline fuel samples.

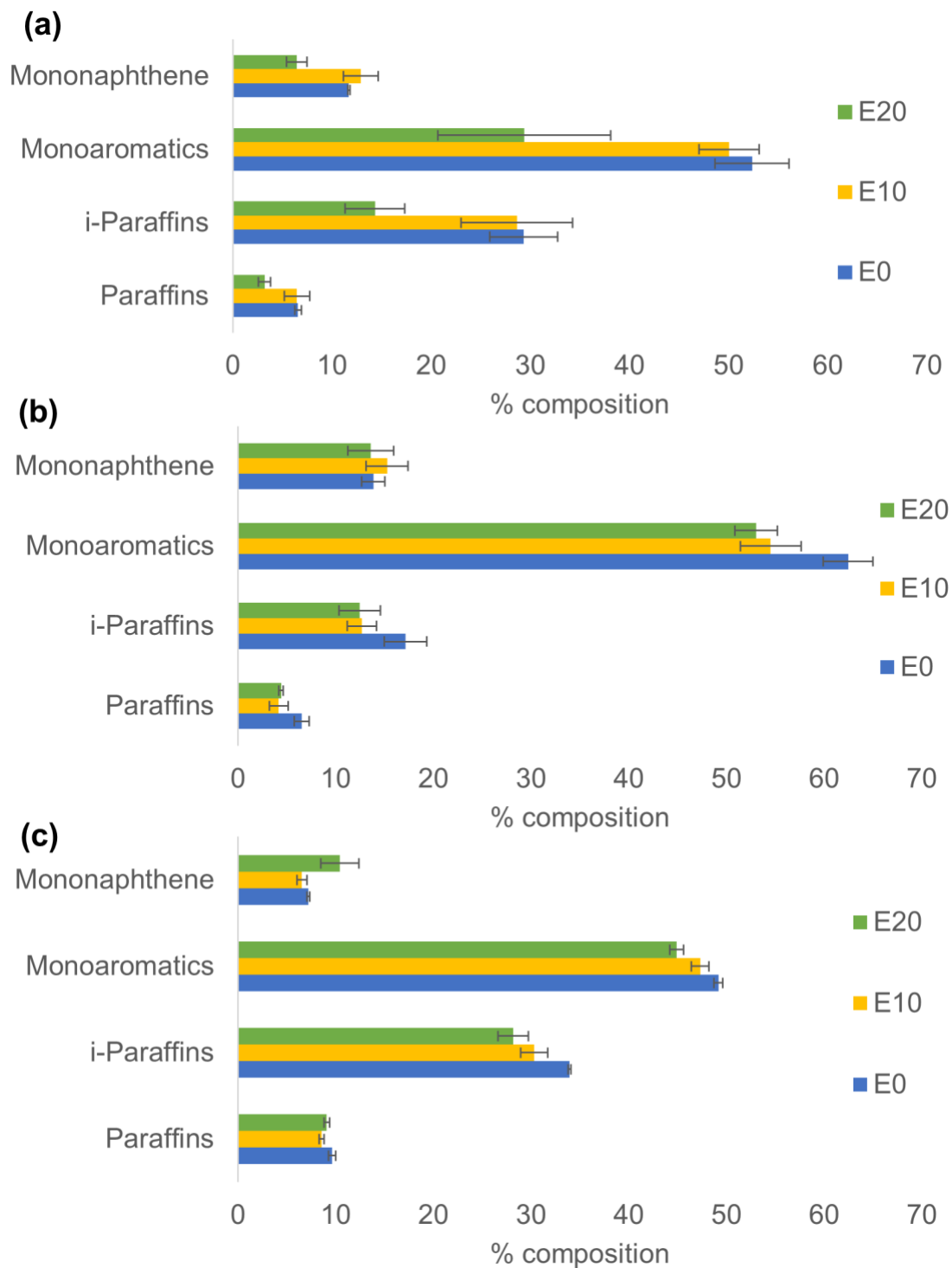


Figure 5. Effect of ethanol on headspace composition of (A) Standard, (B) High-density gasoline and (C) Medium-density gasoline samples at 49 °C

In general, when ethanol is added to E0 standard or gasoline samples, it diluted the samples, and hence it is expected that the percentage composition of studied compounds should decrease accordingly. This is what the experimental results achieved in most cases. Ethanol addition caused a decrease in vapor-phase monoaromatic percentages in all fuel samples (medium and high-density gasoline fuels and standard samples) from ethanol-free samples (E0). The decrease is more pronounced in E20 (20 v/v % ethanol) than E10 from E0 for standard and high-density gasoline samples at higher temperatures (38 and 49 °C), with the range of percentage decreases between 15 to 44%. While at room temperature, the decreases were smaller, between 4 to 20%. Although the monoaromatic percentage decreased for medium-density gasoline, the range was between 4 to 10%. Similar results were obtained in the case of paraffins and *i*-paraffins, in which the vapor-phase composition decreased with increasing ethanol percentage except for the increase of *i*-paraffins composition increased at room temperature. However, the paraffins and *i*-paraffin composition remain similar with the increase of ethanol percentage for medium and high-density gasoline at room temperature. However, for mononaphthene, mixed results were obtained.

The total evaporative emissions were also calculated and illustrated in Figure 6. The total emission of compounds decreased with ethanol addition, since the total chromatographic area decreased in E10 and E20 fuels from the E0 fuel for both medium and high-density fuels at all tested temperatures, except for the high-density fuel at room temperature. However, in case of standard fuel, the evaporative emission increased or remained similar in most cases.

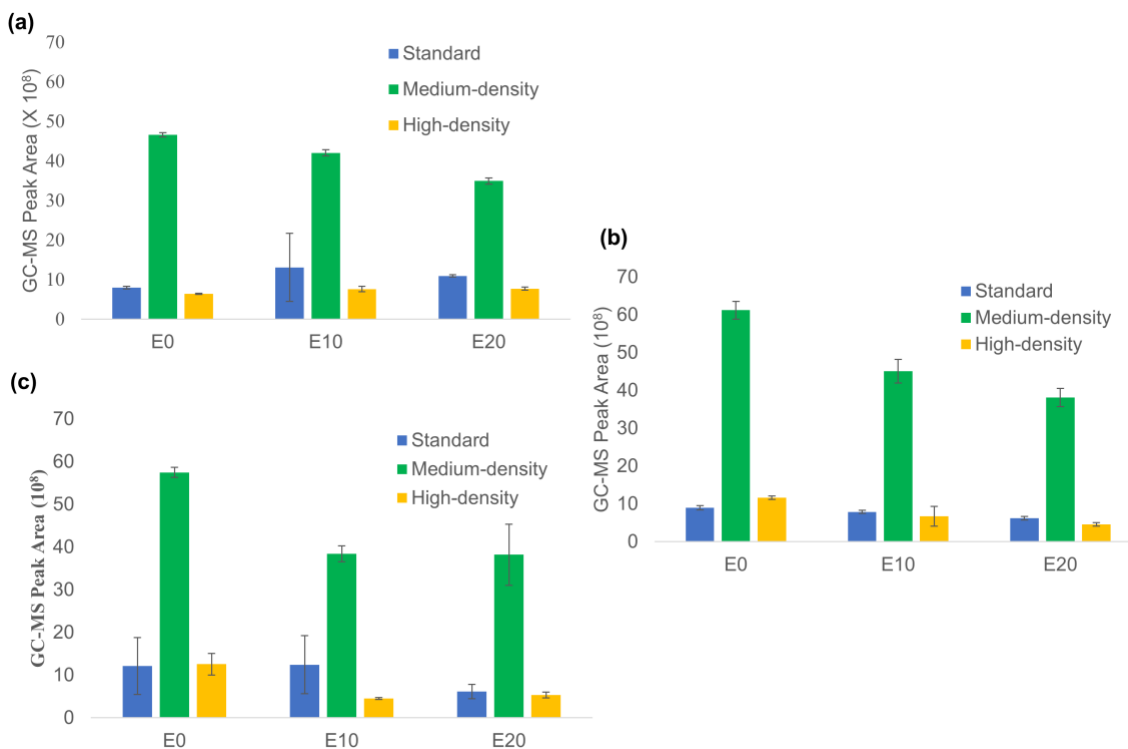


Figure 6. Effect of ethanol on overall evaporative emission of all studied compounds (a) at room temperature, (b) at 38 °C, and (c) at 49 °C. The total GC-MS peak area (X 10⁸) is plotted against E0, E10 and E20 fuels.

2.4.4 Effect of headspace composition of gasoline with the change of temperature

When temperature increases, it is expected that more molecules will transition to vapor phases, and thereby headspace percentage composition of studied compounds should increase. This was noticed in the case ethanol-free samples (Figure 7), as at higher temperatures, the headspace composition of *i*-paraffins and monoaromatics increased. But these results were not true for all samples, as the opposite result was observed for monoaromatics for high-density gasoline samples. However, the percentage change was almost similar for *i*-paraffins in high and medium-density gasoline samples at 38 and 49 °C, as no notable differences in percentage composition were observed at these two temperatures.

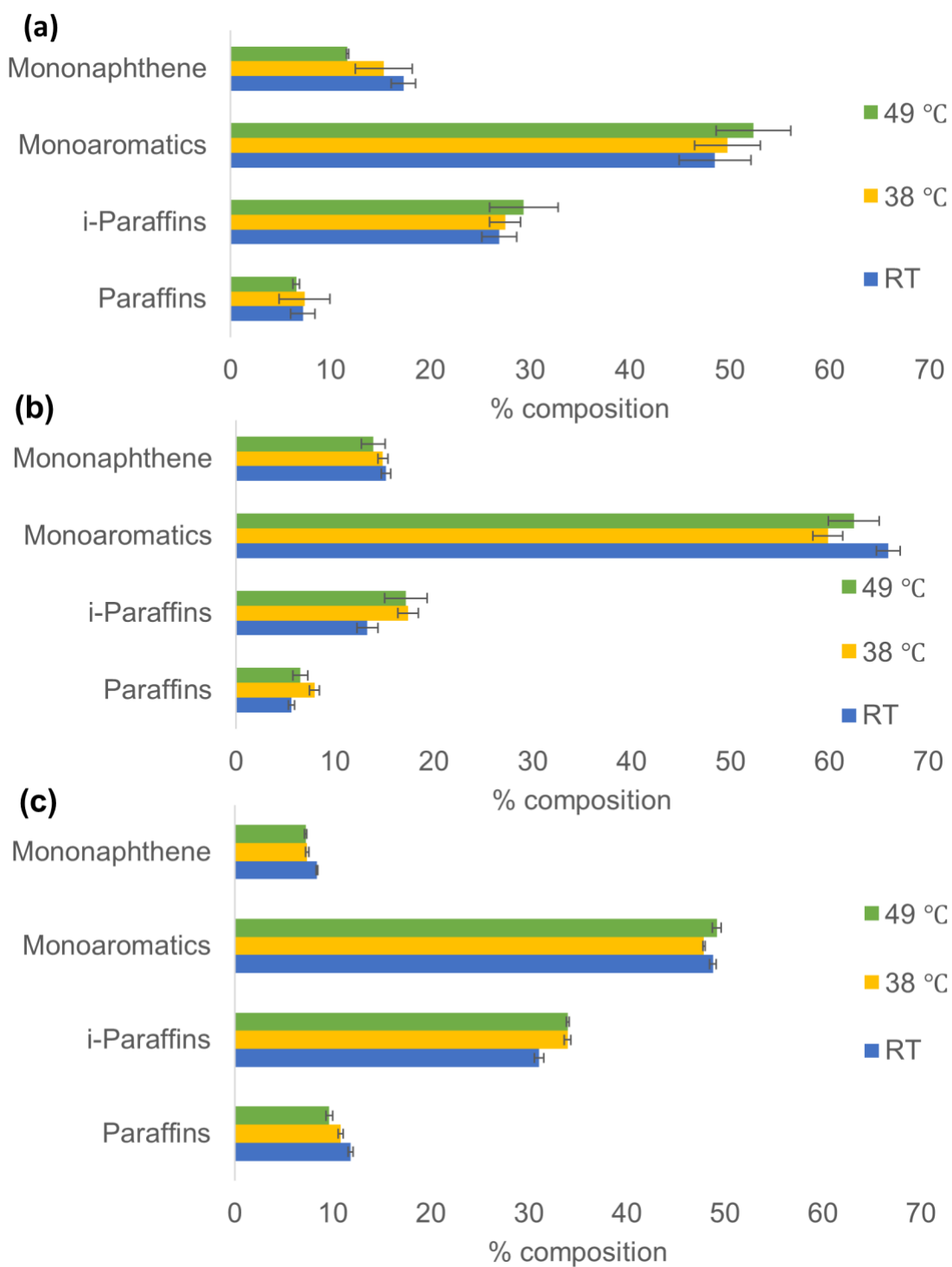


Figure 7. Effect of temperature on the headspace composition of (a) Standard, (b) High-density gasoline and (c) Medium-density gasoline E0 samples

In case of ethanol-blended fuels (Figures 8 and 9), the vapor phase percentage composition of monoaromatics increased with E10 standard and medium-density gasoline fuels at higher temperatures. However, the other results obtained for ethanol-containing samples are confounded, where the percentage composition of paraffins, *i*-paraffins, monoaromatics, and mononaphthene in most samples decreased from room temperature to 49 °C. However, some exceptions were seen for mononaphthene in E10 medium density gasoline and *i*-paraffins in E10 standard fuel, in which the percentage composition remained similar at all temperatures. This suppression in headspace composition is may be due to the fact that ethanol has much higher heat of vaporization compared to gasoline, and much heat is required to vaporize the gasoline components.⁶⁵

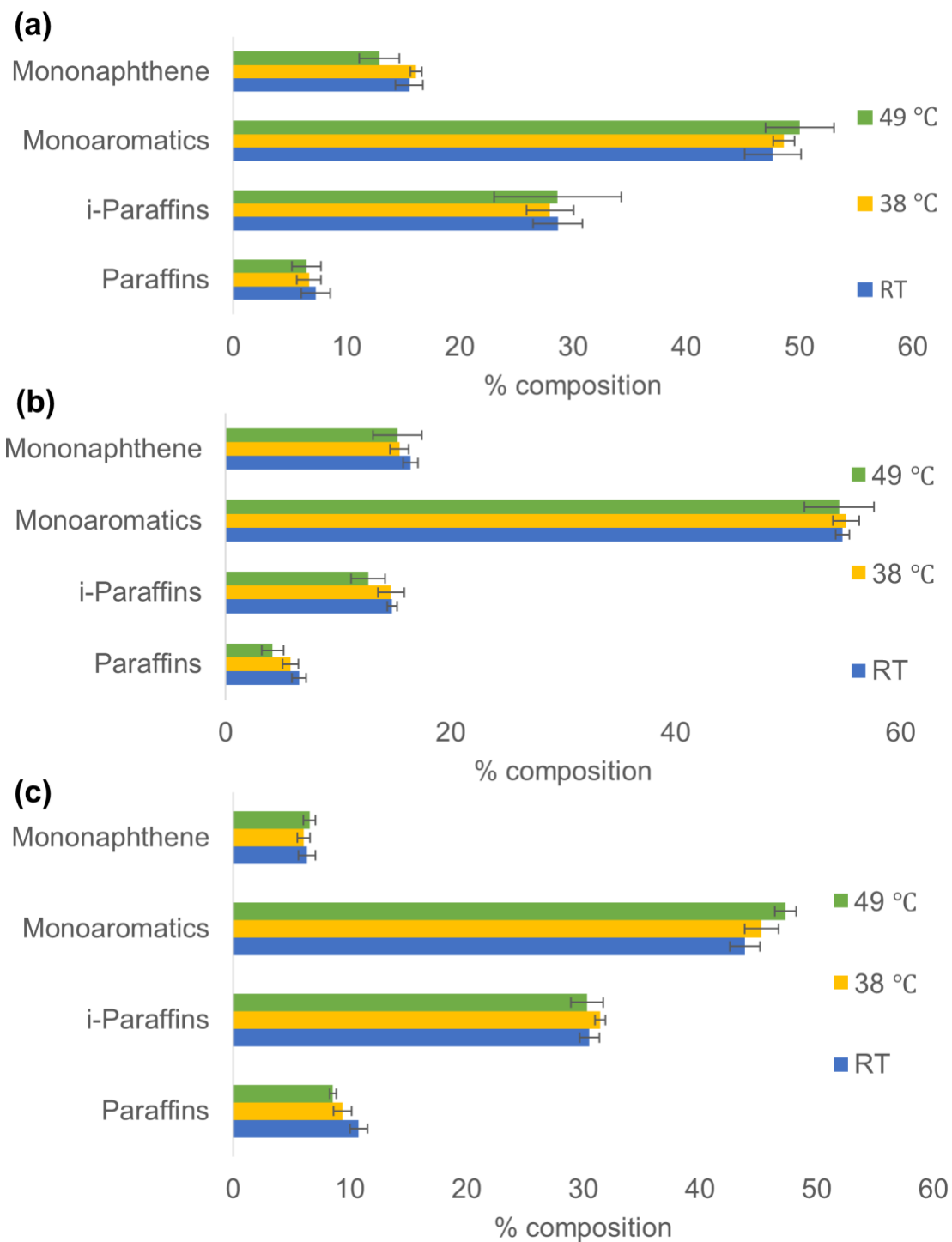


Figure 8. Effect of temperature on the headspace composition of (a) Standard, (b) High-density gasoline and (c) Medium-density gasoline with E10 samples

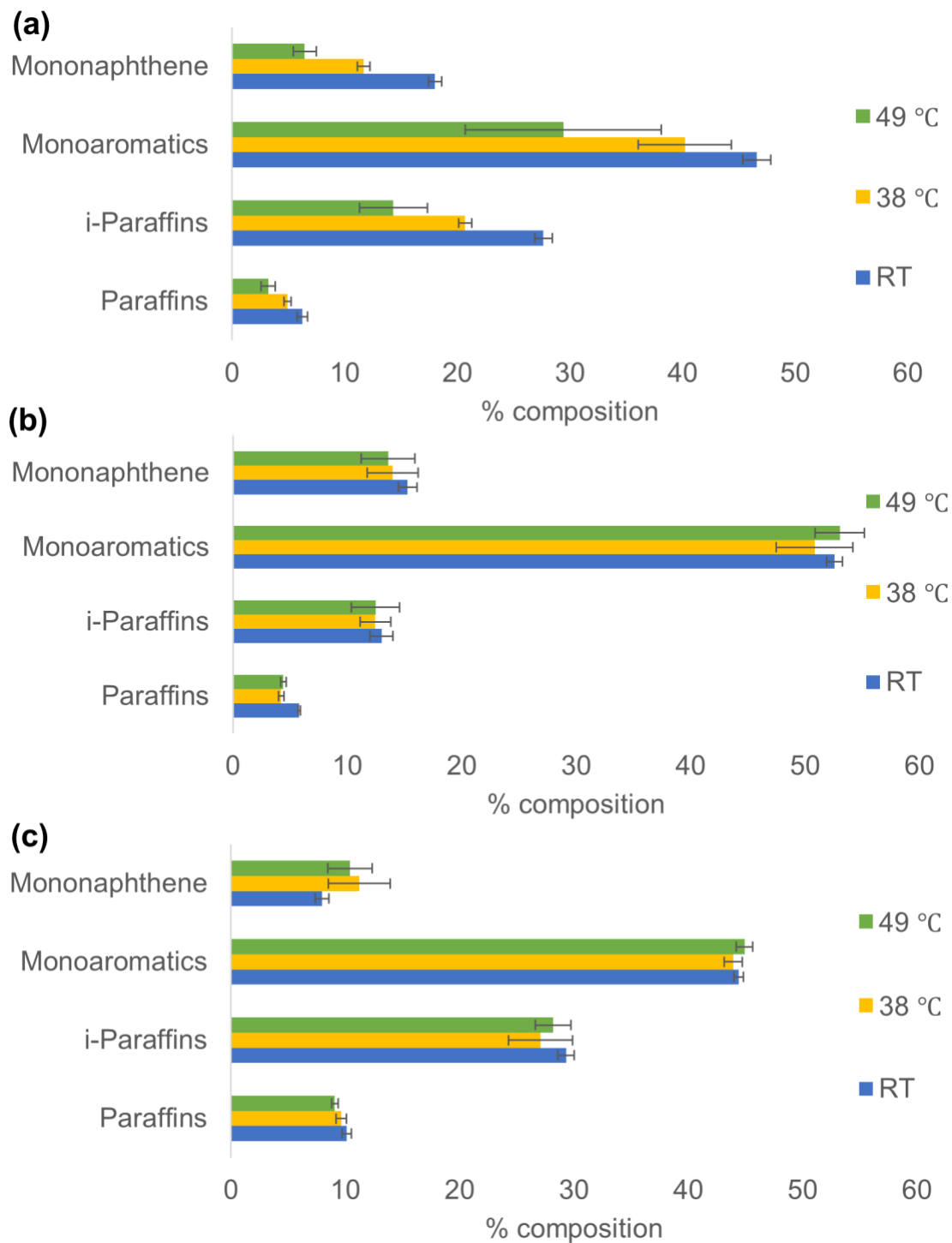


Figure 9. Effect of temperature on the headspace composition of (a) Standard, (b) High-density gasoline and (c) Medium-density gasoline with E20 samples

2.4.5 Change of percentage composition with regards to both temperature and ethanol

The effect of ethanol percentage and temperature on the evaporative emissions were discussed separately in the previous section. Nevertheless, we also wanted to see the effect with regards to ethanol and temperature together. This will be discussed in this section with the help of 3D plots or surface plots (Figures 10, 11, and 12) for both gasoline samples (medium and high density). The Surface plots were drawn by plotting percentage composition in the y-axis, percentage ethanol in the x-axis, and temperature in the z-axis. For data analysis purposes here, the room temperature is considered as 22 °C.

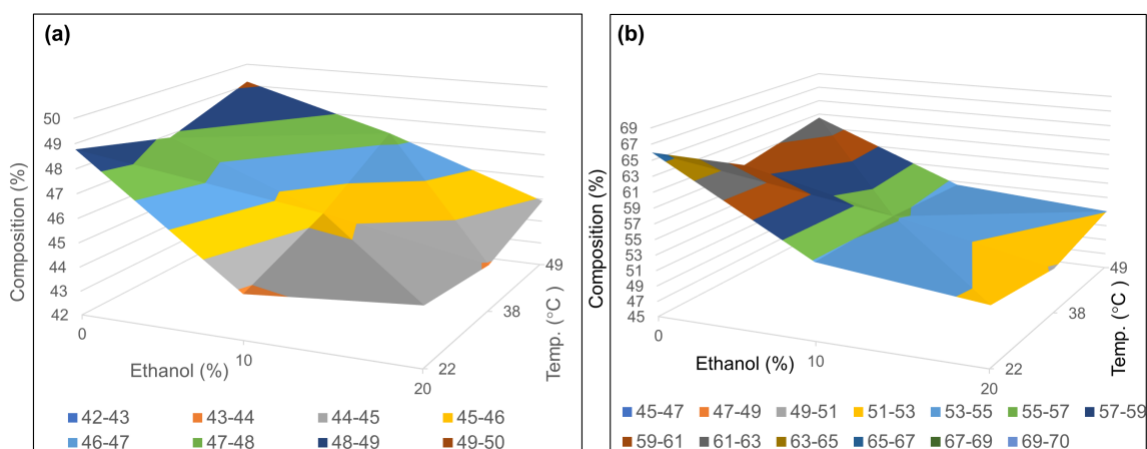


Figure 10. Change of monoaromatics percentage composition with ethanol and temperature (a) medium-density gasoline and (b) high-density gasoline

The plot (Figure 10) shows the change of percentage composition of monoaromatics with respect to ethanol percentage and temperatures for both medium and high-density gasoline. Although the plot illustrates the decrease of percentage composition with the increase of ethanol percentages at a given temperature, not much change was observed due to temperature changes at a given ethanol percentage. So, ethanol here clearly shows a significant impact on emission, while temperatures have a

negligible effect on the emission. The reason might be the narrow temperature range used in this study.

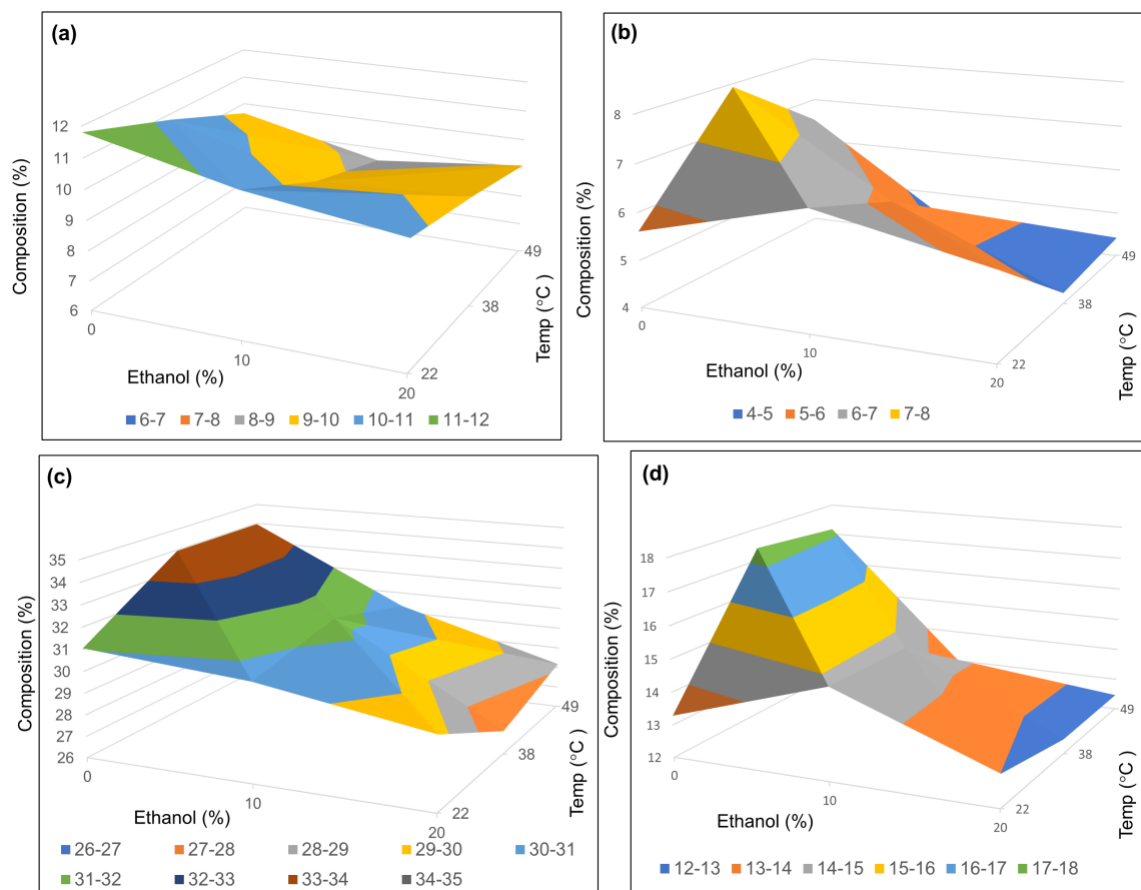


Figure 11. Change of paraffins percentage composition (a) medium-density gasoline and (b) high-density gasoline, and *i*-paraffins composition (c) medium-density gasoline and (d) high-density gasoline with respect to ethanol and temperature

A similar type of results (Figure 11) was obtained for paraffins and *i*-paraffins in terms of temperature effect; however, the decrease of percent composition with regards to increasing ethanol percentage occurred only at higher temperatures (38 and 49 °C), which was already discussed in the previous sections. In the case of mononaphthene (Figure 12), no uniformity in the change of percentage composition was noticed, similar to results discussed in sections 2.4.4 and 2.4.5.

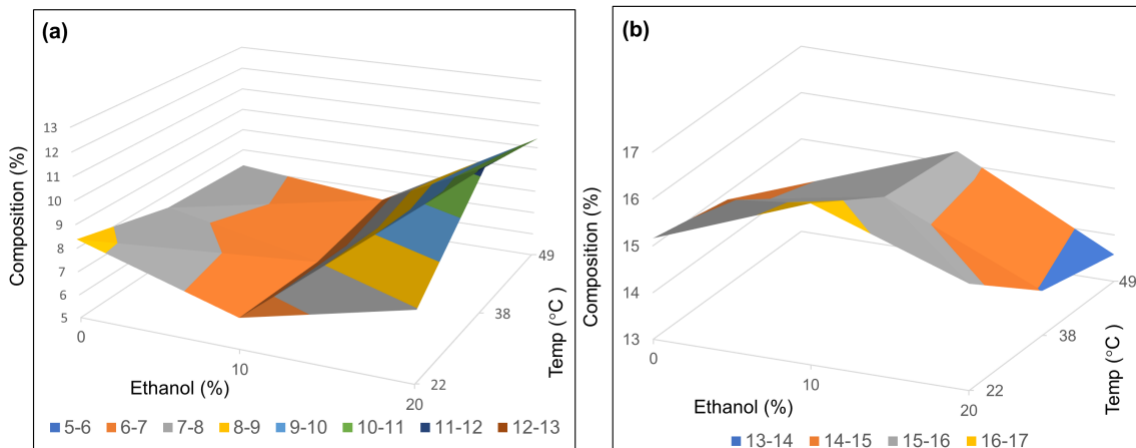


Figure 12. Change of mononaphthene percentage composition with ethanol and temperature (a) medium-density gasoline and (b) high-density gasoline

2.5 Conclusion

In this study the effect of ethanol on the evaporative emissions of components of gasoline were investigated. In all fuels (standard, medium and high-density gasoline), the monoaromatics percentages decreased with increasing ethanol percentages at all tested temperatures. The paraffins and *i*-paraffins also followed a decreasing trend of percentage composition with increasing ethanol percentage at all tested temperature (specially from E0 to E20 samples). These results are similar when compared to the result obtained by Fred et al.³⁵, Kenneth et al.³⁶, Ching et al.³⁷, and Shing et al.³⁸, in which the emissions of total hydrocarbons (THC) decreased with increasing ethanol percentages. However, their results were based on exhaust emissions analysis. However, one study in literature which studied the evaporative emission, found not so much difference in evaporative emissions of THC, while slight growth of BTEX compounds with E10 fuel.⁴²

The temperature effect of evaporative emission was also studied. The experimental results showed inconsistency with no common patterns were observed in all fuel samples. Although in some cases, the mono-aromatics percentages increased at

higher temperatures (standard E0, E10 and medium density E10 samples), but in most other cases the percentage composition of paraffins, i-paraffins, mono-aromatics and mono-naphthene either decreased at higher temperature or remained almost similar.

2.6 Acknowledgement

I would like to thank ICM, Inc. (310 North First Street, Colwich, KS 67030) for their generous funding and support to carry out this work.

3 CHAPTER 3. MICROBIAL DEGRADATION OF PETROLEUM HYDROCARBONS IN KEROSENE AND BIOSURFACTANTS PRODUCTION

3.1 Acknowledgment

This chapter is based on joint work with Pavan Kulkarni, a graduate student and his advisor Dr. Bruce Bleakley at the Department of Biology and Microbiology at South Dakota State University. The biological aspect of the work, such as experimentation regarding inoculation of the bacterial cell in culture media, growth studies, and lipopeptide biosurfactant extraction was done by Pavan Kulkarni. The analytical aspect of the work, such as liquid-liquid extraction, GC-MS, and UHPLC analysis was done by me. I would like to thank Pavan and Dr. Bleakley for their valuable input into this project. Both Pavan and I would also like to thank the department of dairy science for allowing us to use their centrifugation instrument.

3.2 Introduction

Petroleum is one of the most used energy resources of the world. Petroleum products are used as fuel for transportation, heating, electricity generations, and raw materials in petrochemical industries to make various chemicals, plastics, and synthetic materials. US is one the biggest user of petroleum products. In the year 2019, the total petroleum consumption in the US was 20.54 million barrels per day(b/d), of which approximately 45.3 % was gasoline fuel, 20.0 % distillate fuel, and 8.5 % was jet fuel.⁶⁶ Due to its high usage and demand, petroleum has become one of the major organic

pollutants. Petroleum contamination usually occurs due to the leakage of underground storage tanks, accidental spills during transportation, and disposal.

Petroleum pollution is a significant concern of the current world. Petroleum being lighter than water, upon spillage, they float on water and can migrate a long distance, thus release into ground water reservoirs and contaminate drinking and agricultural water supply. Also, as they move and degrade slowly, they persist on the land for a long time. Petroleum impacted soils emit toxic vapors, causing adverse effects to both human health and the environment. A lot of research has been done on the restoration of petroleum contaminated soil.⁶⁷ The most common method can be classified as physical, chemical, microbiological, and plant remediation. Soil removal and replacement, heat treatment and thermal resolution, washing, evaporation, dispersion, extraction, separation, and oxidation are many of the most common physical and chemical methods used in soil remediation.⁶⁷ These methods are more thorough and stable, but they always need processing facilities, chemical agents, and handling of pressure, temperate, and power supply.⁶⁷⁻⁷⁰ These methods are also quite expensive and produce secondary pollution. Due to its limitation to use in small area remediation, they are not widely used in actual applications.⁶⁷

One of the major problems in oil bioremediation is the bioavailability of hydrocarbon components of the oil due to low water solubility. Some hydrocarbon degrading bacteria are capable of producing biosurfactants to increase the uptake of hydrocarbons. Among the biosurfactant producing microorganisms, bacillus species are the major producer of biosurfactants,⁷¹ including lipopeptide biosurfactants such as surfactin, fengycin, lichenysin, iturin, pumilacidin, and bacillomycin.⁷² Biosurfactants

facilitate the emulsification of hydrocarbons in oil-water interface by the formation of micelles, thus increasing the uptake of hydrocarbons by microbial communities.⁷¹

By comparison, bioremediation is considered to be safe, inexpensive, non-destructive, and environment friendly for the removal of hydrocarbons from contaminated site.⁷³ Bioremediation is a process in which biological agents such as bacteria, fungi, or plants remove petroleum hydrocarbons from contaminated soil or water.⁷³ The process enhances the effectiveness of natural biodegradation process of contaminated environment.⁷⁴

Many studies have been conducted with pure culture or isolated bacteria from contaminated sites to investigate the biodegradability of petroleum hydrocarbons.⁷⁵ Several microorganisms have been reported that are able to degrade and utilize petroleum hydrocarbons.⁷⁶ Among the components of petroleum oil, the low molecular weight straight, branched, cyclic, and aromatic hydrocarbons are susceptible to degradation by many microorganisms more readily compared to the high molecular weight polycyclic aromatic hydrocarbons, which biodegrade only slightly due to their higher hydrophobic nature.⁷⁵

The present study aims at assessing the potentiality of two *Bacillus amyloliquifaciens* bacterial isolates in degradation of petroleum hydrocarbons present in kerosene. Previous study by our collaborators in the Biology and Microbiology Department indicated that these isolated microbes produce lipopeptide biosurfactants.⁷⁷ This work investigated the metabolic capability of these bacteria, which were isolated from wheat residue, to degrade and utilize petroleum hydrocarbons present in kerosene. This study also assesses the role of biosurfactants in this process and whether the

presence of petroleum hydrocarbons has any effect on the production of lipopeptide biosurfactants.

3.3 Background

3.3.1 Petroleum hydrocarbons pollutions and its effect

Petroleum hydrocarbons are the most widely used and one of the most dominant energy resources of the world. Because of its high demand and use, pollution results due to leakage or accidental spillage from the underground storage tank or during transportation, exploration, manufacturing etc.

3.3.2 Bioremediation

Bioremediation is a process by which microorganisms remove or biologically degrade components of oil spills from the contaminated sites. Bioremediation is closely affiliated with the term biodegradation. Biodegradation is a natural process of degradation, whereas in bioremediation, microorganisms are artificially introduced to remove contaminants from the environment. It is a technology that uses the metabolic potential of microorganisms to clean up contaminated environments.⁷⁸ It is a natural, green, and cost-effective solution for oil polluted contaminated environments.⁷⁹ Bioremediation has many advantages over traditional techniques such as land filling or incineration: it can be done on the site, is cheap, can clean the site with minimal disruptions, can remove waste permanently, and other physical and chemical methods can be coupled with it.⁸⁰

3.3.3 Biodegradation of petroleum hydrocarbons

Biodegradation of petroleum hydrocarbons is a complex process, and depends on various factors such as types and amount of hydrocarbons present, and microbial

degradation is a natural process of eliminating petroleum hydrocarbon from the environment.⁸¹ When petroleum oil spills, the hydrocarbon components of petroleum oil enter an aquatic system. These hydrocarbons then go through different physical, chemical, or biological effects, getting altered or lost. Volatile components are lost by evaporations, some changed by photochemical reactions, some absorbed in the waste, and some get metabolized or co-metabolized by various living microorganisms.⁸² Many microorganisms have been reported which can degrade hydrocarbons present in crude oil.⁷⁶ Among these microorganisms, bacteria are considered as the most active and primary agents in degradation of petroleum hydrocarbons.⁸¹ Several genera of hydrocarbons utilizing bacteria have been reported, which can grow by using these hydrocarbons as sole carbon and energy sources.^{76, 83} These bacteria are comprised of members mostly aerobic and some anaerobic genera of bacteria,⁸⁴ including *Dietzia*,⁸⁴ *Acinetobacter*,⁸⁵ *Rhodococcus*,⁸⁶ *Alcanivorax*,⁸⁷ *Pseudomonas*,⁷⁵ and *Bacillus*,⁸⁸

3.3.4 Biosurfactants

Biosurfactants are compounds containing both hydrophilic and hydrophobic moieties, produced by microorganism, that can reduce the surface and interfacial tension at the water/oil interfaces.⁸⁹ Biosurfactants can be classified into two groups based on molecular weight.⁹⁰ Low molecular weight compounds generally include glycolipids and lipopeptides, while the high molecular weight compounds are composed of polysaccharides, lipopolysaccharides or lipoprotein biopolymers.^{91, 92} The low molecular weight biosurfactants are effective in decreasing surface and interfacial tension, while the high molecular weight types are more efficient in stabilizing the emulsion of oil in water, and do not offer much in lowering surface tension.^{90, 91}

3.3.5 Role of biosurfactants in bioremediation

One of the main problems in oil remediation is the immiscibility of hydrocarbon fractions of oil in water. Oil is composed of hydrocarbons which are hydrophobic in nature, hence the solubility of these compounds in water is very low. So, the bioavailability of these components is very limited to microorganisms. Low molecular weight biosurfactants can lower the surface and interfacial tension, while high molecular weight biosurfactants decrease the surface area of hydrophobic water insoluble substrates,⁹² thus helping the bioremediation process by increasing the bioavailability of hydrophobic compounds of oil. Moreover, the tendency of surfactants to concentrate at the oil-water interface due to containing both hydrophobic and polar group in their structure, and microorganism being also attached to the surface and concentrated at the interfaces, plays an extra advantage in increasing the bioavailability of hydrophobic compounds to microorganisms.

3.3.6 Biosurfactant producing bacteria

Biosurfactant producing bacteria are ubiquitous in nature.⁹³ Biosurfactants are mainly produced by microorganism in aqueous medium in presence of a soluble (carbohydrates) or insoluble (hydrocarbons, fats and oil) substrates as carbon sources.⁹⁴ Many biosurfactants producing bacteria have been isolated, which are belong to *Bacillus*, *Agrobacterium*, *Streptomyces*, *Pseudomonas*, and *Thiobacillus* as producers of amino acids containing biosurfactants; *Pseudomonas*, *Torulopsis*, *Candida*, *Mycobacterium*, *Micromonospora*, *Rhodococcus*, *Arthrobacter*, *Mycobacterium*, *Corynebacterium*, *Mycobacterium*, and *Arthrobacter* as producers of glycolipids; *Thiobacillus*, *Aspergillus*,

Candida, *Corynebacterium*, *Micrococcus*, and *Acinetobacter* as producers of phospholipids and fatty acids.⁹⁵

3.3.7 Lipopeptide biosurfactants

Lipopeptides are one type of low molecular weight biosurfactant. It is the best known biosurfactants among all the biosurfactant classes and is produced by *Bacillus* species.⁹⁶ Generally, the lipopeptide biosurfactants are a mixture of cyclic lipopeptides that are built from variants of heptapeptides and hydroxy fatty acid chains.⁹⁷ *Bacillus* species produces three types of cyclic lipopeptides: iturins, fengycins, and surfactins.⁹⁸

3.3.7.1 Iturin

Iturins are cyclic lipopeptides, and based on the variation of amino acids in their peptide moieties, it can be classified as iturin A, iturin C, iturin D, iturin E, bacillomycin D, bacillomycin F, bacillomycin L, bacillomycin Lc, and mycosubtilin.⁹⁹ Structure of iturin A consist of a peptide part containing 7 amino acids, linked to hydrophilic tail which is a fatty acid chain with carbon numbers varying from C₁₄-C₁₇ (Figure 13.).¹⁰⁰

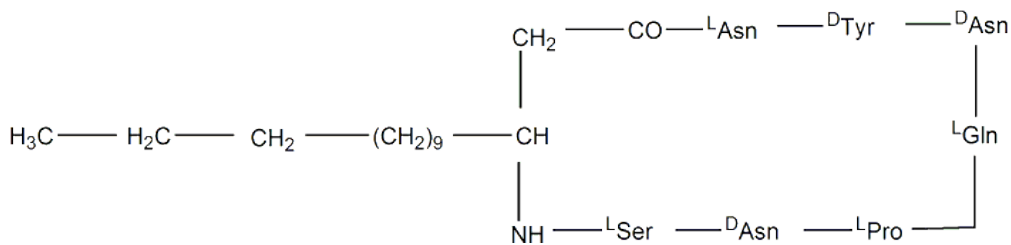


Figure 13. Cyclic structure of Iturin.¹⁰⁰

3.3.7.2 Surfactin

Surfactin is a mixture of cyclic lipopeptides, composed of variants of heptapeptide linked to a β-hydroxy fatty acid group with carbon numbers varying from 13–15.¹⁰¹ The amino acids in the peptide ring have a typical sequence of L-Glu¹-L-Leu²-D-Leu³-L-Val⁴-L-Asp⁵-D-Leu⁶-L-Leu⁷.⁹⁵ Due to the variation in sequence for amino acids and number of

carbons in β -hydroxy fatty acid chain, several isoforms of surfactins can coexist.¹⁰⁰

Surfactin has the following structure:¹⁰⁰

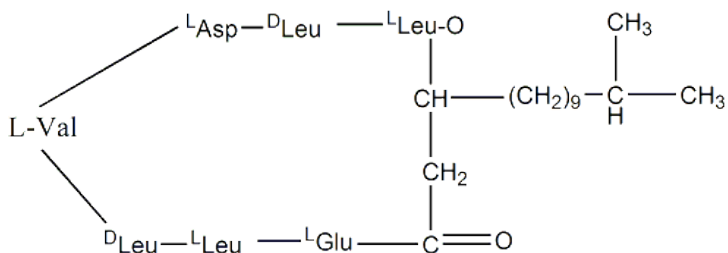


Figure 14. Cyclic structure of Surfactin.¹⁰⁰

3.3.8 *Bacillus amyloliquifaciens*

Bacillus amyloliquifaciens is a gram-positive and non-pathogenic endospore-forming soil bacterium that can act as a biocontrol agent with the ability to suppress diverse bacterial, fungal, and fungal-like pathogens.¹⁰² Work has been done on various isolates of *Bacillus amyloliquifaciens*, 1BA, 1BE, 1BC, and 1D3 by several graduate students in the soil and microbiology lab of the Department of Biology and Microbiology at South Dakota State University. These isolates were isolated from South Dakota wheat foliage and residue, and further tests were performed to confirm that these isolates belong to the genus *Bacillus*.^{77, 103, 104} Results from FAME (fatty acid methyl ester) analysis also showed that the ID3 isolate is closely affinitive to *Bacillus amyloliquifaciens*.^{103, 104}

3.3.9 *B. amyloliquefaciens* and lipopeptide biosurfactants

Bacillus amyloliquifaciens has a close affinity towards *Bacillus subtilis*,¹⁰⁵ which has been known to produce lipopeptide biosurfactants.¹⁰⁶⁻¹⁰⁹ Previous works done in the Biology and Microbiology Department of South Dakota State University also confirmed the ability to produce iturin and surfactin-like biosurfactants by *Bacillus amyloliquifaciens* (1BA).⁷⁷

3.4 Experimental

3.4.1 Bacterial isolates

Two bacterial isolates designated as 1BA and 1D3 were chosen for this study. Both of these isolates were previously isolated from wheat residue in our collaborator's lab in the Department of Biology and Microbiology at SDSU.

3.4.2 Culture media

Two culture media were used to study the biodegradation of petroleum hydrocarbons by both bacterial isolates (1BA and 1D3). One of the media was Tryptic Soy Broth (TSB) culture medium while the other was minimal salt medium. TSB media was used to see if the isolates were capable of co-metabolizing petroleum hydrocarbons while the minimal salt media was used to see if the isolates could metabolize the petroleum hydrocarbons as sole carbon and energy sources.

3.4.2.1 Composition and preparation of culture media

Tryptic Soy Broth (TSB) contained (in g/L): Pancreatic Digest of Casein 17.0 g; Papaic Digest of Soybean 3.0 g; Dextrose 2.5 g; Sodium Chloride 5.0 g; Dipotassium Phosphate 2.5 g. To prepare the media, 30.0 g of the powder was suspended in 1 L of water, followed by mixing and warming it to completely dissolve.

Minimal salt medium was prepared by adding 0.1 g NH_4NO_3 , 0.2 g MgSO_4 , 0.1 mg FeSO_4 , 0.02 g K_2HPO_4 , 0.9 mg KH_2PO_4 , 7 H₂O, 4.0 mg KCl, 1.5 mg CaCl_2 and 0.01 g of yeast extract in to 100 ml of distilled water. The minimal salt medium was then supplemented with 1 ml/L of 1000 X Natchez trace element solution. Both of these media were sterilized by autoclaving at 121 °C for 20 minutes.

3.4.3 Inoculation of bacterial isolates into culture media

The seed cultures were first grown in TSB overnight. The cells were concentrated by centrifugation and from these 1 mL was inoculated into the minimal media, and 500 μ L to TSB media with kerosene, which was filter-sterilized before adding. In case of minimal salt medium, after centrifugation, the cells were washed three times using 0.8% NaCl solution prior to inoculation.

3.4.4 Biodegradation studies of kerosene in culture media

Degradation studies of kerosene by both isolates (1BA and 1D3) were done in both TSB and minimal media culture media. Seed cultures grown in TSB overnight, were inoculated in a 125 mL Erlenmeyer flask with stoppers containing 20 mL of media supplemented with 200 μ L of kerosene oil and incubated on a rotary shaker at 120 rpm at 25°C in dark for 10 days. In case of minimal media, the kerosene oil that was used had been left opened for 1-2 hours in a fume hood to remove volatile hydrocarbons. After every two days, the culture broth was extracted thrice with 10 mL of n-hexane with vortex followed by centrifugation for ten minutes. All extracts were pooled together, adjusted to 30 mL and dried over anhydrous Na₂SO₄. The hydrocarbons were then quantified using GC-MS. The total area of the peaks in the chromatogram were defined as the concentrations of total hydrocarbons (THCs) in kerosene. Then the percentage of kerosene degradation was calculated using the following expressions:

Percentage degradation = [(THCs zero day – THC_s (after 2nd/4th/6th/8th/10th day))/ THC_s zero day]*100. Then the residual kerosene was expressed in term of percentage by subtracting the percentage degradation from 100%. All the samples were carried out in triplicate and the results are shown as mean values and standard deviations.

The bacteria free control was incubated and analyzed in the same way as the experimental group.

3.4.5 GC-MS conditions

Concentration of extracted kerosene was analyzed using an Agilent Technologies 7890 A gas chromatograph (Agilent Technologies, Little Falls, DE), coupled to an Agilent Technologies 5975C triple-axis mass detector, operated in EI mode (with 70 eV ionizing voltage). The column used was a Rxi-1301 Sil MS from Restek, 30 m × 0.25 mm i.d., with 0.25 µm film thickness. The hydrogen carrier flow was kept constant at 2.4 mL/min. 1 µL of extract was injected in split mode (10:1). The GC method begins with an initial oven temperature of 60 °C for 3 min, then ramped at 12 °C/minute to 200°C, held for 1 minute, and finally ramped at 30 °C/minute to 250°C and held for 1 minute. The transfer line temperature was kept at 280 °C. The MS temperatures were ion source 230 °C and quadrupole 150 °C. The scan range was 50-550 amu.

3.4.6 Growth studies to investigate bacterial growth

Growth studies were performed in both TSB and minimal media using both isolates (1BA and 1D3). Values of optical density (OD at 600 nm) were recorded for minimal media while the plate counts were performed for TSB media.

3.4.7 Production of lipopeptide biosurfactants from 1BA and 1D3 isolates

Lipopeptide biosurfactants were prepared from 1BA and 1D3 isolates in both minimal media and TSB media. The isolates were inoculated in the growth media in the same way as the biodegradation of kerosene oil experiment. After five and ten days the lipopeptides produced were extracted from the culture media.

3.4.8 Extraction of lipopeptides from the culture media

Lipopeptides were extracted using the method described by Smyth et al.,2010.¹¹⁰ The culture media was centrifuged at 13,000 x g for 15 minutes at 4 °C to remove the cells. Then the supernatant was acidified using concentrated HCl to pH 2 and stored at 4 °C for 12-24 hours. The sample was then centrifuged at 13,000 x g for 15 minutes at 4 °C to obtain the pellet (crude lipopeptide). Then pellet was collected by dissolving it in methanol. The extracted lipopeptide dissolved in methanol was evaporated to dryness using rotary evaporation.

3.4.9 RP-UHPLC-UV analysis of lipopeptides

Two different type of biosurfactants (iturin A and surfactin) were analyzed using an UltiMate 3000 UHPLC chromatographic system by Thermo Scientific Dionex, USA, equipped with an autosampler and a diode array detector (DAD). A 5 µL aliquot was injected into an ZORBAX Eclipse Plus C18 column (5 µm, 150 mm×4.6 mm) (Agilent Technologies, Little Falls, DE) in the UHPLC system to separate the lipopeptide isoforms. A 100ppm standard mixture of iturin A and surfactin was used to confirm the presence of surfactin isoforms, while no iturin A isoforms were identified. The elution was carried out with gradient solvent systems with a flow rate of 0.3 mL/min at 40 °C. The mobile phase consisted of water (A) and acetonitrile (B). Both mobile phases contained 0.1% trifluoroacetic acid (TFA). The gradient strategy for the acetonitrile-water mobile phase system was as follows: 0-13 min, 30% B to 51% B; 13-18 min, 51% B to 70% B; 18-35 min, 70% B to 100% B; The chromatograms were obtained at 205 nm, and the identified surfactin isoforms were quantified using Thermo Scientific Dionex Chromeleon 7 chromatography data system (CDS).

3.4.9.1 Sample preparation

The extracted lipopeptide dissolved in methanol was evaporated to dryness using rotary evaporation. Then the lipopeptide mixture was dissolved in 1 mL of methanol and filtered through 0.2 μm membrane filter. In case of extracted cultural media containing 1D3 isolates, the samples were further diluted to 1/2 dilution with methanol before injected into UHPLC system

3.4.9.2 Standards

Two lipopeptide standards (iturin A, purity minimum 97% and surfactin, purity \geq 98%) were brought from Sigma-Aldrich. All the standards were prepared in methanol.

3.4.9.3 Preparation of calibration standards

A 3000 ppm of standard stock solution of surfactin was prepared in methanol. Using the stock solution, each calibration standards (100, 200, 400, 600, 800 and 1000, 1200, 1400, 1600, 1800, 2000) were prepared in methanol with 0.1% TFA.

3.4.9.4 Preparation of calibration curve

Two different calibration curves were prepared. Calibration curve for surfactin produced in absence of kerosene were constructed in the range of 1000-2000 ppm, while the calibration curve for surfactin produced in presence of kerosene were constructed in the range of 100-1000 ppm. The calibration curve for surfactin produced in absence of kerosene was made using the peak area (y) versus the concentrations, while for surfactin produced in presence of kerosene, instead of using area, height was used.

3.5 Results and discussion

3.5.1 Analysis of hydrocarbon degradation by GC-MS

Figure 15 shows the sample chromatogram of control (TSB + kerosene + no bacteria) and TSB with 1D3 (no kerosene) after extraction with hexane from the culture broth after day 6. The peaks in control shows the components of kerosene after extraction with hexane.

3.5.1.1 Degradation of kerosene in TSB media

Figure 16 shows the GC-MS results of kerosene degradation study by *B. amyloliquefaciens* 1BA and 1D3 in TSB media. When compared to control, there were some degradation of kerosene, as the residual kerosene % decreased to below 50% (for 1BA) after day 4, and for 1D3 after day 6. But this data was not consistent for all trials (as shown by error bar). The results for up to four to six days are understandable, as when we look at the results from growth studies, as the growth of bacteria were very rapid up to 5 days. As kerosene composed of many volatile hydrocarbons, it was expected that the

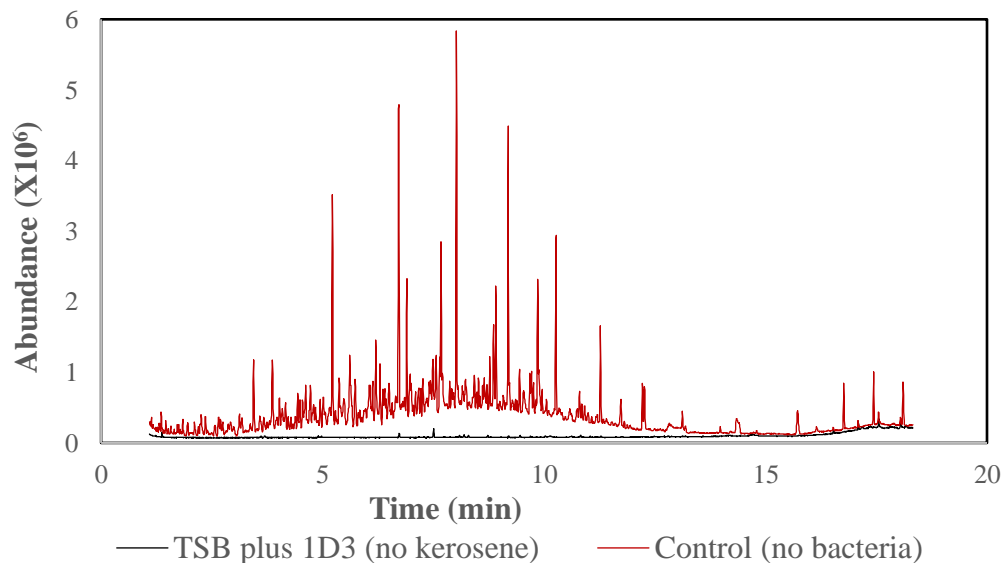


Figure 15. Sample chromatogram showing components of extracted kerosene in control (TSB with kerosene but no bacteria) and in TSB with bacteria but no kerosene

control will lose some hydrocarbons by evaporation, and we expected some difference between control and samples, as we observed in case of 1BA for up to four days, and for 1D3 for up to day 6. However, beyond day 6 for 1D3, the results were opposite, as we saw there were higher % of residual kerosene in samples than for control.

3.5.1.2 Degradation of kerosene in minimal media

Figure 17 shows the degradation results obtained from the culture broth of *B. amyloliquefaciens* 1BA, 1D3 in minimal media. Although the residual % kerosene is less in minimal media consist of 1BA and 1D3 after most days compared to control but the difference is insignificant to decide whether these bacteria degrade the hydrocarbons by utilizing them.

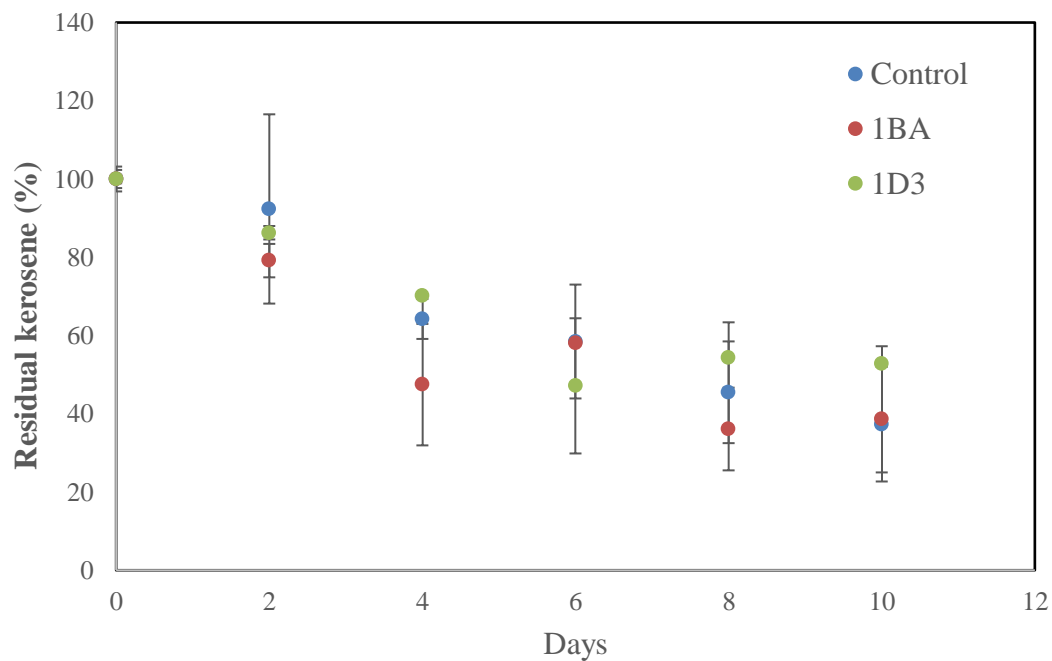


Figure 16. Degradation of kerosene by *B. amyloliquifaciens* 1BA and 1D3 in TSB media

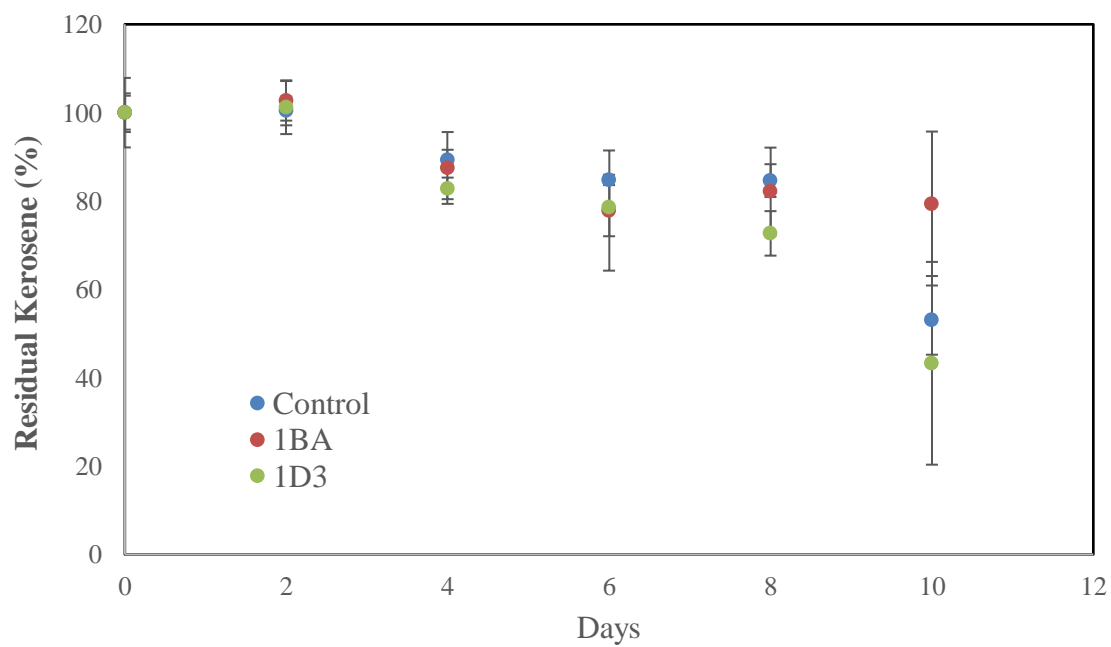


Figure 17. Degradation of kerosene by *B. amyloliquifaciens* 1BA and 1D3 in minimal media

3.5.2 Determination of bacterial growth by growth studies

3.5.2.1 Growth studies of *B. amyloliquefaciens* 1BA and 1D3 in TSB media

Figure 18 shows the growth of *B. amyloliquefaciens* 1BA and 1D3 in TSB media. The CFU or colony forming units count is used to tell how many microbes or colonies are present in the solution. Figure 18 shows that the amount of microbes were raised very rapidly for up to five days, then it increased little bit, and then started to decrease and finally comes to a plateau after 10 days.

3.5.2.2 Growth studies of *B. amyloliquefaciens* 1BA and 1D3 in minimal media

Bacterial growth was studied by determining the optical density (OD). Optical density is used to investigate the growth of bacteria under different conditions. OD measurements are measured assuming that the obtained OD value is proportional to cell number.¹¹¹ OD is also a measure of turbidity.¹¹¹ So a higher OD value suggest that the solution is more turbid, and hence the possibility of more bacterial cells. Figure 19 shows an OD curve for *B. amyloliquefaciens* 1BA and 1D3 measured at 600 nm.

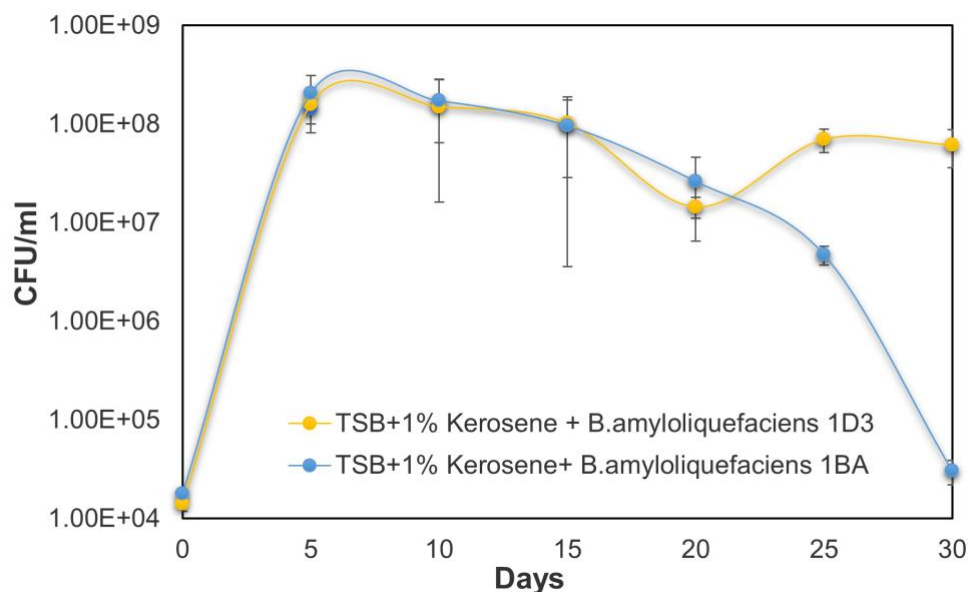


Figure 18. Growth curve of *B. amyloliquefaciens* 1D3 and 1BA using CFU counts

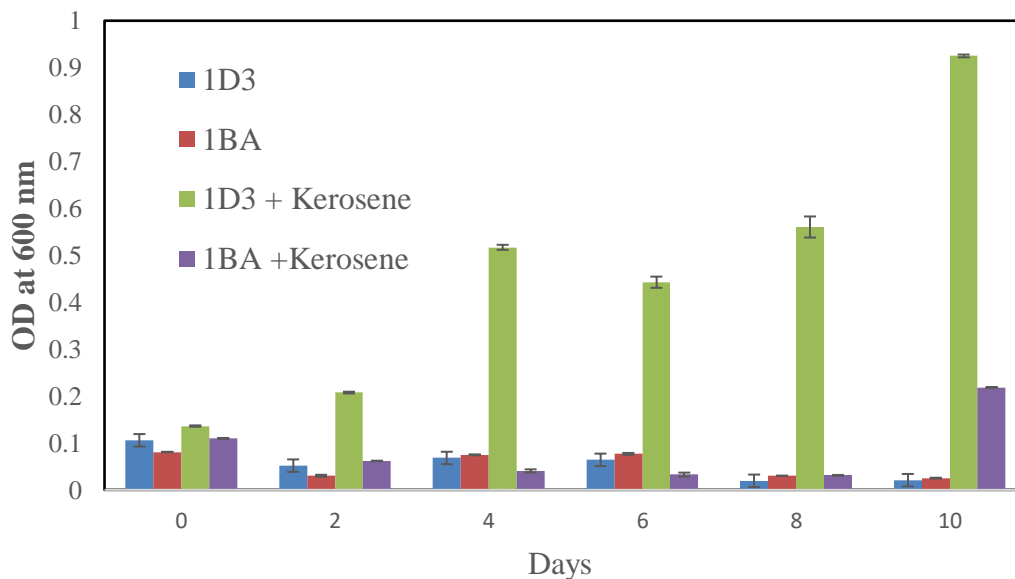


Figure 19. Growth curve of *B. amyloliquifaciens* 1D3 and 1BA using OD600 measurements

The OD curve for 1D3 with kerosene in minimal media shows gradual increase of OD as the day progresses, meaning proliferation of 1D3 in define conditions. However, the other curve showing lower growth than 1D3, and the difference between each curve are not significant.

3.5.3 UHPLC analysis of lipopeptide biosurfactants

Two different types of biosurfactant lipopeptides (iturin A and surfactin) were analyzed using the UHPLC method described above. A standard mixture of iturin A and surfactin at 100ppm was also prepared. The chromatogram of mixture of standard iturin A and surfactin (100ppm) and sample chromatogram obtained from 1D3 isolates in TSB in absence of kerosene are shown in Figure 20. The itruin and surfactin are mixture of various isoforms. The different isoforms are due to the varying number of carbon chain length, peptide sequence, difference in nutritional supplements in the culture broth and difference in types of bacterial strains.^{112, 113} The retention times for iturin A in the

mixture were recorded at 8.29, 8.62, 9.52, 10.01, 10.24, 12.16, 12.52, 13.87 and 14.05 and for surfactin were recorded at 25.91, 27.06, 27.20, 27.50, 28.80, 29.12, 29.41, 29.64, 30.29, 30.40, 30.69, 31.23, 31.98, and 32.32 min. The peaks obtained from the sample shows similarity with surfactin peaks, while no iturin A peaks were observed in the sample. Figures 21 and 22 display details from Figure 20.

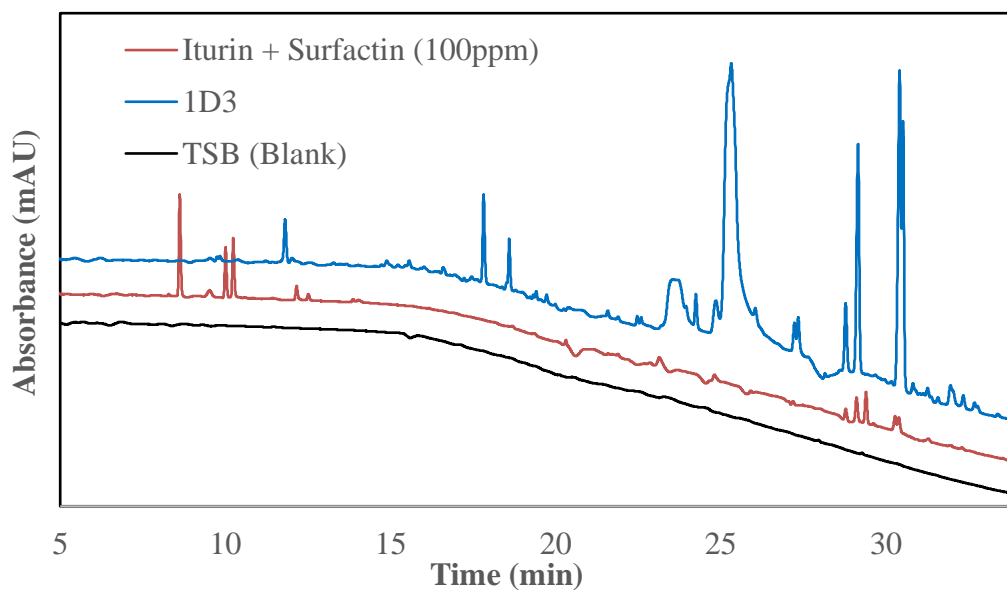


Figure 20. Sample chromatogram of standard conc. of iturin A and surfactin (100 ppm), extracted lipopeptide from TSB culture broth containing *B. amyloliquifaciens* 1D3, and extracted TSB media with no bacteria in absence of kerosene after day 10

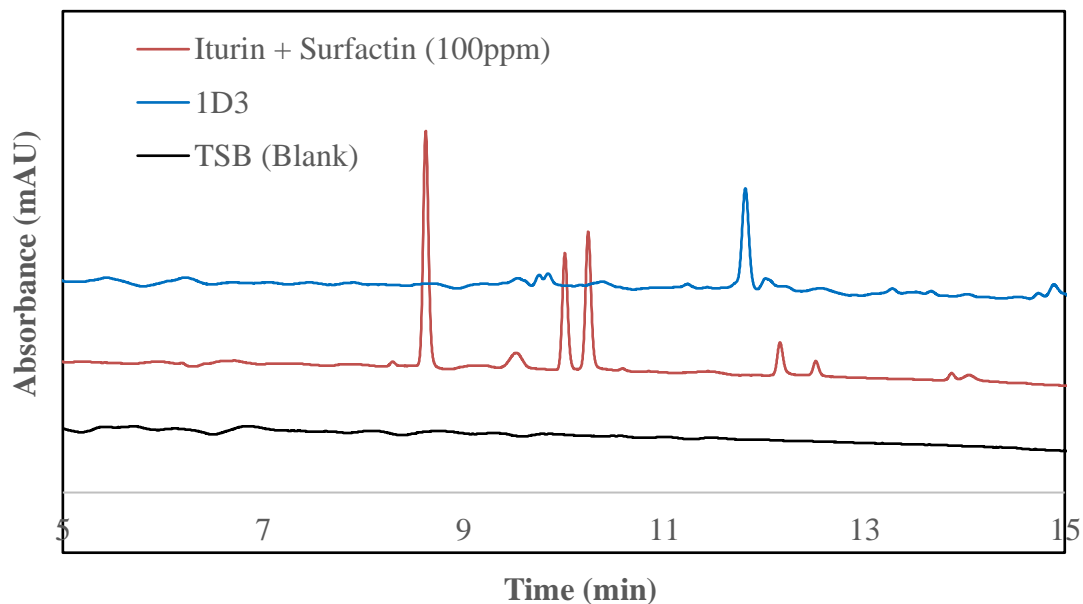


Figure 21. Chromatogram showing iturin A fractions (zoomed in version of Figure 20).

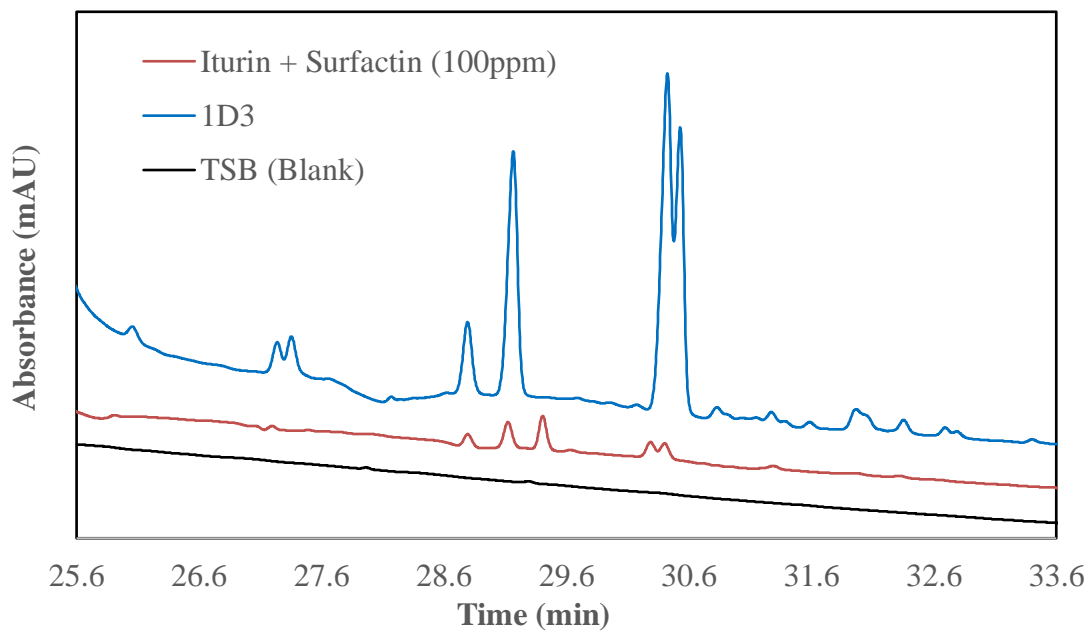


Figure 22. Chromatogram showing surfactin fractions (zoomed in version of Figure 20).

3.5.3.1 Lipopeptides production in minimal media in absence of kerosene

Figure 23 shows the UHPLC chromatogram for iturin A and surfactin standard concentration at 100 ppm and samples of extracted lipopeptides from the culture broth

(made of minimal medium) of *B. amyloliquefaciens* 1BA and 1D3. When the chromatogram of surfactin from 1D3 were compared with surfactin peaks in the standard chromatogram, only three of the peaks were similar to the standard chromatogram (indicated in the figure), and also as the intensity was very low, the amount produced are likely very insignificant. Although there is another peak at around 29 min, which is similar to surfactin standard peak, but this peak was also seen in the extracted minimal media with no bacteria (also included in Figure 23), and hence it was not considered. However, for samples containing *B. amyloliquefaciens* 1BA, no surfactin peaks were identified.

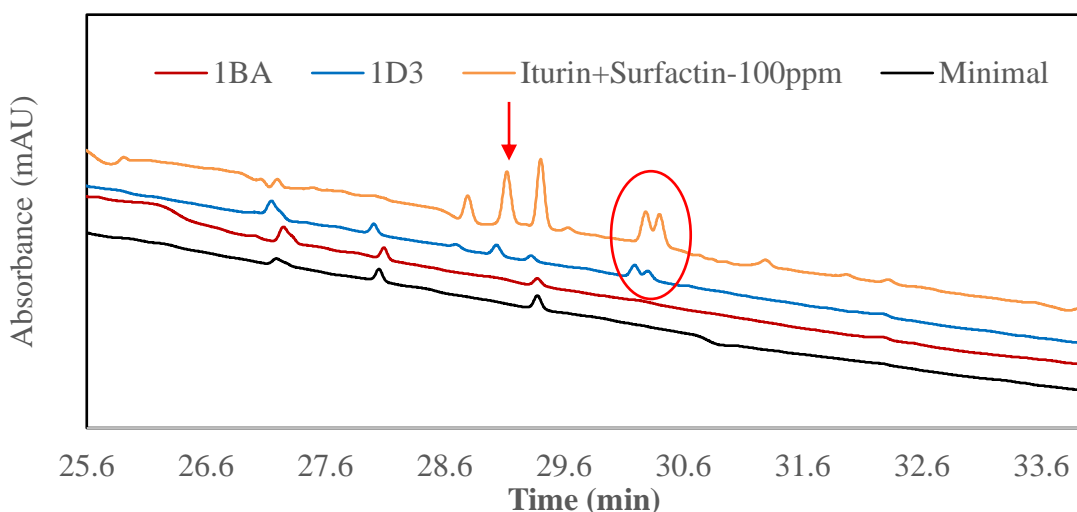


Figure 23. Chromatogram showing extracted minimal media with no bacteria, lipopeptides from the culture broth (minimal media) of *B. amyloliquefaciens* 1D3 and 1BA in absence of kerosene after day 10 and standard mixture of iturin A and surfactin (100ppm)

3.5.3.2 Lipopeptide production in minimal media in presence of kerosene

Lipopeptide production was also carried out in presence of kerosene. Figure 24 shows the chromatogram of lipopeptides produced by *B. amyloliquefaciens* 1BA and 1D3 in minimal media culture broth in presence of kerosene and the chromatogram for the

mixture of iturin A and surfactin standard concentration at 100 ppm. When compared to the standard no surfactin peaks were identified in lipopeptide samples.

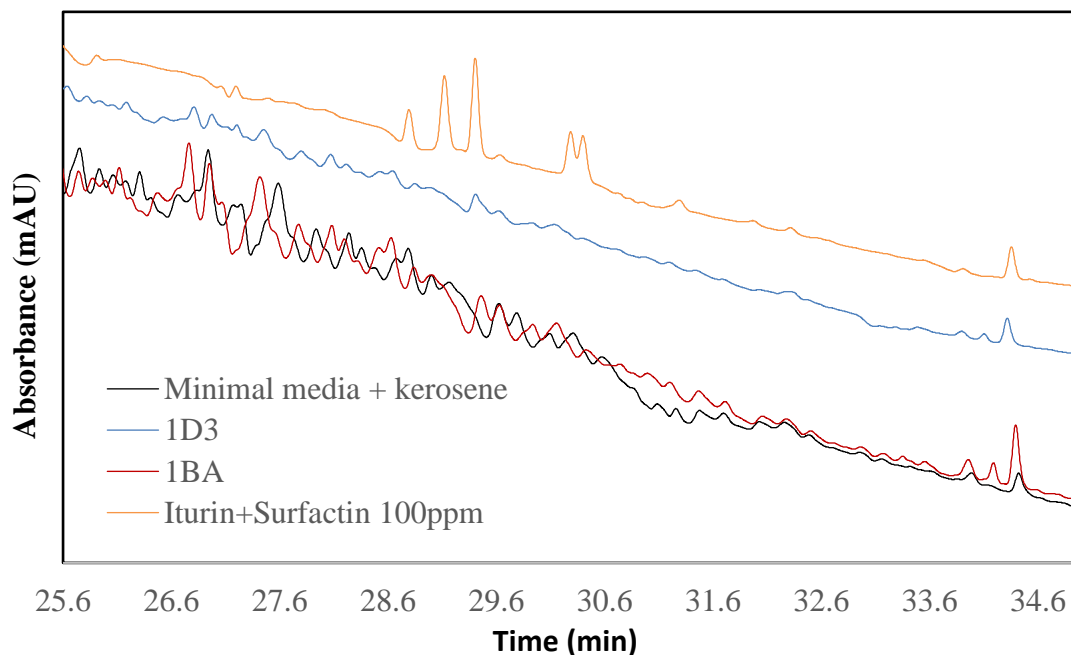


Figure 24. Chromatogram showing extracted minimal media with no bacteria and extracted lipopeptides from the culture broth (minimal media) of *B. amyloliquefaciens* 1D3 and 1BA in presence of kerosene after day 10, and standard mixture of iturin A and surfactin (100 ppm)

3.5.3.3 Lipopeptide production in TSB media in absence of kerosene

Figure 25 shows the chromatograms of extracted surfactin from culture broth (TSB media) of *B. amyloliquefaciens* 1BA, 1D3 and standard surfactin concentration at 1600 ppm. The retention times of standard surfactin concentrations at 1600 ppm in the figure were recorded at 25.91, 27.07, 27.19, 27.51, 27.63, 28.81, 29.17, 29.31, 29.41, 29.66, 30.34, 30.46, 30.77, 30.86, 30.99, 31.22, 31.56, 31.92, 32.01, 32.35, 32.69, and 32.79 min. When the standard chromatogram was compared with *B. amyloliquefaciens* 1BA and 1D3 similar chromatogram was obtained for 1D3 isolates, while 1BA did not produce any identical surfactin peaks.

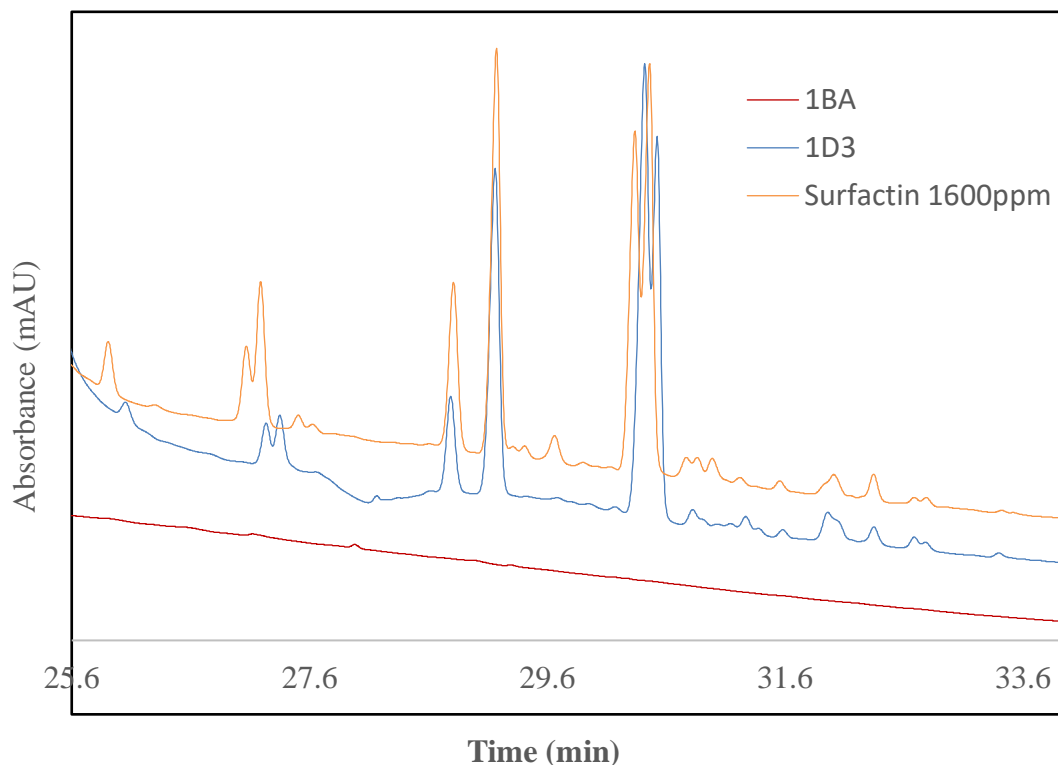


Figure 25. Chromatogram showing extracted lipopeptides from the culture broth (TSB media) of *B. amyloliquefaciens* 1D3 and 1BA in absence of kerosene after day 10 and standard conc. of surfactin at 1600 ppm

3.5.3.4 Lipopeptide production in TSB media in presence of kerosene

Similar results were obtained for extracted surfactin from culture broth (TSB media) of *B. amyloliquefaciens* 1BA and 1D3 in presence of kerosene, as is shown in Figure 26. However, only three surfactin isoforms were able to identified (indicated in the figure), when compared to the retention times of standard surfactin concentration at 600 ppm (recorded at 25.97, 26.35, 27.12, 27.23, 27.55, 27.67, 28.84, 29.18, 29.33, 29.45, 29.70, 30.35, 30.47, 30.80, 30.89, 31.02, 31.26, 31.60, 32.06, and 32.40 min). The peaks that were less intense in the standard, could not be identified because of the baseline noise in the chromatogram coming from the kerosene, which can be seen in the chromatogram of extracted TSB media with kerosene.

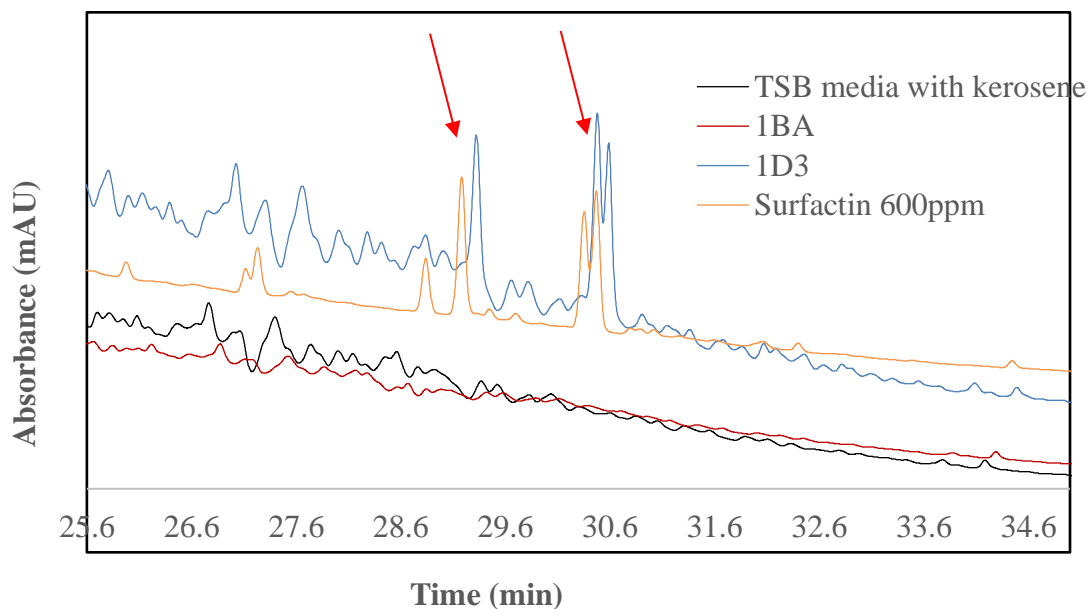


Figure 26. Chromatogram showing extracted TSB media with no bacteria and extracted lipopeptides from the culture broth (TSB media) of *B. amyloliquefaciens* 1D3 and 1BA in presence of kerosene after day 10, and standard conc. of surfactin at 600ppm

3.5.4 Determination of concentrations of extracted surfactin

Extracted surfactin concentration were determined using the calibration curves described above. Here the concentration of extracted surfactin from the culture broth (TSB media) of *B. amyloliquefaciens* 1D3 were quantified both in presence and absence of kerosene. As the amount of surfactin produced by *B. amyloliquefaciens* 1D3 in minimal media with no kerosene were very insignificant when compared to 100 ppm standard surfactin solution, and while no surfactin peaks were able to identify in presence of kerosene, quantification was not carried out in case of minimal media.

Two different calibration curves, one with the concentrations in the range of 1000-2000 ppm and another in the range of 100 -1000 ppm were used to quantify the surfactin produced by *B. amyloliquefaciens* 1D3. The R^2 and curve equation for both calibration curves are given in Table 6.

Table 6. R² values and curve equation for calibration curve used for surfactin quantification

Curve Used for Surfactin Quantification	Calibration Range (ppm)	R ²	Equations
In absence of kerosene	1000-2000	0.9869	$y = 0.0917x + 72.707$
In presence of kerosene	100-1000	0.9941	$y = 1.5001x + 50.823$

The quantification result for surfactin concentrations is summarized in Tables 7 and 8. The tables show that the concentration produced in absence of kerosene are much higher than that of surfactin concentrations in presence of kerosene. The higher ratio of C:N in the later might be reason for the decrease in lipopeptide production.

Table 7. Concentration of extracted surfactin in TSB by *B. amyloliquefaciens* 1D3 in absence of kerosene.

Replicate	Days	Diluted Conc. (ppm)	Undiluted Conc. (ppm)	Average (ppm)	Std. dev	% RSD
1	5	1792.88332	3585.76663	3310	390	11.78
2	5	1517.29662	3034.593239			
1	10	1507.32606	3014.652126	2869	210	7.32
2	10	1361.21265	2722.4253			

Table 8. Concentration (in ppm) of extracted surfactin in TSB by *B. amyloliquefaciens* 1D3 in presence of kerosene.

Repl- icates	Days	Diluted Conc.	Undiluted Conc.	Avg.	Std. dev.	% RSD	Overall Avg.	Std. dev	% RSD
1-1	5	465.600293	931.200587	987	48	4.90	907	110	12
1-2	5	509.557363	1019.11473						
1-3	5	504.957669	1009.91534						
2-1	5	411.083928	822.167855	827.0	4.6	0.55			
2-2	5	413.737084	827.474168						
2-3	5	415.623625	831.24725						
1-1	10	537.188854	1074.37771	1079.2	7.3	0.68	1045	120	11
1-2	10	537.775482	1075.55096						
1-3	10	543.781748	1087.5635						
2-1	10	420.829945	841.659889	914	63	6.85			
2-2	10	477.639491	955.278981						
2-3	10	471.953203	943.906406						
3-1	10	586.512233	1173.02447	1143	28	2.45			
3-2	10	558.974068	1117.94814						
3-3	10	568.406773	1136.81355						

3.6 Conclusion

In this study, two bacterial isolates of *B. amyloliquefaciens* were investigated for potential usefulness for bioremediation efforts for petroleum hydrocarbons present in kerosene. Both of these isolates were grown in two different media, minimal and TSB, in presence or absence of kerosene, to determine whether these isolates could metabolize or co-metabolize hydrocarbons components of kerosene. These bacterial isolates were also analyzed for the production of lipopeptide biosurfactants in presence or absence of kerosene to find out the correlation between biosurfactant production and hydrocarbons utilization. Our results from GC-MS performed on extracted kerosene from TSB culture broth showed there were some degradation for up to four days. For minimal media, there were some difference in % residual kerosene compared to control for both the isolates for up to six days, and after that kerosene degradation by 1D3 was highest, as the residual kerosene came down to around 43% after day 10. Our UHPLC results shows the presence

of surfactin lipopeptide in TSB media by *B. amyloliquefaciens* 1D3 both in presence and absence of kerosene, while the determined concentration in absence of kerosene were significantly higher than that of in presence of kerosene. For minimal media, surfactin lipopeptides was found in culture broth consist of 1D3 in absence of kerosene, but qualitatively the amount was very little compared to the 100 ppm standard mixture. However, in presence of kerosene no surfactin was identified by UHPLC analysis. There was no positive correlation found between surfactin production and hydrocarbon utilization. Although the GC data shows some degradation caused by isolates 1D3 and 1BA, UHPLC data shows lower (in TSB media) to zero (in minimal media) surfactin produced in presence of kerosene, which implies that bacteria were less likely utilizing the kerosene to grow and produce lipopeptide surfactants.

4 CHAPTER 4. DRY HERB VAPORIZER AS A HEADSPACE SAMPLER FOR SOLID-PHASE MICROEXTRACTION

4.1 Introduction

Solid-phase microextraction (SPME) is a sampling technique developed by Pawliszyn to provide a first sample preparation by integrating sampling, sample preparation, and extraction in a single step.^{114, 115} This technique provides solutions to the problems associated with traditional sample preparation techniques by shortening analysis time, avoiding organic solvents, and decreasing manual labor due to automation.¹¹⁶ SPME is a method based on the adsorption of compounds from the gaseous or liquid sample by using a fiber coated with different polar or nonpolar sorbents.¹¹⁷ The adsorbed compounds are then thermally desorbed into the GC injection port or removed by appropriate solvent for analysis using HPLC or other types of instruments.

SPME is often accompanied by heating, especially when adsorbing gaseous compounds from the sample matrix. Since headspace SPME allows direct extraction of volatile and semivolatile compounds from any matrix, the analyte compounds have to come out from the sample matrix freely. The most convenient way of doing this is by providing heat. Heating at elevated temperatures increases the vapor pressure of the compound and helps to break the strong affinity associated with the matrix to facilitate the release of compounds from the matrix.^{118, 119} The sample is usually heated in the laboratory on hot plate with oil bath, sand, or aluminum heating block. Although these techniques are cheap, quite available, and convenient, it requires continuous monitoring of temperature and in-house lab arrangements.

In this study, we proposed a technique to replace the traditional heating arrangement with a commercially dry herb vaporizer (vape) device. Although this device was not intended to use laboratory samples, with some arrangements it can be used to heat and extract sample directly from it. This type of vape device has the potential to offer many advantages such as it is cheap, automatic temperature controlled, can be operated at high temperature, and very easy to use. This proposed technique can also be combined with field portable analytical techniques such as portable GC-MS to offer a time-saving and cost-effective technique to provide many real-time decisions, especially in the case of environmental remediation and characterization of materials from contaminated sites. With the emergence of field analytical chemistry and the development of new portable analytical instruments, we believe our proposed technique can be very useful.

The objective of this study was to develop an analytical technique using a commercial vape device as a potential sampling device to heat up samples to analyze the volatile organic compounds extracted from the headspace of the vape. This was accomplished by heating various food and environmental samples (horseradish, cinnamon, and gasoline spiked soil) inside a vape device followed by analyzing the headspace component of vape using solid-phase microextraction (HS-SPME) coupled with gas chromatography- mass spectrometry (GC-MS).

4.2 Background

4.2.1 Headspace analysis

Headspace analysis is a technique in which volatile compounds are directly analyzed from the sample matrix. In this method, the sample matrix of interest is heated

in a closed vial, and then the volatile components in the gas phase are collected and send to GC system for separating them.

A sample matrix can be volatile, nonvolatile, or a mixture of both. However, GC will analyze the volatile components of the sample. For example, samples like blood, polymer, plastic, or cosmetics can consist of high molecular weight nonvolatile components. If these samples are directly inserted to GC system, they may remain in the GC inlet and break down volatile compounds, hence giving unwanted peaks or producing poor analytical response. So, in order to analyze these types of samples, always prior works or extensive sample preparation need to be done, either in the form of extraction to extract the analyte of interest or to precipitate unwanted nonvolatile compounds by using appropriate solvents. Obviously, these sample preparation steps are time consuming, and may dilute the analyte of interest resulting in poorer response. Sometimes the nonvolatile materials are difficult to avoid and can accumulate at the injector, causing degradation of chromatographic performances. There is a way in which the volatile component in these types of samples can be analyzed without doing any prior sample handling or liquid extraction, simply by placing them in a closed container and analyze the gas phase above the sample matrix. The gas or vapor phase is referred to as headspace (HS), and the investigation as a whole is termed as headspace analysis (HSA)

4.2.2 Principal of headspace analysis

In headspace analysis, the original sample matrix (solid or liquid) is placed in a closed container. The volatile component of the sample phase is diffuse through the gas phase (or HS) and will continue to do so until an equilibrium is established between the gas phase and sample phase. Based on the fundamental law of physics, the volatile

components will remain on both phases, and their relative concentrations in the respective phases depends on the partial pressure of the compounds.¹²⁰ An aliquot of the gas sample is collected from the headspace and sent it to GC system for separation.

Apart from vapor pressure or volatility of compounds, the diffusion of volatile components in the headspace also depends on the affinity of the compounds to the sample phase. The ability of a compound to migrate to the gas phase depends on the factor called partition coefficient. Partition coefficient (K) is the ratio of the concentration of the compound (analyte) in the sample phase to the concentration of the analyte in the gas phase (equation 1). the lower the K value, the more readily a compound can migrate into the gas phase, resulting in high responses and low limits of detection. As the objective is to analyze sample in headspace, a lower K value of analyte is favored. This can be

$$K = \frac{c_s}{c_g} \dots\dots\dots \text{Equation 1}$$

where, Cs = concentration of analyte in sample phase

Cg = concentration of analyte in gas phase

achieved by increasing the temperature of the vial or by salting-out (adding salts to aqueous sample). In addition to partition coefficient, phase ratio also affect the concentration of an analyte in headspace. Phase ratio (β) is defined as the volume ratio of two phases in sample vial (equation 2). A lower β value ensures higher response of volatile analyte.

$$\beta = \frac{V_g}{V_s} \dots\dots\dots \text{Equation 2}$$

where,

Vs = Volume of sample phase

V_g = Volume of gas (headspace) phase

However, a lower β value does not always favor a higher response, and often the combination of partition coefficient and phase ratio (equation 3) can determine the concentration of analyte in the headspace. A lower value of $(K + \beta)$ will ensure a higher concentration of analyte in the headspace and better sensitivity.

$$C_g = \frac{C_o}{(K + \beta)} \dots\dots\dots \text{Equation 3}$$

Where,

C_o = original concentration of analyte in the sample

C_g = concentration of analyte in gas phase

4.2.3 Types of headspace analysis

During headspace analysis a solid and liquid sample is placed in a closed vessel (typically vial) with gas volume or headspace above it, and then the vial along with the sample is thermostated at a certain temperature until an equilibrium is established between the two phases. Once the equilibrium is established, an aliquot of the gas phase (headspace) is transferred into the carrier gas stream, which carries it into the column, either by using a gas tight syringe (manually) or using an automated vial pressurized system. This procedure is known as static headspace (HS) analysis which both the phases are in static condition, and the gas phase is only transferred when the phases reach equilibrium state. All this procedure can be carried out in another way in which the removal of gas phase occurs continuously, thus the establishment of equilibrium is not necessary here, and at the end, all the volatile analytes are collected for analysis. This is called dynamic headspace analysis. One type of dynamic headspace is purge and trap

method, where purge gas (helium or nitrogen) is used to drive the gas phase (headspace) to a trap. The trap is usually made of adsorbent material that retain the analyte. Once the extraction is finished, the trapped analyte is removed by heating or backflushing into GC system for analysis. Thermal desorption is another type of gas extraction technique, quite similar to the purge and trap method. However, it differs from the purge and trap technique in that instead of using an inert gas to purge the analyte to a thermal desorption trap, the analyte sample is loaded into a trap. The trap is a tube made of glass or stainless steel packed with adsorbent materials. The tube is then heated to desorb the compounds into a carrier gas stream, which carries the compounds to a second trap to refocus the compounds, finally transferred to a GC column for GC analysis.

4.2.4 Headspace solid-phase microextraction analysis

Solid-phase microextraction (SPME) is an alternate form of dynamic headspace analysis.¹²¹ It is similar to dynamic headspace, but instead of inserting purging gas into the vial to drive the gas to a trapping device, it uses a trap inside the vial. The trap is usually an inert needle, coated with adsorbent materials, placed in the gas phase (headspace) above the sample phase. Once the volatile analyte is adsorbed in the coating materials, it is introduced into the GC injection port to thermally desorb the extracted analyte into the GC column via carrier gas stream. In SPME technique, sampling, extraction, and preconcentration are all done in a single step.¹²² During headspace analysis, the sample phase interact with headspace, and also the headspace interacts with SPME fiber coating. Hence two thermodynamic system exist in which the sample phase try to reach equilibrium with headspace while the headspace seeks to achieve equilibrium

with the fiber coating. Due to this, two partition coefficients are seen in the case of the headspace SPME system.

$$K_{FG} = \frac{C_F}{C_G} \dots\dots\dots \text{Equation 4}$$

$$K_{SG} = \frac{C_S}{C_G} \dots\dots\dots \text{Equation 5}$$

Where,

K_{FG} = Partition coefficient between the fiber coating and headspace phase

K_{SG} = Partition coefficient between the sample phase and the headspace phase

C_F = concentration of analyte in the fiber coating

C_g = concentration of analyte in the headspace (gas) phase

C_S = concentration of analyte in the sample phase

The relationship (equation 6) between these phases can be derived using equation 4 and 5. So a higher K_{FS} indicates more analyte in fiber coating phase, hence favors headspace SPME analysis.

$$K_{FS} = \frac{C_F}{C_S} = \frac{K_{FG}}{K_{SG}} \dots\dots\dots \text{Equation 6}$$

Where,

K_{FS} = Partition coefficient between the fiber coating and the sample phase

4.2.5 Field analytical chemistry

Field analytical chemistry has become very important research area, where analytical measurements are carried out at the location of analyte. Traditionally the analytes are collected and brought to analytical lab from the site, where they are stored until the analysis is completed. One of the major problems associated with this traditional approach is time-consuming. Sample collection, transfer, storage, and analysis take a lot of time that sometimes it takes weeks before the identity of samples can be known, hence

cause delays in decision making for some sites, some of which are concerning regarding human safety and quality of products.

4.2.6 Importance of field analytical chemistry

Field analytical chemistry not only saves time but is also cost effective. By knowing the identity of analyte, many real-time decisions can be taken, especially decisions about environmental remediation or characterization of on-site materials, cost of an operation can be reduced. For example, during cleaning oil contaminated site, if the results of the analysis are known on the site, the cleanup or other treatment can be completed without returning to the site once again after getting the information from the lab.

4.2.7 Portable field laboratory instruments

Over the years, a lot of portable instruments have been developed by many manufactures to aid on-site analysis. These instruments, which are often battery powered, can range from single function handheld instruments to suitcase size instruments. Although these instruments are portable and may be smaller in size, their capabilities are comparable to their benchtop counterparts. Some of the commercially available portable instruments include portable balances, conductivity meter, portable GC-MS, spectrometer/handheld spectrometer, photosynthesis analyzer, Raman spectrometer, TOC analyzer, portable X-ray fluorescence (XRF) analyzers, etc.

4.2.8 Vaporizer device

A vaporizer device is used to inhale the vapor of many plants' substances such as cannabis, tobacco, or other herbs. Sometimes liquids such as essential oil or liquid containing nicotine are also used. Examples of vape devices include e-cigarette

vaporizers, dry herb vaporizers, medical vaporizers, etc. For the purpose of our study, a dry herb vaporizer was used. The description of this device will be discussed further in the experimental section.

4.3 Experimental

4.3.1 Samples

Three samples were analyzed, two food samples and one gasoline spiked soil samples. The food samples were commercially available horseradish (Kelchner's brand) and ground cinnamon (Great Value brand) and were collected from local grocery stores. The gasoline fuel was supplied by ICM, Inc. The non-spiked soil was collected from an SDSU construction site.

4.3.2 Dry herb vaporizer

The commercially available dry herb vaporizer (vape) used in this experiment was purchased from Jedi. It consists of a 14 mm ceramic chamber surrounded by a metallic body. It has a real temperature control with temperature can be set between 150 to 240 °C. It also includes a glass mouthpiece which can be connected with the ceramic chamber. So, this could be used as a potential heating pod in which the samples can be filled inside the chamber to heat it, followed by extraction of the headspace composition with the help of a SPME fiber assembly and manual holder through the mouthpiece. Figure 27 shows the Jedi vape device accompanied by a mouthpiece, a 13 mm Black Top Hat Cap, and a cylinder-shaped container made with aluminum foil in order to make easy clean up after each experiment. When the mouthpiece is screw tight to vaping chamber, the volume of the device is estimated to be 3 mL. This volume was

estimated by combining the volume of space inside the chamber and the volume of the mouthpiece.

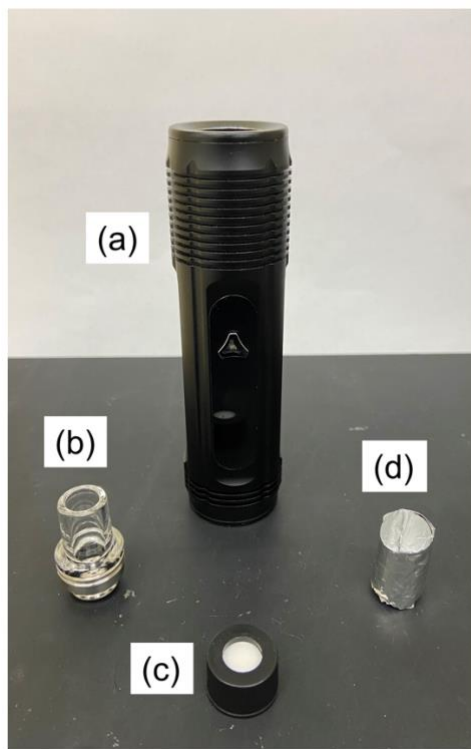


Figure 27. Jedi dry herb vaporizer (a) with mouthpiece (b), top hat cap, and (d) aluminum foil container

4.3.3 Analytical procedure

Analysis of samples was done using two analytical procedures, one with the heating sample inside the vaporizer (vape) followed by extraction of headspace components with the SPME fiber (procedure A) and another procedure consists of heating and extracting the sample inside a headspace vial (procedure B). Extracted headspace components were both analyzed using GC-MS

4.3.3.1 Procedure A (using vape)

Specific mass of respective samples (horseradish (500 mg), cinnamon (20 mg) and gasoline spiked soil (400 mg) were loaded in the ceramic chamber containing the

aluminum foil container (Figure 28 (a)). The mouthpiece was attached on the top of the chamber, followed by a 4ml vial top hat cap on the top of the mouthpiece in order to stop the vapor escaping to outside. The vape was then turned on at the respective extraction temperature (150, 200, and 240 °C) to incubate the sample for five minutes (Figure 28 (b)).

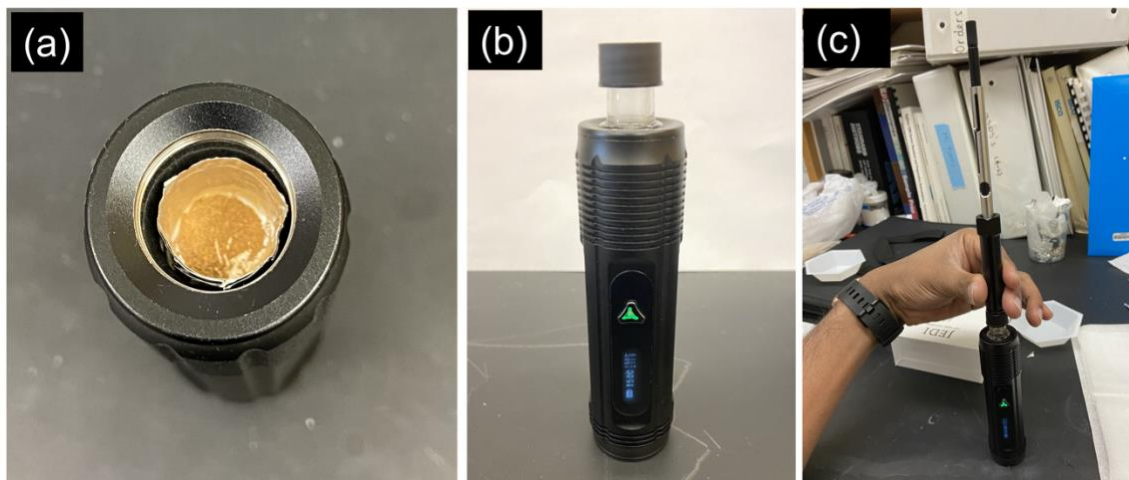


Figure 28. Experimental set up for vape extraction a) sample loading b) incubation c) extraction

Following the incubation, the headspace components of the sample were extracted using PDMS coated SPME fiber using a manual holder (Figure 28 (c)). The adsorbed components were thermally desorbed at the GC injection port for GC-MS analysis. The incubation and extraction time here include the time required by the vape device to reach the respective temperature, which varies from samples to samples (Table 9).

Table 9. Time (s) required to reach incubation and extraction temperature

Samples/Temp.	Incubation time (s)			Extraction time (s)		
	150 °C	200 °C	240 °C	150 °C	200 °C	240 °C
Horseradish	35.3 ± 7.1	66 ± 32	136 ± 55	9.3 ± 1.5	17.0 ± 4.6	48 ± 22
Cinnamon	11.67 ± 0.58	18.0 ± 2.6	57 ± 21	6.67 ± 0.58	10.3 ± 1.2	20.7 ± 4.7
Spiked soil	10.3 ± 2.1	35.3 ± 7.1	31.7 ± 1.5	6.0 ± 1.0	8.7 ± 2.1	10.7 ± 1.2

4.3.3.2 Procedure B (using conventional headspace set up)

The experimental set up for conventional headspace was almost similar to the vape set up except the sample was heated in a traditional 10 milliliter headspace vial in a silicon oil bath at 40, 150 and 200 °C (240 °C was avoided since silicon oil can withstand temperature up to 200 °C) followed by extracting the headspace component using PDMS coated SPME fiber using manual holder (Figure 29). The adsorbed components were desorbed in the GC injection port for GC-MS analysis. The septa of the vial was cut in “X” shape before use to avoid explosion due to pressure buildup inside the vial at higher temperatures.

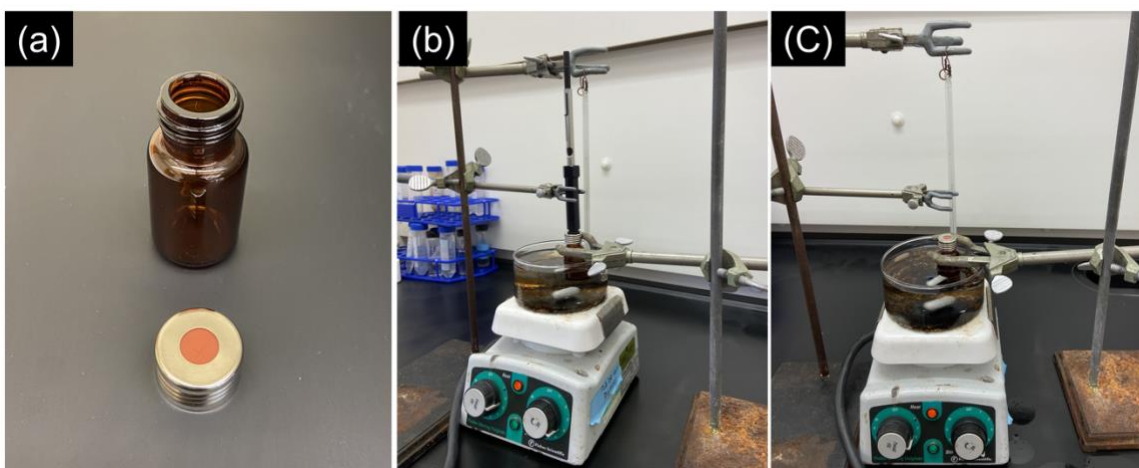


Figure 29. Experimental set up for conventional headspace extraction a) vial and cap b) sample incubation c) sample extraction

4.3.4 Headspace solid-phase microextraction (HS-SPME) analysis

A Specific mass of respective samples (horseradish 500 mg, cinnamon 20 mg, and gasoline spiked soil 400 mg) were transferred to the ceramic chamber of the vape or 10 mL headspace vials. SPME of headspace sample components was carried out using a 100 μm polydimethylsiloxane coated fiber by rapidly inserting it into the headspace of the ceramic chamber or the vial. The SPME fiber and the SPME manual holder used in this

experiment were purchased from Supelco (Bellefonte, PA, USA). Extraction temperature was chosen as 150, 200, and 240 °C for vape analysis and 40, 150, 200 °C for conventional headspace analysis. The fiber was preconditioned for 30 minutes in the GC injection port at 250 °C before each extraction. The extracted sample was desorbed in the GC injection port at 250 °C for 5 min, and the experiment was carried out in triplicate for each sample.

4.3.5 GC-MS analysis

All samples were analyzed using an Agilent 7890B gas chromatograph (Agilent Technologies, Little Falls, DE) coupled to an Agilent Technologies 5977B mass spectrometer and fitted with a 30-m x 0.25-mm, 0.25- μ m DB-5MS column (Agilent Technologies, Little Falls, DE). The hydrogen carrier flow was kept constant at 1.2 mL/min. Split injection was performed with the injection port at 250 °C. The mass spectrometer was operated in electron ionization mode (with 70 eV ionizing voltage). The transfer line temperature was kept at 250 °C. The MS temperatures were ion source 250 °C and quadrupole 150 °C. The scan range was 30-400 U (3.9 scans/s). Mass spectrometer analysis were done in full scan mode, and the data were processed using ChemStation software (Agilent Technologies). The compounds were identified by comparing the mass spectra of extracted compounds to the mass spectra of National Institute of Standard and Technology (NIST) library. The oven temperature program and the split ratio were varied from sample to sample and are described here below:

Horseradish sample: The GC method begins with an initial oven temperature of 40 °C for 2 min, then ramped at 8 °C/minute to 250°C and held for 5 min for a total run time of 33.25 min. Split ratio 5:1 was used.

Cinnamon sample: The GC method begins with an initial oven temperature of 40 °C for 2 min, then ramped at 8 °C/minute to 250°C and held for 5 min, for a total run time of 33.25 min. Split ratio 100:1 was used.

Gasoline spiked soil: The GC method begins with an initial oven temperature of 35 °C for 1 min, then ramped at 10 °C/minute to 220°C and held for 1 min, followed by a final ramp at 50 °C/minute to 250°C and held for 5 min for a total run time of 26.10 min. Split ratio 5:1 was used.

4.3.6 Data analysis

Analysis of results obtained from GC-MS was done by determining the relative percent peak area of identified compounds. Only few major compounds were selected to calculate the relative percent peak. Relative percent peak was calculated using the following equation:

$$\text{Relative percent peak area} = \frac{X_1}{X_{total}}$$

Where X_1 is the area of an identified compound and X_{total} is the total peak area of detected compounds, calculated using the autointegration function in ChemStation software (Agilent Technologies).

4.4 Results and discussion

4.4.1 HS-SPME-GC-MS analysis of horseradish components

Figure 31 shows a representative total ion chromatogram (TIC) of headspace extract from horseradish sample using both vapo and headspace (conventional) method. As stated previously the figure does not include extraction at 240 °C for headspace method. So, instead of 240 °C, extraction at 40 °C was included, since it is the most

commonly used extraction temperature for headspace method. Another form of figure 31 with expanded y-axis is also given Figure 32. Horseradish, a condiment made from roots of horseradish plants, is used in some cuisine to add an extra burst of flavor to food. D'auria et al., extracted 18 compounds from fresh horseradish samples, and the main compounds were allyl isothiocyanate, 4-isothiocyanato-1-butene, and 2-phenylethyl isothiocyanate.¹²³ In our study, we were able to identify allyl thiocyanate (ATC), allyl isothiocyanate (AITC), 2-isothiocyanatobutane, 4-isothiocyanato-1-butene, benzenepropanenitrile (BPN), and 2-phenethyl isothiocyanate. Among these, allyl thiocyanate (ATC), allyl isothiocyanate (AITC), benzenepropanenitrile (BPN), and phenethyl isothiocyanate (PITC) were chosen for analysis since these were able to be picked up by ChemStation software using autointegration. The structures of the chosen compounds are shown in Figure 30.

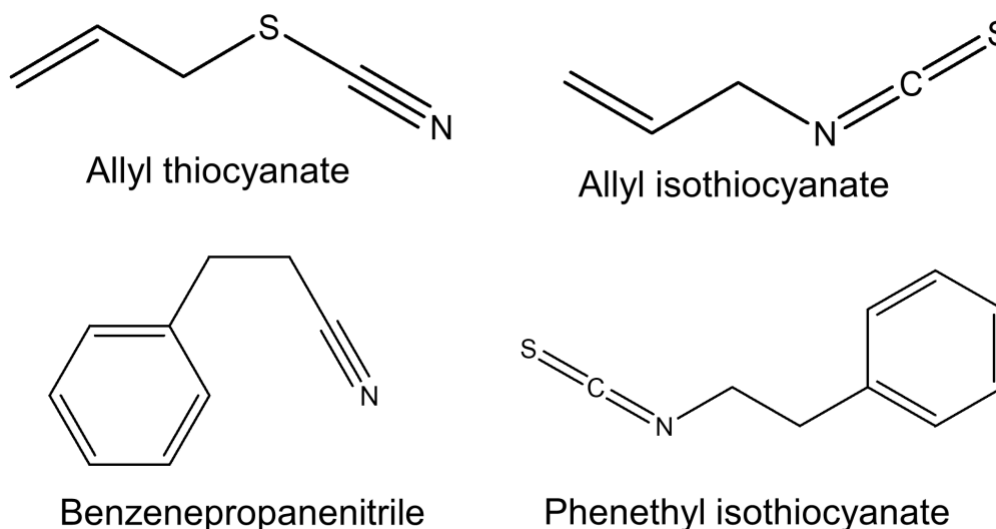


Figure 30. Structure of horseradish components chosen for analysis

Although both methods gave similar chromatograms in terms of the number of identified peaks (Figure 31), in terms of the number of total extracted compounds, the

vape method produced more compounds peaks compared to the headspace methods (Figure 32). Compared to peak intensity, the vape method is also a more concentrated method, as the peak intensity is much higher. The figure also shows chromatograms at different extraction temperatures, and as the temperature was increased, the peak intensity was decreased. Besides doing the extraction at higher temperatures, the headspace method was also done at 40 °C, a very common extraction temperature for headspace analysis. At this temperature, the peak intensity is much higher compared to extraction at 150 or 200 °C for the headspace method.

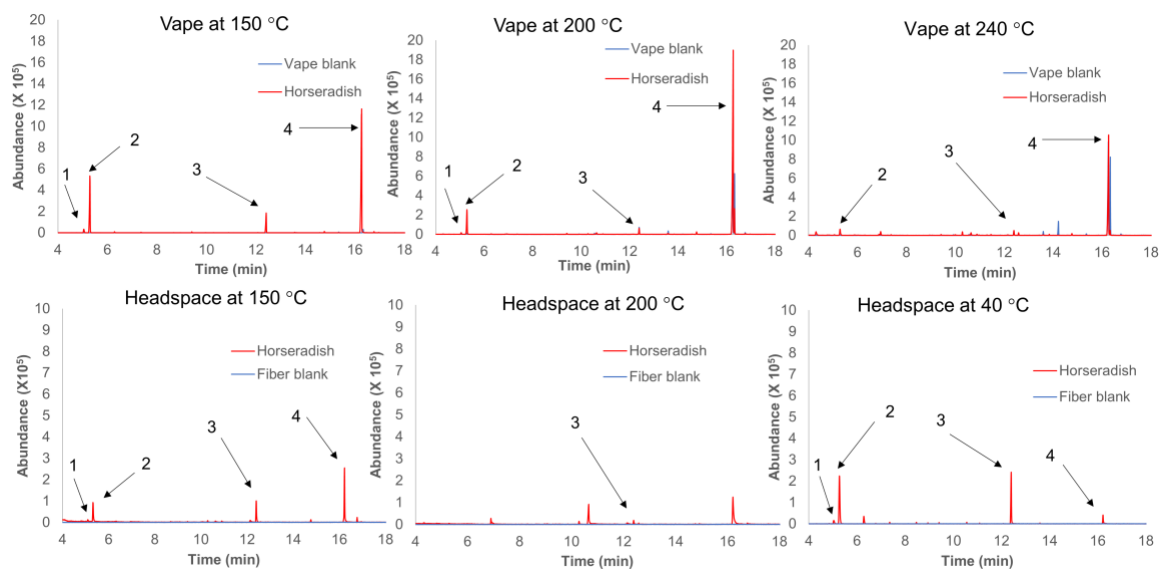


Figure 31. Chromatograms of extracted horseradish components at different temperature using both vape and headspace method. The abundance ($\times 10^5$) is plotted against retention times in min. 1. Allyl thiocyanate, 2. Allyl isothiocyanate, 3. Benzenepropanenitrile and 4. Phenethyl isothiocyanate

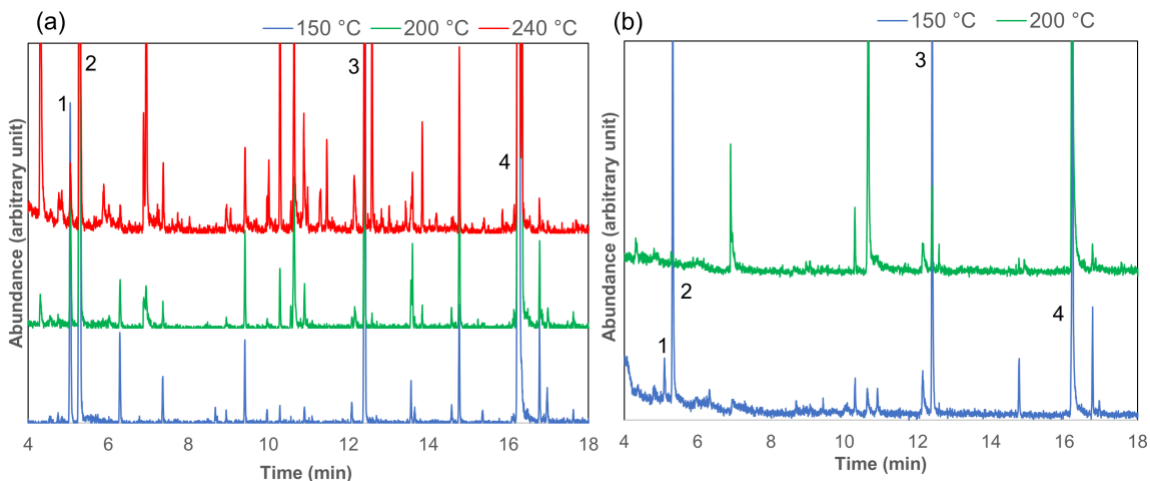


Figure 32. Chromatograms of extracted horseradish components at different temperature with expanded y-axis (a) vape method and (b) headspace method

The relative percent area of identified compounds was also calculated to quantify the horseradish compounds. The relative percent area results are summarized in Table 10.

Table 10. Relative Percent Peak Area of Horseradish Components.

	Temp. (°C)	Vape method			Headspace method		
		Avg.	Std.Dev	% RSD	Avg.	Std.Dev	% RSD
Allyl thiocyanate	40				2.92	0.22	7.6
	150	0.32	0.12	37	0.46	0.5	107
	200	0.33	0.12	37	-	-	-
	240	-	-	-			
Allyl isothiocyanate	40				34.4	2.4	7
	150	4.5	2	44	5.9	4.4	75
	200	3.9	2.1	54	-	-	-
	240	1.14	0.65	57			
Benzenepropanenitrile	40				25.4	4.6	18
	150	1.57	0.35	22	2.5	1.9	76
	200	0.89	0.11	13	0.084	0.093	110
	240	1.31	0.34	26			
Phenethyl isothiocyanate	40				5.7	2.3	41
	150	12	2.7	23	24	20	83
	200	27.5	12.8	46	-	-	-
	240	18.5	5.8	31			

Although both methods gave a very similar relative percent of compounds, however, the percent area was slightly higher for the headspace method for all compounds at 150 °C. These methods are not comparable at 200 °C as most of the identified peaks were missing at 200 °C for the headspace method. This could be due to the reason that the horseradish samples are not that stable at higher temperature, as the decomposition of the samples was observed at the higher temperature. This is evident by the change of color of the samples (yellow/white to brown and eventually became black in Figure 33). The percent area result obtained with the headspace method at 40 °C also suggests that the temperature stability of the samples at the lower temperature.

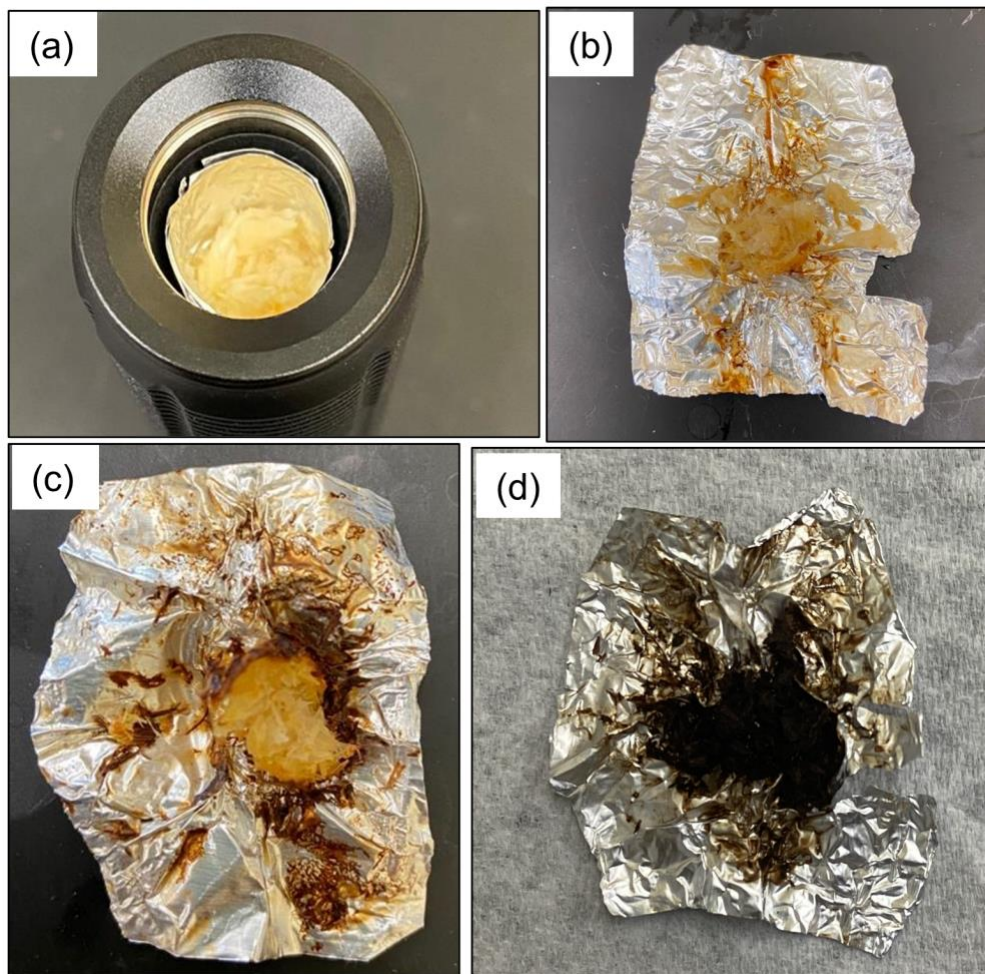


Figure 33. Horseradish samples (a) pre-extraction, (b) post-extraction at 150 °C, (c) post-extraction at 200 °C, and (d) post-extraction at 240 °C

4.4.2 HS-SPME-GC-MS analysis of cinnamon components

The TIC in Figure 35 shows the components of cinnamon using both vial and headspace procedures at different extraction temperatures, with a different form of the chromatogram with expanded y-axis are also shown in Figure 36. Since extraction was not carried out at 240 °C for headspace method, a most commonly used extraction temperature at 40 °C was included in Figure 35 for comparison purposes. Cinnamon, an important spice, is mainly used to add flavor to a wide variety of cuisines. Cinnamon is mainly composed of cinnamaldehyde, trans or E-cinnamaldehyde, cinnamic acid,

cinnamate, etc., with E-cinnamaldehyde being one of the important constituents of cinnamon.¹²⁴ In our study, we identified E-cinnamaldehyde, α -copaene, α -muurolene, and δ -cadinene being the major components of cinnamon extracts. The structures of these compounds are illustrated in Figure 34.

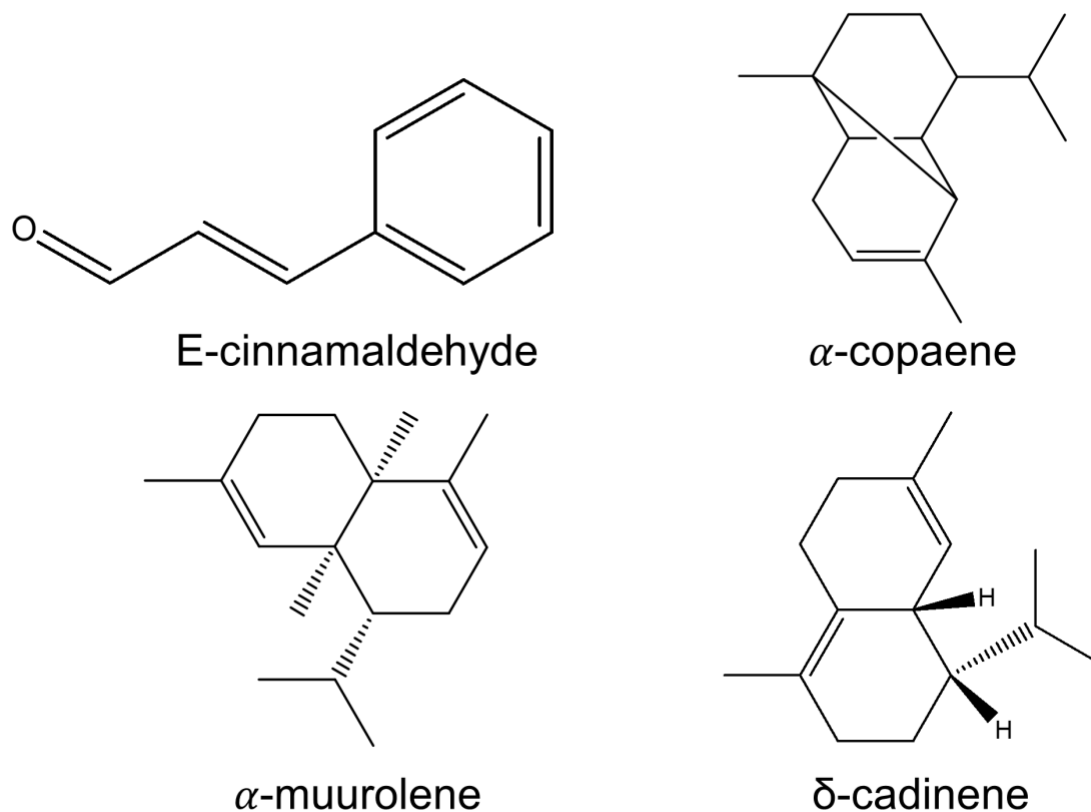


Figure 34. Structure of cinnamon components chosen for analysis

Although all four compounds are observed in chromatograms for both methods, the peak intensity was significantly higher in the vape method. The temperature plays a significant role in headspace extraction. When the temperature is increased, more molecules are transitioned to headspace. Therefore, peak intensity should increase. This is observed in the case of E-cinnamaldehyde for the vape method, as the peak intensity of E-cinnamaldehyde increased with increasing extraction temperature. However, for the

other three compounds, the change of peak intensity with increasing temperature remained similar. Almost similar results were obtained for all other unidentified peaks, as the intensity of the peaks either remained similar or decreased with increasing temperatures (Figure 36). However, this decrease in intensity was very high in the headspace method (except E-cinnamaldehyde), that some peaks disappeared at 200 °C. Both methods are comparable in terms of the number of peaks at 150 °C, however, as the intensity decreases with temperature, the headspace method lost numbers of eluting peaks at 200 °C.

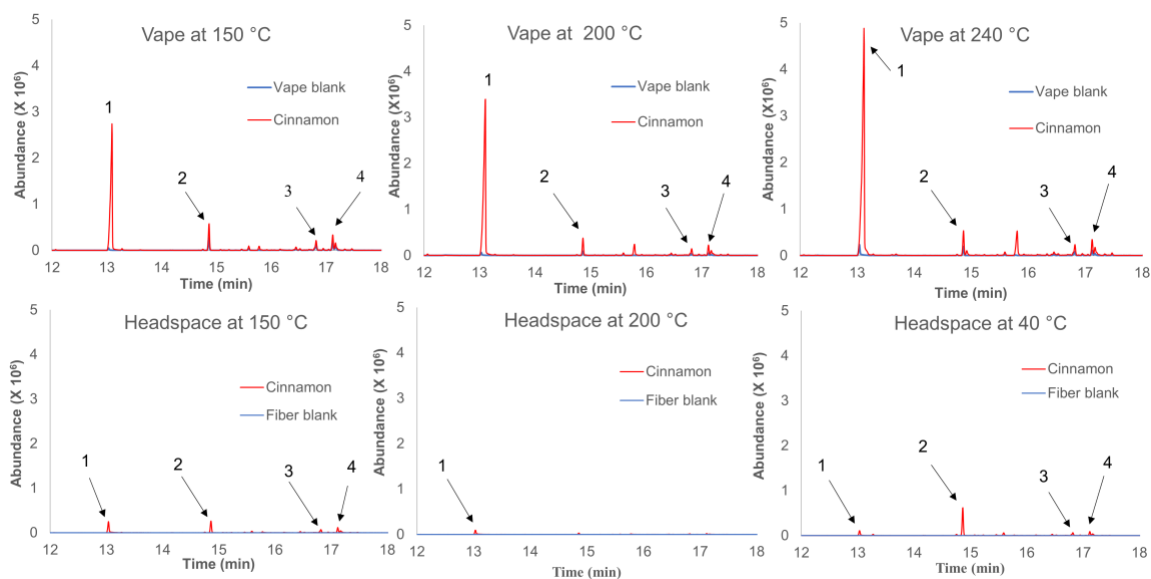


Figure 35. Chromatograms of extracted cinnamon components at different temperature using both vapo and headspace method. The abundance ($\times 10^6$) is plotted against retention times in min. 1. E-cinnamaldehyde, 2. α -copaene, 3. α -muurolene and 4. δ -cadinene

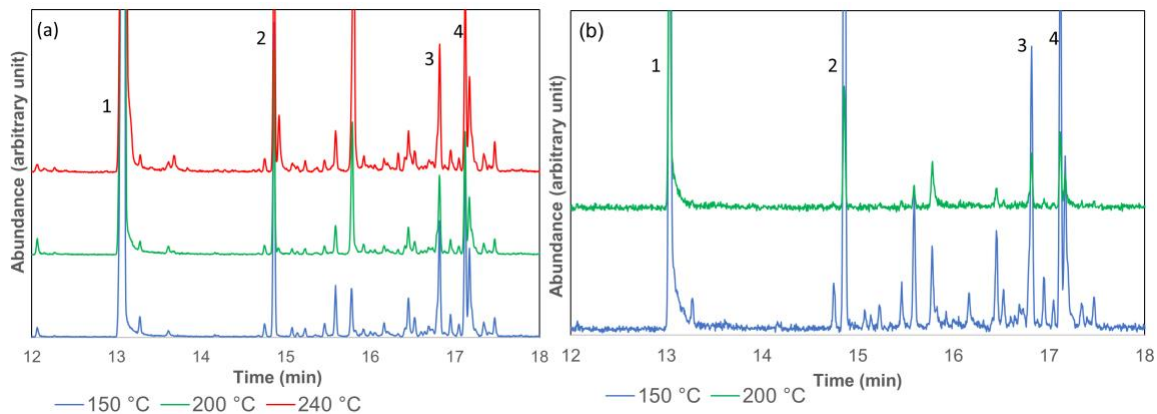


Figure 36. Chromatograms of extracted cinnamon components at different temperature with expanded y-axis (a) vape method and (b) headspace method. 1. E-cinnamaldehyde, 2. α -copaene, 3. α -murolene and 4. δ -cadinene

The relative percent area of identified compounds was also calculated. Table 11 shows the relative content of cinnamon extracted compounds in terms of relative percent peak area.

Table 11. Relative percent peak area of cinnamon components.

	Temp. (°C)	Vape method			Headspace method		
		Avg.	Std.Dev	% RSD	Avg.	Std.Dev	% RSD
E-cinnamaldehyde	40				11.16	0.29	2.6
	150	58	14	23	35.4	2.9	8.2
	200	81.5	1.4	1.7	93	12	12
	240	77.9	4.2	5.4			
α -copaene	40				60.87	0.42	0.70
	150	7.9	1.8	23	36.1	4.6	13
	200	4.69	0.61	13	20	—	—
	240	3.3	1.1	35			
α -murolene	40				7.62	0.12	1.5
	150	3.4	1.1	32	11.48	0.77	6.7
	200	2.33	0.10	4.1	-	-	-
	240	2.14	0.40	19			
δ -cadinene	40				8.96	0.24	2.6
	150	4.4	1.3	28	13.28	0.25	1.9

200	3.00	0.23	7.6	-	-	-
240	2.51	0.52	21			

The headspace method is seemed to be more effective in relative percent peak area, as these areas were higher for all compounds for the headspace method except for E-cinnamaldehyde at 150 °C and α -muurolene at 200 °C. The headspace method produced the highest yield (in terms of percent peak area) of E-cinnamaldehyde at 200 °C. The extraction temperature had a very significant effect on extracted compounds, as E-cinnamaldehyde gave a higher yield at 200 °C for both methods. While for all compounds except E-cinnamaldehyde, the relative percent area decreased with temperature. A possible explanation may be degradation, followed by char formation of cinnamon at 240 °C, which was also evident by the color of the cinnamon powder changed to black after the extraction (Figure 37).

The headspace method also gave a similar result as cinnamaldehyde percent increased at higher temperatures. However, in this case, cinnamaldehyde was not the highest yield compound, as α -copaene percent peak year was higher at 150 °C. Similar to the vapo method, all the compounds except cinnamaldehyde yield decreased with the increase of temperature. The result obtained in 40 °C was very interesting as at this temperature, the amount of extracted E-cinnamaldehyde was lowest among all the conditions, suggesting 40 °C is the least favorable condition for extraction of E-cinnamaldehyde.

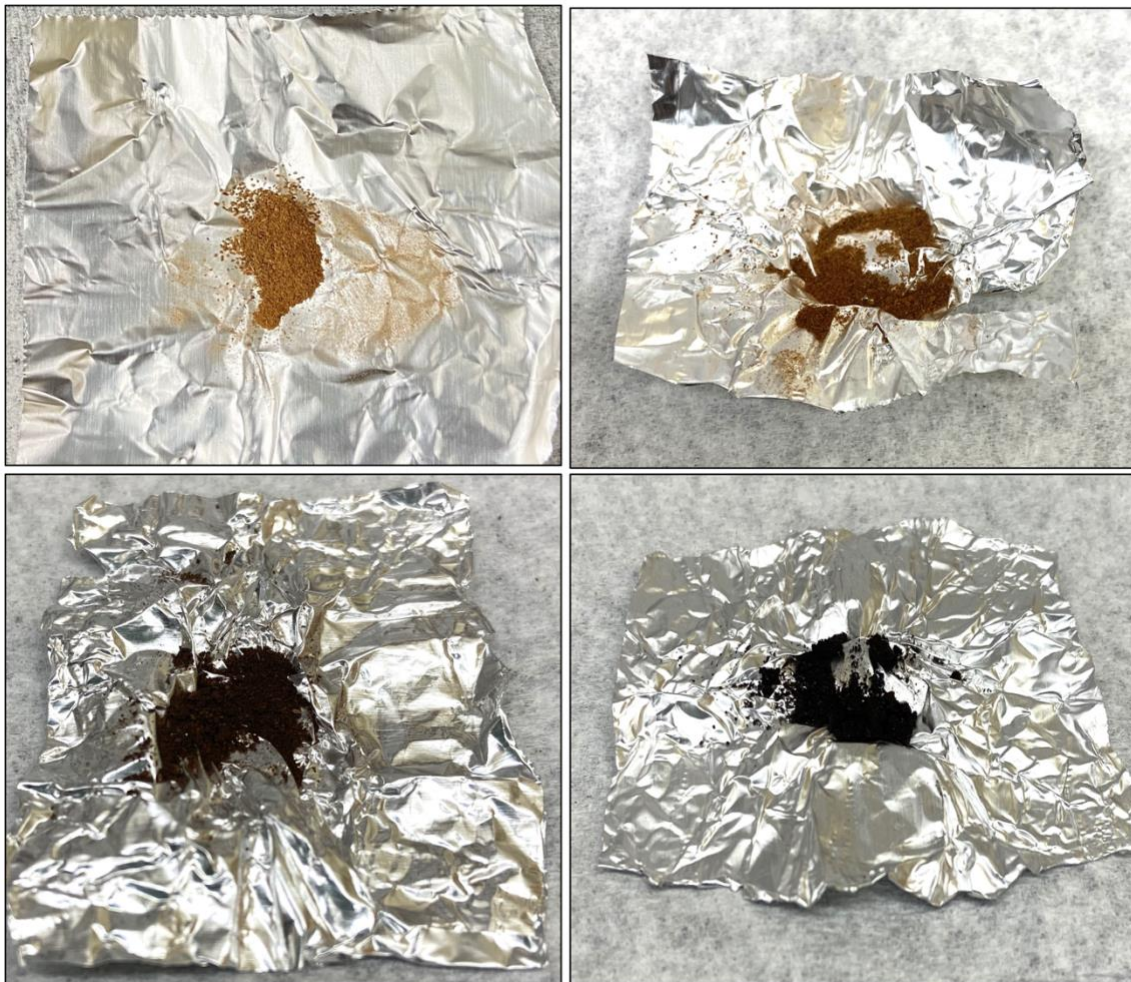


Figure 37. Cinnamon samples (a) pre-extraction, (b) post-extraction at 150 °C, (c) post-extraction at 200 °C, and (d) post-extraction at 240 °C

4.4.3 HS-SPME-GC-MS analysis of gasoline spiked soil

Figure 39 shows a representative total ion chromatogram (TIC) of gasoline components obtained from headspace extraction of gasoline spike soil using vapo and headspace (conventional) procedure at different extraction temperature. Similar to horseradish and cinnamon samples, the figure does not include extraction at 240 °C for headspace method, and instead of 240 °C, extraction at 40 °C was included. A different form of the chromatogram, showing expanding y-axis, is also illustrated in Figure 40. Gasoline, a hydrocarbon rich fluid, contains hundreds of components. However, for the

purpose of our study, some major components (based on peak size) were identified to evaluate the efficacy of our extraction method. The structure of the selected compounds are shown in Figure 38.

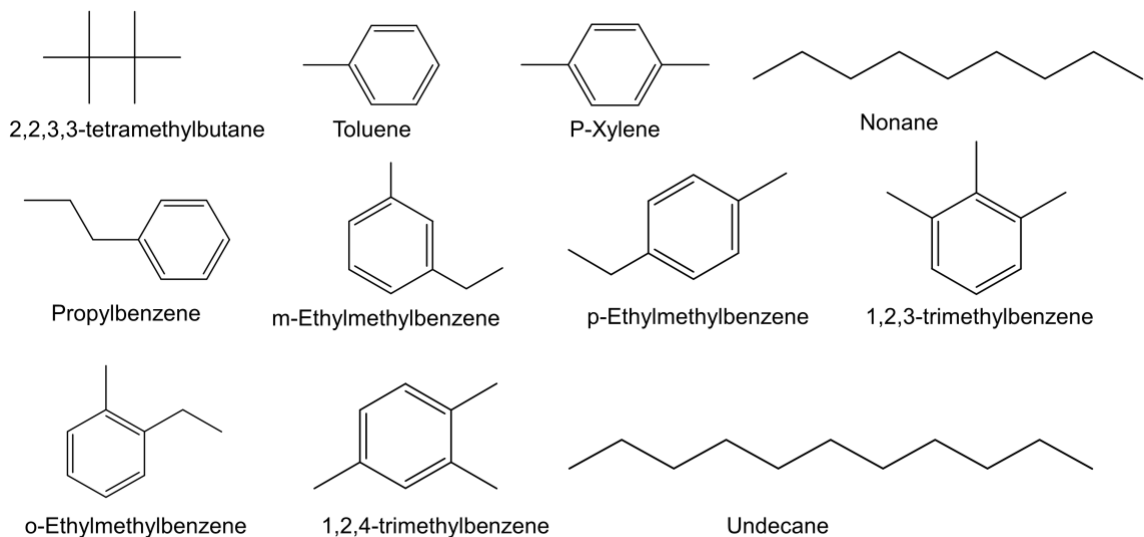


Figure 38. Structure of gasoline spiked soil components chosen for analysis

Comparable chromatograms were obtained in terms of the number of peaks for both vapo and headspace methods, however, the peak intensity is much higher (about ten magnitudes) in the vapo method. The temperature also affects the intensity of the peak, as at higher temperature peak intensity decreased, with the most drastic fall of intensity was observed at 240 °C. Although much similar, the extraction carried out at the usual condition (at 40 °C) seems to be more effective, as the peak intensity was slightly higher compared to the peak intensity at 150 and 200 °C using the headspace method. As we were dealing with very high volatile compounds, the compounds tend to lose more in the headspace method at higher temperatures.

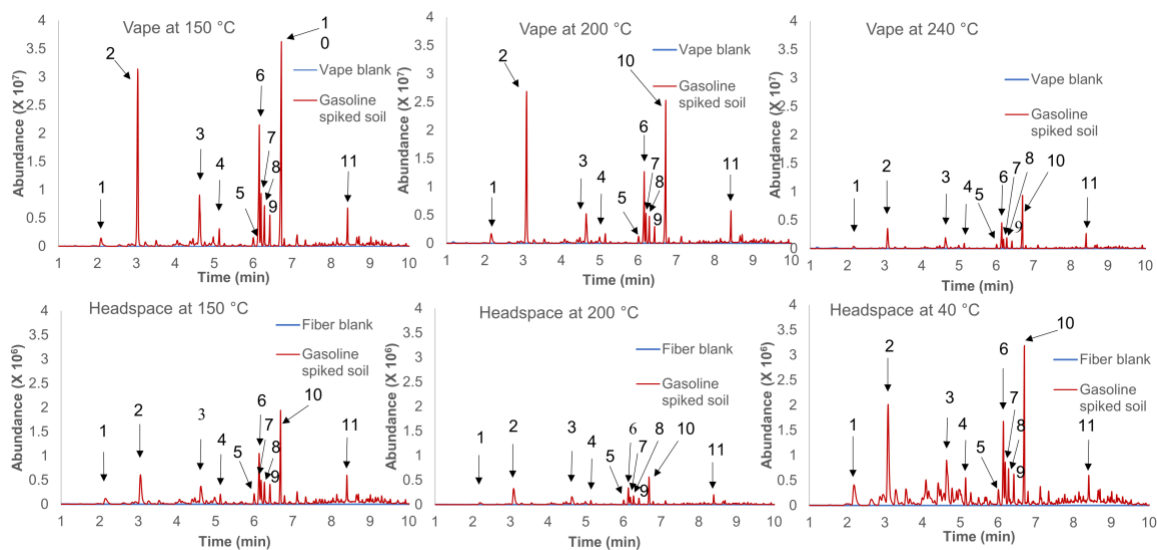


Figure 39. Chromatograms of components of gasoline spiked soil at different temperature using both vapo and headspace method. The abundance ($\times 10^7$ (for vapo) and $\times 10^6$ (for headspace)) is plotted against retention times in min. 1. 2,2,3,3-tetramethylbutane, 2. Toluene, 3. p-Xylene, 4. Nonane, 5. Propylbenzene, 6. m-Ethylmethylbenzene, 7. p-Ethylmethylbenzene, 8. 1,2,3-trimethylbenzene, 9. o-Ethylmethylbenzene, 10. 1,2,4-trimethylbenzene, and 11. Undecane

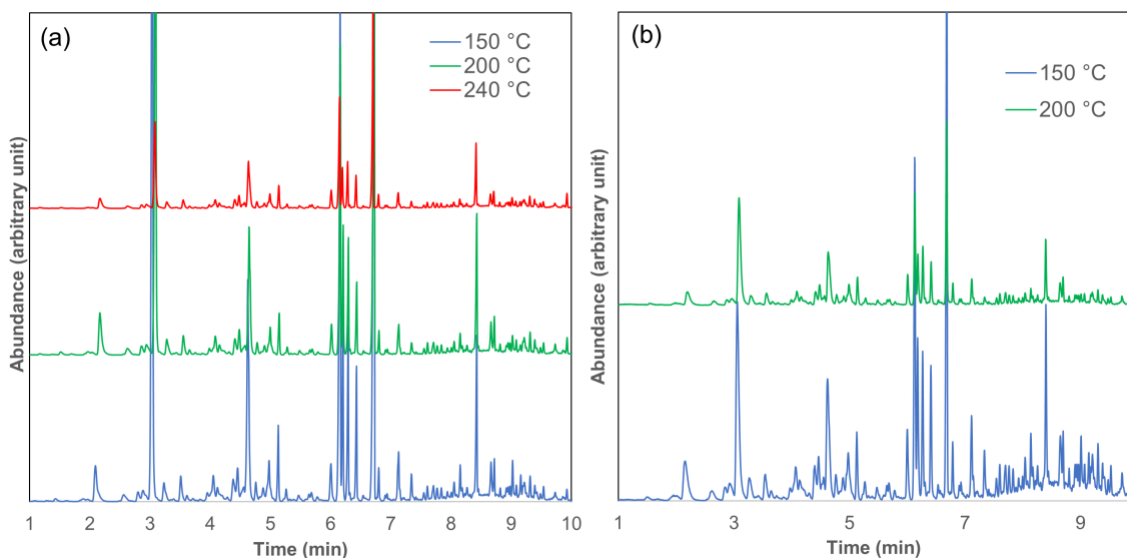


Figure 40. Chromatograms of components of gasoline spiked soil at different temperature with expanded y-axis (a) vapo method and (b) headspace method.

The relative content of extracted compounds was also calculated and is expressed here in terms of percent peak area. The results are summarized in Table 12. Although the vape method is more concentrated based on peak intensity, but in terms of the relative percent peak area, mixed results were obtained. At 150 °C the vape method was seen to be more effective in terms of relative percent peak area for most of the identified compounds. However, the headspace method was more effective at 200 °C. The temperature affected the experiment differently for vape and headspace methods. The increasing temperatures positively affected the headspace method, with all components saw an increase in relative percent area from 40 to 200 °C. In the case of the vape method, the relative percent area decreased for most compounds at 200 and 240 °C from 150 °C, except for an increase of toluene at 200 °C, nonane at 240 °C, and propylbenzene at both 200 and 240 °C from 150 °C.

Table 12. Relative percent peak area of gasoline spiked soil components

	Temp. °C	Vape method			Headspace method		
		Avg.	Std.Dev	% RSD	Avg.	Std.Dev	% RSD
Tetramethylbutane	40				0.19	0.15	79
	150	1.40	0.58	42	2.14	0.58	27
	200	1.5	1.2	82	3.46	0.64	18
	240	1.18	0.96	81			
Toluene	40				7.7	6.6	86
	150	13.7	4.7	34	9.80	0.56	5.8
	200	15.8	5.5	34	18.9	3.2	17
	240	8.0	3.2	40			
p-Xylene	40				4.0	3.4	85
	150	7.37	0.67	9.1	5.75	0.17	3.0
	200	5.35	0.54	10	9.99	0.98	9.8
	240	5.1	1.6	32			
Nonane	40				1.1	1.0	85
	150	1.15	0.15	13	1.517	0.010	0.68
	200	0.95	0.15	16	2.57	0.12	4.7
	240	1.27	0.51	40			
Propylbenzene	40				0.85	0.73	85
	150	0.80	0.18	23	1.708	0.058	3.4
	200	0.88	0.16	18	2.88	0.12	4.1
	240	1.22	0.51	42			
m-Ethylmethylbenzene	40				3.4	2.9	85
	150	10.23	0.39	3.8	7.50	0.31	4.2
	200	8.38	0.97	12	9.51	0.39	4.1
	240	8.2	1.3	16			
p/o-Ethylmethylbenzene	40				1.6	1.4	85
	150	3.35	0.17	5.0	3.334	0.027	0.81
	200	2.98	0.47	16	4.64	0.14	3.1
	240	2.90	0.43	15			
1,2,3-Trimethylbenzene	40				1.3	1.1	85
	150	3.75	0.85	23	2.964	0.027	0.91
	200	3.12	0.42	13	4.698	0.025	0.53
	240	3.45	0.69	20			
p/o-Ethylmethylbenzene	40				1.2	1.0	85
	150	2.27	0.17	7.5	2.79	0.15	5.4
	200	1.94	0.29	15	3.94	0.18	4.6
	240	2.14	0.30	14			
1,2,4-trimethylbenzene	40				5.2	4.4	85
	150	17.56	0.93	5.3	12.1	1.2	10
	200	18.1	2.8	16	13.26	0.30	2.3
	240	17.6	1.6	9.2			
Undecane	40				1.5	1.3	85
	150	5.5	2.3	41	4.10	0.16	3.8
	200	7.0	3.0	43	4.58	0.35	7.7
	240	7.9	3.4	44			

Overall, the analytical technique we developed here has shown promising results in the application of headspace extraction. The extracted compounds have significantly higher intensity in the vape method compared to the headspace method. The reason, we think that the vape method was more efficient in keeping the headspace vapor trapped inside the sample chamber and the volume being significantly smaller for vape compared to the headspace vials. The relative content of the compounds in terms of relative percent peak area in the headspace method was higher compared to the vape method for horseradish and cinnamon samples, while mixed results were obtained in the case of soil samples. The temperature played an important role in extraction as the intensity, as well as the relative content, both decreased with increasing temperature for most of the extracted compounds from all studied samples. However, at higher temperature, some compounds peaks were missing in headspace method, while in vape method the peak intensity although decreased, but all the compound peak was still detectable at the higher temperature. Based on our research, the vape method have several advantages:

- It is very easy and convenient to use
- Programmable temperature control
- Portable and can be performed on site
- Concentrated method, minimal amount of sample is needed
- Extraction can be performed at a high temperature range (150 -200 °C)

Although not many, this method has some disadvantages. The cleaning of the sample chamber is tough. Although the problem can be minimized by using aluminum foil, some unwanted peaks, although intensity-wise is very low, probably coming out from the device itself and previous runs, is an issue.

4.5 Conclusion

In this study, we presented a simple, portable, and convenient commercial vape device, which can be used as a heating and extraction medium for the headspace solid-phase microextraction method. We have shown that this method can analyze food and environmental samples at a temperature higher than usual headspace extraction temperatures. We have also compared this method with the headspace method accompanied by traditional heating arrangement and found that the vape method not only gave comparable results but, in some cases, it was better, considering how concentrated this method can be by using a very small amount of sample. Since, as per our knowledge, this is the first time such a device has been used to carry out headspace extraction, with some modification of the device and method optimization, this method can become very efficient in analyzing a wide variety of samples, both in house and onsite analysis.

5 CONCLUSION

The vapor phase composition of ethanol blended gasoline was determined using an HS-SPME coupled with the GC-MS method to understand the effect of ethanol addition on the evaporative emission of gasoline components. This method successfully showed how the vapor phase composition of paraffins, *i*-paraffins, monoaromatics, and mononaphthene changes with the change of ethanol percentages at different temperatures.

A GC-MS method was developed to investigate the biodegradation of petroleum hydrocarbons from kerosene by *B. amyloliquefaciens* isolates. A UHPLC-DAD method was also developed to identify and quantify the lipopeptide biosurfactants produced by the isolates. Based on the GC-MS and UHPLC results, not enough evidence was found to confirm that the bacterial isolates were utilizing or degrading petroleum hydrocarbons from kerosene to grow and produce lipopeptide biosurfactants.

A simple, portable, and convenient analytical technique using a commercial dry herb vaporizer was developed to analyze the VOCs using an HS-SPME-GC-MS method. When the results were compared to the traditional headspace SPME-GC-MS, although similar results were obtained in terms of relative percent peak area, the vape method proved to be more concentrated.

Overall, the work is done, and results obtained in this dissertation have shown the understanding of evaporative emission characteristics of gasoline components, and the effect of ethanol percentage on hydrocarbon components, especially more toxic ones such as BTEX or monoaromatics. Based on the result from biodegradation studies, this work has shown whether a bacterial isolate could potentially biodegrade petroleum

hydrocarbons. Moreover, a new analytical technique has been introduced in this dissertation work, which is portable and has the potential to complement currently developed headspace SPME analysis of volatile organic compounds.

6 REFERENCES

1. Nugent, O., *The smog primer*. Pollution Probe: 2002.
2. Hinrichs, R.; Kleinbach, M. H., *Energy: Its Use and the Environment*. Cengage Learning: 2013.
3. Filippidou, E.; Koukouliata, A. J. P. H. S., Ozone effects on the respiratory system. **2011**, *1*, 144-55.
4. Sharma, S. B.; Jain, S.; Khirwadkar, P.; Kulkarni, S. J. I. J. o. R. i. P.; Biotechnology, The effects of air pollution on the environment and human health. **2013**, *1* (3), 391-396.
5. Simanzhenkov, V.; Idem, R., *Crude oil chemistry*. CRC Press: 2003.
6. Hester, R. E.; Harrison, R. M., *Volatile organic compounds in the atmosphere*. Royal Society of Chemistry: 1995.
7. Wolkoff, P. J. I. A., Suppl, Volatile organic compounds. **1995**, *3*, 1-73.
8. Rajabi, H.; Mosleh, M. H.; Mandal, P.; Lea-Langton, A.; Sedighi, M. J. S. o. T. T. E., Emissions of volatile organic compounds from crude oil processing—Global emission inventory and environmental release. **2020**, 138654.
9. Lubes, G.; Goodarzi, M. J. C. r., Analysis of volatile compounds by advanced analytical techniques and multivariate chemometrics. **2017**, *117* (9), 6399-6422.
10. Hillel, D.; Hatfield, J. L., *Encyclopedia of Soils in the Environment*. Elsevier Amsterdam: 2005; Vol. 3.
11. Speight, J., *Handbook of Petroleum Analysis*. Hoboken. NJ: John Wiley and Sons: 2001.
12. Chilcott, R. P. J. H. P. A. C. H.; Poisons Division . Chilton, D., Oxfordshire, OX11 0RQ, United Kingdom, Compendium of chemical hazards: kerosene (fuel oil). **2006**.
13. Curl, H. C.; O'Donnell, K., Chemical and physical properties of refined petroleum products. **1977**.
14. Adeniji, A.; Okoh, O. O.; Okoh, A. I. J. J. o. C., Analytical methods for the determination of the distribution of total petroleum hydrocarbons in the water and sediment of aquatic systems: A review. **2017**, *2017*.
15. Okparanma, R. N.; Mouazen, A. M. J. A. S. R., Determination of total petroleum hydrocarbon (TPH) and polycyclic aromatic hydrocarbon (PAH) in soils: a review of spectroscopic and nonspectroscopic techniques. **2013**, *48* (6), 458-486.
16. Demeestere, K.; Dewulf, J.; De Witte, B.; Van Langenhove, H. J. J. o. c. A., Sample preparation for the analysis of volatile organic compounds in air and water matrices. **2007**, *1153* (1-2), 130-144.
17. Mosier-Boss, P.; Lieberman, S. J. A. C. A., Detection of volatile organic compounds using surface enhanced Raman spectroscopy substrates mounted on a thermoelectric cooler. **2003**, *488* (1), 15-23.
18. Bacsik, Z.; Mink, J.; Keresztury, G. J. A. s. r., FTIR spectroscopy of the atmosphere. I. Principles and methods. **2004**, *39* (3), 295-363.
19. Lin, T.-Y.; Sree, U.; Tseng, S.-H.; Chiu, K. H.; Wu, C.-H.; Lo, J.-G. J. A. E., Volatile organic compound concentrations in ambient air of Kaohsiung petroleum refinery in Taiwan. **2004**, *38* (25), 4111-4122.

20. Semb, S. I.; Pedersen-Bjergaard, S.; Brevik, E. M. J. C., Solid-phase microextraction coupled with atomic emission spectroscopy—rapid screening for volatile chlorinated compounds. **2002**, *49* (10), 1349-1355.
21. Wang, M.; Zeng, L.; Lu, S.; Shao, M.; Liu, X.; Yu, X.; Chen, W.; Yuan, B.; Zhang, Q.; Hu, M. J. A. M., Development and validation of a cryogen-free automatic gas chromatograph system (GC-MS/FID) for online measurements of volatile organic compounds. **2014**, *6* (23), 9424-9434.
22. Cervera, M.; Beltran, J.; Lopez, F.; Hernandez, F. J. A. c. a., Determination of volatile organic compounds in water by headspace solid-phase microextraction gas chromatography coupled to tandem mass spectrometry with triple quadrupole analyzer. **2011**, *704* (1-2), 87-97.
23. Wang, Z.; Fingas, M. J. J. o. C. A., Differentiation of the source of spilled oil and monitoring of the oil weathering process using gas chromatography-mass spectrometry. **1995**, *712* (2), 321-343.
24. Yamada, H. J. S. o. t. t. e., Contribution of evaporative emissions from gasoline vehicles toward total VOC emissions in Japan. **2013**, *449*, 143-149.
25. Wei, W.; Wang, S.; Hao, J.; Cheng, S. J. A. e., Projection of anthropogenic volatile organic compounds (VOCs) emissions in China for the period 2010–2020. **2011**, *45* (38), 6863-6871.
26. Ye, Y.; Galbally, I.; Weeks, I.; Duffy, B.; Nelson, P. J. A. E., Evaporative emissions of 1, 3-butadiene from petrol-fuelled motor vehicles. **1998**, *32* (14-15), 2685-2692.
27. Yuan, B.; Hu, W.; Shao, M.; Wang, M.; Chen, W.; Lu, S.; Zeng, L.; Hu, M. J. A. C.; Physics, VOC emissions, evolutions and contributions to SOA formation at a receptor site in eastern China. **2013**, *13* (17), 8815-8832.
28. Duan, J.; Tan, J.; Yang, L.; Wu, S.; Hao, J. J. A. R., Concentration, sources and ozone formation potential of volatile organic compounds (VOCs) during ozone episode in Beijing. **2008**, *88* (1), 25-35.
29. Huang, R.-J.; Zhang, Y.; Bozzetti, C.; Ho, K.-F.; Cao, J.-J.; Han, Y.; Daellenbach, K. R.; Slowik, J. G.; Platt, S. M.; Canonaco, F. J. N., High secondary aerosol contribution to particulate pollution during haze events in China. **2014**, *514* (7521), 218.
30. Anderson, J. E.; Leone, T. G.; Shelby, M. H.; Wallington, T. J.; Bizub, J. J.; Foster, M.; Lynskey, M. G.; Polovina, D. *Octane numbers of ethanol-gasoline blends: measurements and novel estimation method from molar composition*; 0148-7191; SAE Technical Paper: 2012.
31. Hunwartz, I. *Modification of CFR test engine unit to determine octane numbers of pure alcohols and gasoline-alcohol blends*; 0148-7191; SAE technical paper: 1982.
32. Andersen, V. F.; Anderson, J.; Wallington, T.; Mueller, S.; Nielsen, O. J. J. E.; Fuels, Vapor pressures of alcohol– gasoline blends. **2010**, *24* (6), 3647-3654.
33. Reid, R. C.; Prausnitz, J. M.; Poling, B. E., *The properties of gases and liquids*. **1987**.
34. Furey, R. L. *Volatility characteristics of gasoline-alcohol and gasoline-ether fuel blends*; 0148-7191; SAE Technical Paper: 1985.

35. Stump, F. D.; Knapp, K. T.; Ray, W. D. J. J. o. t. A.; Association, W. M., Influence of ethanol-blended fuels on the emissions from three pre-1985 light-duty passenger vehicles. **1996**, *46* (12), 1149-1161.
36. Knapp, K. T.; Stump, F. D.; Tejada, S. B. J. J. o. t. A.; Association, W. M., The effect of ethanol fuel on the emissions of vehicles over a wide range of temperatures. **1998**, *48* (7), 646-653.
37. Wang, C.-H.; Lin, S.-S.; Chang, H.-L. J. J. o. E. S.; Health, P. A., Effect of oxygenates on exhaust emissions from two-stroke motorcycles. **2002**, *37* (9), 1677-1685.
38. Leong, S. T.; Muttamara, S.; Laortanakul, P. J. A. E., Applicability of gasoline containing ethanol as Thailand's alternative fuel to curb toxic VOC pollutants from automobile emission. **2002**, *36* (21), 3495-3503.
39. Pouloupoulos, S.; Philippopoulos, C. J. J. o. e. f. g. t.; power, The effect of adding oxygenated compounds to gasoline on automotive exhaust emissions. **2003**, *125* (1), 344-350.
40. He, B.-Q.; Wang, J.-X.; Hao, J.-M.; Yan, X.-G.; Xiao, J.-H. J. A. E., A study on emission characteristics of an EFI engine with ethanol blended gasoline fuels. **2003**, *37* (7), 949-957.
41. Suarez-Bertoa, R.; Zardini, A. A.; Keuken, H.; Astorga, C., Impact of ethanol containing gasoline blends on emissions from a flex-fuel vehicle tested over the Worldwide Harmonized Light duty Test Cycle (WLTC). *Fuel* **2015**, *143*, 173-182.
42. Li, L.; Ge, Y.; Wang, M.; Peng, Z.; Song, Y.; Zhang, L.; Yuan, W., Exhaust and evaporative emissions from motorcycles fueled with ethanol gasoline blends. *Science of The Total Environment* **2015**, *502*, 627-631.
43. Yüksel, F.; Yüksel, B., The use of ethanol-gasoline blend as a fuel in an SI engine. *Renewable Energy* **2004**, *29* (7), 1181-1191.
44. Najafi, G.; Ghobadian, B.; Tavakoli, T.; Buttsworth, D.; Yusaf, T.; Faizollahnejad, M. J. A. E., Performance and exhaust emissions of a gasoline engine with ethanol blended gasoline fuels using artificial neural network. **2009**, *86* (5), 630-639.
45. Koç, M.; Sekmen, Y.; Topgül, T.; Yücesu, H. S., The effects of ethanol-unleaded gasoline blends on engine performance and exhaust emissions in a spark-ignition engine. *Renewable Energy* **2009**, *34* (10), 2101-2106.
46. Kondyli, A.; Schrader, W., High-resolution GC/MS studies of a light crude oil fraction. *J Mass Spectrom* **2019**, *54* (1), 47-54.
47. Wang, H.; Geppert, H.; Fischer, T.; Wieprecht, W.; Moller, D., Determination of volatile organic and polycyclic aromatic hydrocarbons in crude oil with efficient gas-chromatographic methods. *J Chromatogr Sci* **2015**, *53* (5), 647-54.
48. Liu, Y.; Shen, J.; Zhu, X. D., Headspace Solid-phase Microextraction for the Determination of Volatile Organic Compounds in Larix Gmelini Particles. *Physics Procedia* **2012**, *32*, 605-613.
49. Banan, N.; Latif, M. T.; Juneng, L.; Ahamad, F. J. A.; Research, A. Q., Characteristics of surface ozone concentrations at stations with different backgrounds in the Malaysian Peninsula. **2012**, *13* (3), 1090-1106.
50. Gérin, M.; Siemiatycki, J.; Désy, M.; Krewski, D. J. A. j. o. i. m., Associations between several sites of cancer and occupational exposure to benzene, toluene, xylene, and styrene: Results of a case-control study in Montreal. **1998**, *34* (2), 144-156.

51. Pang, Y.; Fuentes, M.; Rieger, P., Trends in the emissions of Volatile Organic Compounds (VOCs) from light-duty gasoline vehicles tested on chassis dynamometers in Southern California. *Atmospheric Environment* **2014**, *48*, 127-135.
52. Abbey, D. E.; Burchette, R. J.; Knutsen, S. F.; McDonnell, W. F.; Lebowitz, M. D.; Enright, P. L. J. A. j. o. r.; medicine, c. c., Long-term particulate and other air pollutants and lung function in nonsmokers. **1998**, *158* (1), 289-298.
53. Künzli, N.; Lurmann, F.; Segal, M.; Ngo, L.; Balmes, J.; Tager, I. B. J. E. r., Association between lifetime ambient ozone exposure and pulmonary function in college freshmen—results of a pilot study. **1997**, *72* (1), 8-23.
54. Uysal, N.; Schapira, R. M. J. C. o. i. p. m., Effects of ozone on lung function and lung diseases. **2003**, *9* (2), 144-150.
55. Marino, E.; Caruso, M.; Campagna, D.; Polosa, R. J. T. a. i. c. d., Impact of air quality on lung health: myth or reality? **2015**, *6* (5), 286-298.
56. Nadim, F.; Zack, P.; Hoag, G. E.; Liu, S. J. E. P., United States experience with gasoline additives. **2001**, *29* (1), 1-5.
57. Thomas, V. J. A. R. o. E.; Environment, t., The elimination of lead in gasoline. **1995**, *20* (1), 301-324.
58. Shapouri, H.; Duffield, J. A.; Wang, M. Q. *The energy balance of corn ethanol: an update*; 2002.
59. Squillace, P. J.; Pankow, J. F.; Korte, N. E.; Zogorski, J. S. J. E. T.; Chemistry, Review of the environmental behavior and fate of methyl tert-butyl ether. **1997**, *16* (9), 1836-1844.
60. McCarthy, J. E.; Tiemann, M., MTBE in gasoline: clean air and drinking water issues. **2006**.
61. Cassada, D.; Zhang, Y.; Snow, D.; Spalding, R. J. A. C., Trace analysis of ethanol, MTBE, and related oxygenate compounds in water using solid-phase microextraction and gas chromatography/mass spectrometry. **2000**, *72* (19), 4654-4658.
62. Song, C.-L.; Zhang, W.-M.; Pei, Y.-Q.; Fan, G.-L.; Xu, G.-P. J. A. E., Comparative effects of MTBE and ethanol additions into gasoline on exhaust emissions. **2006**, *40* (11), 1957-1970.
63. Al-Hasan, M. J. e. c.; management, Effect of ethanol–unleaded gasoline blends on engine performance and exhaust emission. **2003**, *44* (9), 1547-1561.
64. Frena, M.; Tonietto, A. E.; Madureira, L. A. d. S. J. J. o. t. B. C. S., Application of solid phase microextraction and gas chromatography for the determination of BTEX in solid petroleum residues. **2013**, *24* (9), 1530-1536.
65. Chen, Y.; Zhang, Y.; Cheng, W. K. *Effects of ethanol evaporative cooling on particulate number emissions in GDI engines*; 0148-7191; SAE Technical Paper: 2018.
66. Short-Term Energy Outlook. https://www.eia.gov/outlooks/steo/report/us_oil.php (accessed November 11).
67. Wang, S.; Xu, Y.; Lin, Z.; Zhang, J.; Norbu, N.; Liu, W. In *The harm of petroleum-polluted soil and its remediation research*, AIP Conference proceedings, AIP Publishing: 2017; p 020222.
68. Han, J., Introduction to land engineering. Beijing: Science Press: 2013.
69. Zhang, H.; Li, P.; Sun, T. J. J. o. a.-e. s., Bioremediation on 4 soils contaminated by petroleum oils using prepared bed processes. **2001**, *20* (2), 76-80.

70. Thapa, B.; Kc, A. K.; Ghimire, A. J. K. u. j. o. s., engineering; technology, A review on bioremediation of petroleum hydrocarbon contaminants in soil. **2012**, 8 (1), 164-170.
71. Das, P.; Mukherjee, S.; Sen, R. J. C., Improved bioavailability and biodegradation of a model polyaromatic hydrocarbon by a biosurfactant producing bacterium of marine origin. **2008**, 72 (9), 1229-1234.
72. Vater, J.; Kablitz, B.; Wilde, C.; Franke, P.; Mehta, N.; Cameotra, S. S. J. A. E. M., Matrix-assisted laser desorption ionization-time of flight mass spectrometry of lipopeptide biosurfactants in whole cells and culture filtrates of *Bacillus subtilis* C-1 isolated from petroleum sludge. **2002**, 68 (12), 6210-6219.
73. Maletić, S.; Dalmacija, B.; Rončević, S. J. E. b. V. K., Petroleum hydrocarbon biodegradability in soil—Implications for bioremediation. **2013**, 43.
74. Sheppard, C., *World Seas: An Environmental Evaluation: Volume III: Ecological Issues and Environmental Impacts*. Academic Press: 2018.
75. Zhang, Z.; Hou, Z.; Yang, C.; Ma, C.; Tao, F.; Xu, P. J. B. T., Degradation of n-alkanes and polycyclic aromatic hydrocarbons in petroleum by a newly isolated *Pseudomonas aeruginosa* DQ8. **2011**, 102 (5), 4111-4116.
76. Chaillan, F.; Le Flèche, A.; Bury, E.; Phantavong, Y.-h.; Grimont, P.; Saliot, A.; Oudot, J. J. R. i. m., Identification and biodegradation potential of tropical aerobic hydrocarbon-degrading microorganisms. **2004**, 155 (7), 587-595.
77. Baye, N. *Bacillus* Strains Used for Biological Control of *Fusarium* Head Blight: Identification, Growth Studies, and Lipopeptide Production. M.S. Thesis, South Dakota State University, Brookings, SD, 2007.
78. Watanabe, K. J. C. o. i. b., Microorganisms relevant to bioremediation. **2001**, 12 (3), 237-241.
79. Atlas, R. M. J. I. B.; Biodegradation, Bioremediation of petroleum pollutants. **1995**, 35 (1-3), 317-327.
80. Boopathy, R. J. B. t., Factors limiting bioremediation technologies. **2000**, 74 (1), 63-67.
81. Das, N.; Chandran, P., Microbial degradation of petroleum hydrocarbon contaminants: an overview. *Biotechnol Res Int* **2011**, 2011, 941810.
82. Cooney, J.; Silver, S.; Beck, E. J. M. e., Factors influencing hydrocarbon degradation in three freshwater lakes. **1985**, 11 (2), 127-137.
83. Prince, R. C., The microbiology of marine oil spill bioremediation. In *Petroleum microbiology*, American Society of Microbiology: 2005; pp 317-335.
84. Wang, X.-B.; Chi, C.-Q.; Nie, Y.; Tang, Y.-Q.; Tan, Y.; Wu, G.; Wu, X.-L. J. B. t., Degradation of petroleum hydrocarbons (C6–C40) and crude oil by a novel *Dietzia* strain. **2011**, 102 (17), 7755-7761.
85. Sakai, Y.; Maeng, H. J.; Tani, Y.; Kato, N. J. B., biotechnology,; biochemistry, Use of long-chain n-alkanes (C13-C44) by an isolate, *Acinetobacter* sp. M-1. **1994**, 58 (11), 2128-2130.
86. Van Hamme, J. D.; Ward, O. P. J. A. E. M., Physical and metabolic interactions of *Pseudomonas* sp. strain JA5-B45 and *Rhodococcus* sp. strain F9-D79 during growth on crude oil and effect of a chemical surfactant on them. **2001**, 67 (10), 4874-4879.

87. Liu, Y.-C.; Li, L.-Z.; Wu, Y.; Tian, W.; Zhang, L.-P.; Xu, L.; Shen, Q.-R.; Shen, B. J. B. t., Isolation of an alkane-degrading *Alcanivorax* sp. strain 2B5 and cloning of the *alkB* gene. **2010**, *101* (1), 310-316.
88. Das, K.; Mukherjee, A. K. J. B. t., Crude petroleum-oil biodegradation efficiency of *Bacillus subtilis* and *Pseudomonas aeruginosa* strains isolated from a petroleum-oil contaminated soil from North-East India. **2007**, *98* (7), 1339-1345.
89. Cunha, C.; Do Rosario, M.; Rosado, A.; Leite, S. J. P. B., *Serratia* sp. SVGG16: a promising biosurfactant producer isolated from tropical soil during growth with ethanol-blended gasoline. **2004**, *39* (12), 2277-2282.
90. Ron, E. Z.; Rosenberg, E. J. C. o. i. b., Biosurfactants and oil bioremediation. **2002**, *13* (3), 249-252.
91. Banat, I. M.; Franzetti, A.; Gandolfi, I.; Bestetti, G.; Martinotti, M. G.; Fracchia, L.; Smyth, T. J.; Marchant, R. J. A. m.; biotechnology, Microbial biosurfactants production, applications and future potential. **2010**, *87* (2), 427-444.
92. Ron, E. Z.; Rosenberg, E. J. E. m., Natural roles of biosurfactants: Minireview. **2001**, *3* (4), 229-236.
93. Gudiña, E.; Teixeira, J.; Rodrigues, L. J. M. d., Biosurfactants produced by marine microorganisms with therapeutic applications. **2016**, *14* (2), 38.
94. Silva, R.; Almeida, D.; Rufino, R.; Luna, J.; Santos, V.; Sarubbo, L. J. I. j. o. m. s., Applications of biosurfactants in the petroleum industry and the remediation of oil spills. **2014**, *15* (7), 12523-12542.
95. Liu, J.-F.; Mbadanga, S.; Yang, S.-Z.; Gu, J.-D.; Mu, B.-Z. J. I. j. o. m. s., Chemical structure, property and potential applications of biosurfactants produced by *Bacillus subtilis* in petroleum recovery and spill mitigation. **2015**, *16* (3), 4814-4837.
96. Pornsunthorntawe, O.; Arttaweeporn, N.; Paisanjit, S.; Somboonthanate, P.; Abe, M.; Rujiravanit, R.; Chavadej, S. J. B. E. J., Isolation and comparison of biosurfactants produced by *Bacillus subtilis* PT2 and *Pseudomonas aeruginosa* SP4 for microbial surfactant-enhanced oil recovery. **2008**, *42* (2), 172-179.
97. Zhang, J.; Xue, Q.; Gao, H.; Lai, H.; Wang, P. J. M. c. f., Production of lipopeptide biosurfactants by *Bacillus atrophaeus* 5-2a and their potential use in microbial enhanced oil recovery. **2016**, *15* (1), 168.
98. Hbid, C.; Jacques, P.; Razafindralambo, H.; Mpoyo, M. K.; Meurice, E.; Paquot, M.; Thonart, P. In *Influence of the production of two lipopeptides, Iturin A and Surfactin S1, on oxygen transfer during Bacillus subtilis fermentation*, Seventeenth Symposium on Biotechnology for Fuels and Chemicals, Springer: 1996; pp 571-579.
99. He, C.; Fan, L.; Wu, W.; Liang, Y.; Li, R.; Tang, W.; Zheng, X.; Xiao, Y.; Liu, Z.; Zheng, F. J. G.; GMR, m. r., Identification of lipopeptides produced by *Bacillus subtilis* Czkl isolated from the aerial roots of rubber trees. **2017**, *16* (1).
100. Meena, K. R.; Kanwar, S. S. J. B. r. i., Lipopeptides as the antifungal and antibacterial agents: applications in food safety and therapeutics. **2015**, *2015*.
101. Haddad, N. I.; Liu, X.; Yang, S.; Mu, B. J. P.; letters, p., Surfactin isoforms from *Bacillus subtilis* HSO121: separation and characterization. **2008**, *15* (3), 265-269.
102. Belbahri, L.; Chenari Bouket, A.; Rekik, I.; Alenezi, F. N.; Vallat, A.; Luptakova, L.; Petrovova, E.; Oszako, T.; Cherrad, S.; Vacher, S. J. F. i. M., Comparative genomics of *Bacillus amyloliquefaciens* strains reveals a core genome with

- traits for habitat adaptation and a secondary metabolites rich accessory genome. **2017**, *8*, 1438.
103. Hansen, S. A. G. Identifying and Evaluating Potential Microbial Biological Control Agents of Tan Spot and Head Scab of Wheat. M.S. Thesis, South Dakota State University, Brookings, SD, 1996.
104. Luo, Y. Bacillus Strains as Biological Control Agents of Tan Spot and Fusarium Head Blight of Wheat. M.S. Thesis, South Dakota State University, Brookings, SD, 2000.
105. Peiest, F.; Goodfellow, M.; Shute, L.; Berkeley, R. J. I. J. S. B., *Bacillus amyloliquefaciens* sp. nov. norn. rev. **1987**, *37*, 69-71.
106. Kim, H.-S.; Yoon, B.-D.; Lee, C.-H.; Suh, H.-H.; Oh, H.-M.; Katsuragi, T.; Tani, Y. J. J. o. f.; bioengineering, Production and properties of a lipopeptide biosurfactant from *Bacillus subtilis* C9. **1997**, *84* (1), 41-46.
107. Kim, P. I.; Ryu, J.; Kim, Y. H.; Chi, Y.-T. J. J. M. B., Production of biosurfactant lipopeptides Iturin A, fengycin and surfactin A from *Bacillus subtilis* CMB32 for control of *Colletotrichum gloeosporioides*. **2010**, *20* (1), 138-145.
108. Jacques, P.; Hbid, C.; Destain, J.; Razafindralambo, H.; Paquot, M.; De Pauw, E.; Thonart, P. In *Optimization of biosurfactant lipopeptide production from Bacillus subtilis S499 by Plackett-Burman design*, Twentieth Symposium on Biotechnology for Fuels and Chemicals, Springer: 1999; pp 223-233.
109. Al-Wahaibi, Y.; Joshi, S.; Al-Bahry, S.; Elshafie, A.; Al-Bemani, A.; Shibulal, B. J. C.; Biointerfaces, S. B., Biosurfactant production by *Bacillus subtilis* B30 and its application in enhancing oil recovery. **2014**, *114*, 324-333.
110. Smyth, T.; Perfumo, A.; McClean, S.; Marchant, R.; Banat*, I. J. H. o. h.; microbiology, I., Isolation and analysis of lipopeptides and high molecular weight biosurfactants. **2010**, 3687-3704.
111. Stevenson, K.; McVey, A. F.; Clark, I. B.; Swain, P. S.; Pilizota, T. J. S. r., General calibration of microbial growth in microplate readers. **2016**, *6*, 38828.
112. Mubarak, M. Q. E.; Hassan, A. R.; Hamid, A. A.; Khalil, S.; Isa, M. H. M. J. S. M., A simple and effective isocratic HPLC method for fast identification and quantification of surfactin. **2015**, *44* (1), 115-120.
113. OKA, K.; HIRANO, T.; HOMMA, M.; ISHII, H.; MURAKAMI, K.; MOGAMI, S.; MOTIZUKI, A.; MORITA, H.; TAKEYA, K.; ITOKAWA, H. J. C.; bulletin, p., Satisfactory separation and MS-MS spectrometry of six surfactins isolated from *Bacillus subtilis* natto. **1993**, *41* (5), 1000-1002.
114. Arthur, C. L.; Pawliszyn, J. J. A. c., Solid phase microextraction with thermal desorption using fused silica optical fibers. **1990**, *62* (19), 2145-2148.
115. Zhang, Z.; Yang, M. J.; Pawliszyn, J. J. A. c., Solid-phase microextraction. A solvent-free alternative for sample preparation. **1994**, *66* (17), 844A-853A.
116. Ross, C.; Pawliszyn, J., EXTRACTION| Solid-Phase Microextraction. **2005**.
117. Kyle, P., Toxicology: GCMS. In *Mass Spectrometry for the Clinical Laboratory*, Elsevier: 2017; pp 131-163.
118. Tang, B.; Isacson, U. J. E.; Fuels, Analysis of mono-and polycyclic aromatic hydrocarbons using solid-phase microextraction: state-of-the-art. **2008**, *22* (3), 1425-1438.

119. Carasek, E.; Pawliszyn, J. J. J. o. A.; Chemistry, F., Screening of tropical fruit volatile compounds using solid-phase microextraction (SPME) fibers and internally cooled SPME fiber. **2006**, *54* (23), 8688-8696.
120. Kolbe, B.; Ettre, L. S. J. C. W. V., Static Headspace–Gas Chromatography: Theory and Practice. **1997**.
121. Pawliszyn, J., *Comprehensive sampling and sample preparation: analytical techniques for scientists*. Academic Press: 2012.
122. Menéndez, J. F.; Sánchez, M. F.; Martínez, E. F.; Uría, J. S.; Sanz-Medel, A. J. T., Static headspace versus head space solid-phase microextraction (HS-SPME) for the determination of volatile organochlorine compounds in landfill leachates by gas chromatography. **2004**, *63* (4), 809-814.
123. D'auria, M.; Mauriello, G.; Racioppi, R. J. I. j. o. f. s., SPME-GC-MS ANALYSIS OF HORSERADISH (ARMORACIA RUSTICANA). **2004**, *16* (4).
124. Rao, P. V.; Gan, S. H. J. E.-B. C.; Medicine, A., Cinnamon: a multifaceted medicinal plant. **2014**, *2014*.